The Dependence of Polymer Structure and Morphology

on Catalytic Activity

in Molecularly Imprinted Nanogels

Inaugural-Dissertation

zur

Erlangung des Doktorgrades der

Mathematisch-Naturwissenschaftlichen Fakultät

der Heinrich-Heine-Universität Düsseldorf

vorgelegt von

Byong-Oh Chong

aus Seoul, Korea

2005

Gedruckt mit der Genehmigung der Mathematisch-Naturwissenschaftlichen Fakutät der Heinrich-Heine-Universität Düseeldorf

1. Berichtstatter: Prof. Dr. G. Wulff
2. Berichtstatter: Prof. Dr. H. Ritter

Tag der mündlichen Prüfung: 12. 07. 2005

Die vorliegende Arbeit wurde in der Zeit von Mai 1999 bis November 2004 am Institut für Organische Chemie und Makromolekulare Chemie II der Heinrich-Heine-Universität Düsseldorf unter der Leitung Prof. Dr. Günter Wulff durchgeführt.

감사의 글

이 곳 독일에 온지도 어언 6 년이 지났습니다.

그리고 지난 6 년 동안 저는 아버지 세 분을 새롭게 만났습니다. 항상 저를 인도하시는 하나님 아버지, 저를 낳고 길러주신 아버지, 그리고 배움의 즐거움을 알게 해 주신 Wulff 교수님 아버지. 제가 이 분들께 드릴 수 있는 감사는 항상 모자람이 있어 두려울 뿐입니다. 다시 한 번 깊은 감사를 드립니다.

아울러 제 실험실 동료 Dr. Marco Emgenbroich 와 Dr. Karsten Knorr 를 떠올립니다. 지난 시간 동안 그들과 같이 보낸 시간들은 온통 즐거움이었음을 전합니다. 가장 믿을만한 두 명의 독일인 친구를 만난 것은 제겐 무엇보다 소중한 경험입니다. 둘 다 앞으로도 좋은 학문적 성과와 화목한 가정의 두 마리 토끼를 잘 잡기 기도합니다.

지금은 중국 Beijing 에 있는 Dr. Jun-Qiu Liu 에게도 감사를 전합니다. 그가 아침에 실험실 문을 열어 놓으면 저녁엔 제가 그 문을 닫고 나가던 그 시절은 앞으로도 무척 그리울 것입니다. 또한 제 마지막 실험실 동료가 된 Sarah Schmidt 와 Sebastian Sinnwell 에게도 고마움을 전하며 앞으로의 학업에도 좋은 결과 있기를 바라는 마음입니다.

최수환 박사님께도 특히 깊은 감사의 뜻을 전합니다. 아직도 앞뒤를 잘 가릴 줄 모르는 저에게 선배로서의 폭 넓은 경험과 깊은 안목으로 큰 도움을 주셨습니다. 그것은 학문적으로뿐만 아니라 독일 생활에서 필요한 부분들이었기에 더욱 감사를 드립니다.

일일이 그 이름을 여기에 적지는 못하지만 항상 좋은 추억을 갖게 해준 많은 다른 동료들에게도 따뜻한 감사의 마음 전합니다. 제 졸업 시험 때에 그들이 정성으로 만들어 준 Doktorwagen 과 Doktorhut 는 앞으로도 결코 잊지 못할 것입니다.

제 논문에 실린 TEM 분석을 도와주신 Johannes Gutenberg-Universität Mainz 의 Dr. Ute Kolb 에게도 감사를 전합니다. 그리고 처음엔 졸필에 지나지 않았던 이 논문을 이렇게 멋진 글과 적절한 표현으로 가다듬어준 Universität Dortmund 의 Dr. Andrew Hall 에게도 고마운 마음 전합니다.

뒤셀도르프 순복음교회 식구들에게도 이 기쁜 마음을 전합니다. 전한다고는 하지만 다 전해질지는 모르겠습니다. 김광덕 목사님과 사모님, 한사무엘 목사님과 사모님, 장로님, 권사님, 집사님들 그리고 많은 성도님들. 비록 고국과 가족을 떠나 살아온 지난 독일 생활이었지만 결코 한시도 고국과 가족을 떠나지 않은듯한 기분을 들게 해 준 고마운 분들이었음을 여기 감사한 마음으로 밝힙니다. 특히 청년부와 성가대 지체들은 잊을 수 없으리라 믿습니다. 여기서 새로 만난 가족들이니까요. 항상 점심식사 때마다 멘자(학교식당)에서 즐거운 시간을 보낸 'Mensa Team'에게도 특별한 감사의 말 전합니다. 제가 독일을 떠나도 서로 같이 기다려 준 그 시간들과 수다 떨며 비운 그 커피잔들은 항상 그 자리에 기억으로 남을 것입니다.

다시 한 번 아버지와 어머니께 감사를 드립니다. 결코 갚을 수 없는 사랑을 받았습니다. 그리고 항상 온 가족을 위해 기도하시는 할머니께도 감사의 말씀을 드려야 하겠습니다. 늘 건강하시길. 제가 여기 다 적지는 못하지만 항상 저희 가족을 위해 염려하시고 기도해 주시는 모든 분들께도 깊은 감사를 드립니다.

마지막으로 나의 아내 혜섭과 딸 혜원이에게 제 모든 사랑을 전합니다. 혹시 제가 받을 축하의 말과 수고에 대한 위로의 말이 있다면 그것은 제 것이 아니라 그 동안 묵묵히 기다리며 인내해 준 제 가족들의 것입니다. 정말 사랑합니다.

정병오 올림

For

S.T .Chong

Abstract

A series of imprinted nanogels was prepared by solution polymerization to catalyze the hydrolysis of diphenylcarbonate (DPC). Diphenylphosphate (DPP) employed as a template molecule and *N,N'*-diethyl(4-vinylphenyl)amidine (DEVPA) as a binding molecule and these were mixed with an excess of EDMA and MMA. The monomer mixture was highly diluted with cyclopentanone, which was found to be a good solvent for preparation of MMA-based nanogels, and polymerized with AIBN under a variety of conditions.

The resultant nanogels, generally nano-sized particles, were found to give stable solutions in appropriate solvents and, thus, make it possible to carry out the kinetic experiments under homogeneous conditions. Due to their good solubility, it is expected that the nanogels will exhibit good mass transfer properties, one of the known limitations of traditional bulk-polymerized imprinted polymers. Further, this series of nanogels could be characterized by standard techniques available for soluble macromolecules, such as GPC, NMR and membrane osmometry. This relieves the problems associated with the characterization of insoluble materials, such as traditional imprinted polymers.

Moreover, direct proof of the size and shape of an individual nanogel particle was obtained via a special electron microscopy technique. After the characterization of membrane osmometry and potentiometric titration, the number of active sites per 40,000 of absolute number-averaged molecular weight (M_{abs}) could be calculated to show the relative density of active sites in the nanogels. From these results, it was possible to synthesize an imprinted nanogel which possesses one active site per one individual particle.

This nanogel showed significant catalytic activity in the hydrolysis of DPC and, after modification of polymer structure, displayed even better performance. The most improved result was an approximately 290-fold increase in rate constant compared to that measured in buffer solution, with this nanogel remaining soluble.

A Michaelis-Menten kinetic experiment was also performed, yielding a value of k_{cat}/K_m ratio for the imprinted nanogel that was 65.6 times higher than for a control nanogel.

Introduction

Enzyme-mimicking with molecularly imprinted polymers (MIPs)

In nature, most reactions are catalyzed with high activity and selectivity by enzymes. They are extraordinary catalysts. It is well known that the rate enhancements brought about by enzymes are often in the range of 7 to 14 orders of magnitude (*Table 1*). Furthermore, enzymes have a high degree of selectivity for their substrates and they accelerate particular chemical reactions with remarkable chemo-, regio- and stereoselectivity. The reactions usually function in aqueous solutions with high levels of

Table 1. Some rate enhancements produced by enzymes.

Carbonic anhydrase	10^7
Phosphoglucomutase	10^{12}
Succinyl-CoA transferase	10^{13}
Urease	10^{14}

efficiency. Owing to these unique properties, enzymes have long attracted the attention and imagination of chemists and biologists to create efficient artificial enzymes.

Countless attempts and studies have been carried out for enzyme mimicking, such as making use of host-guest chemistry,[1] like supramolecular complexes,[2] cyclodextrins,[3] cryptands,[4] and crown ether.[5] Furthermore, functionalized linear polymers,[6] modified micelles and vesicles,[7] artificial polypeptides[8,9] and catalytic antibodies[10,11] have also been used. Molecularly imprinted polymers (MIPs) are another possibility; they have shown promising efficiency in this respect as well.[12]
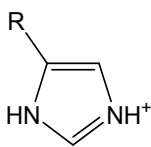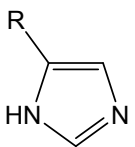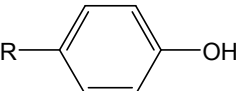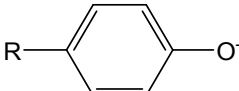
Indeed, there has also been the traditional way of using synthetic polymers for making enzyme models.[13,14] Especially after the elucidation of the mechanism of chymotrypsin in the late 1960s, the activity in the polymer field became more prominent.[15,16] Synthetic polymers are regarded as good candidates for enzyme mimicking, because they are usually stable against heat, chemicals, solvents and some other harsh environments. Furthermore, they can

be easily produced in forms suitable for industrial application. These are advantages compared to the properties of natural enzymes.

Nature builds up three major biopolymers, namely polypeptides, nucleic acids (DNA, RNA), and polysaccharides. This means that natural enzymes are themselves polymers. Actually, many of the unique features of enzymes are directly related to their polymeric nature. This is particularly true for the high cooperativity of the functional groups and dynamic effects such as induced fit, the allosteric effect and the steric strain exhibited by enzymes. Thus, artificial polymeric enzyme models can provide advantages in imitating enzymes if the macromolecular properties of enzymes are considered.

The introduction of functional groups into the polymer at the right positions is the key procedure to fulfill this goal. Functional groups in natural enzyme systems, which can participate in the catalytic process, are both binding and catalytic sites. Important catalytic groups are proton donors or proton acceptors. The active sites of most enzymes contain amino acids with such functional groups (*Table 2*).

Table 2. List of amino acids possessing functional side groups.

Amino acid residues	General acid form (Proton donor)	General base form (Proton acceptor)
Glu, Asp	R-COOH	R-COO$^-$
Lys, Arg	R-NH$_3^+$	R-NH$_2$
Cys	R-SH	R-S$^-$
Ser	R-OH	R-O$^-$
His		
Tyr		
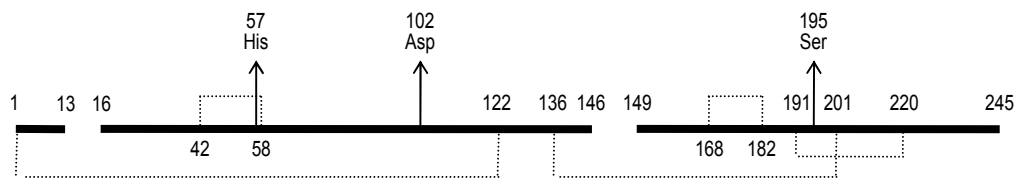
Scheme 1. A representation of the primary structure of α-chymotrypsin, showing disulfide bonds (dashed lines) and the location of key amino acids. Note that the protein consists of three polypeptide chains.

In many cases, these functional groups interact with each other to establish arrangements of higher cooperation for better catalytic activity. In the well-known example of the serine-protease α-chymotrypsin, three key amino acids cooperate in the active site, namely 57-His, 102-Asp and 195-Ser, respectively. In the primary structure, the locations of the single groups of this "catalytic triad"[17] are distant from each other; thus, there seems to be no sign of cooperation between these amino acids (*Scheme 1*).

However, in the three-dimensional arrangement, due to the α-helix or β-sheet conformation of proteins and five disulfide bridges from cysteine, the spatial distance of these amino acids is close, thus giving the proper orientation for the catalytic activity.

The shape of the active site as well as the arrangement of suitable binding site groups is
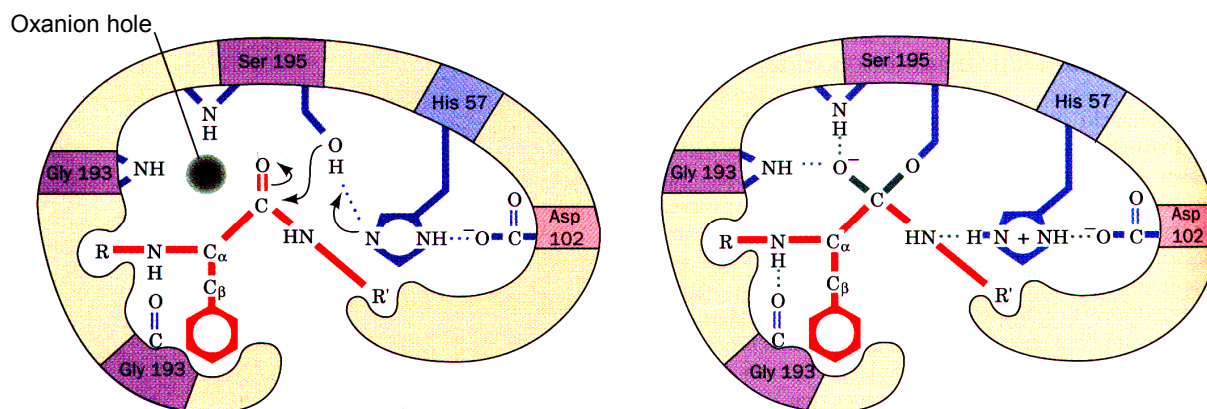
Scheme 2. Schematic of the mechanism of α-chymotrypsin action in the hydrolysis of an L-phenylalaninamide.

complementary to the chemical structure of the substrate that is preferably bound. Thus, it shows selectivity for the substrate molecule, in *Scheme 2* for L-phenylalaninamide. When the substrate interacts with functional groups in the active site, an appreciable change in the three-dimensional conformation of the peptide chain and of the amino acid residues inside the cavity occurs. This is called 'induced fit'.[18]
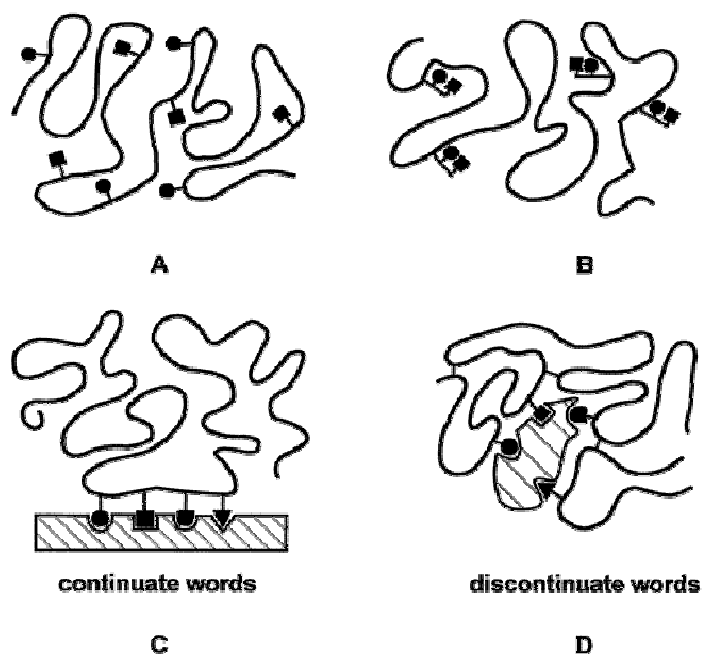
Scheme 3. Possible arrangements of functional groups in synthetic and natural polymers.

This observation of how nature works implies that, to prepare proper synthetic macromolecular enzymes, it is important to introduce the functional groups in the correct positions. There have been several concepts to mimic the arrangement of functional groups in synthetic and natural polymers, as illustrated in *Scheme 3*.[19]

Firstly, catalytically active functional groups can be introduced into polymers by copolymerization of the appropriate monomers possessing the desired functionalities, providing a random distribution of functional groups all over the polymer chains (*Scheme 3-*

A). Another possibility is to attach side chains containing functionalities with desired arrangement onto the parent polymer (*Scheme 3-B*).[20]

It seems that these two strategies are significantly different with respect to how the information is stored. While the latter (*B*) already has the information "encoded" into a one-dimensional arrangement sequence in space to obtain certain cooperation, in the former arrangement (*A*) this information is "decoded" into a statistical arrangement. From this point of view, the former arrangement (*A*) constitutes a situation similar to denatured enzymes. However, to arrange a desired functionality in a cavity by this method seems to be rather difficult, because there is insufficient driving force in normal polymer networks to arrange the randomly distributed functional groups in a way suitable for the substrate.

Another approach is the polycondensation or polymerization of monomers with a desired sequence. In this case, the functional groups are localized in linear arrangement in the main chain, as is observed in some hormone receptors (*Scheme 3C*).[21]

Although in a few cases significantly high catalytic activities have been observed, especially with *3A*,[22,23] these attempts have, in general, brought rather limited success. This is due to the impossibility of orienting the functional groups into a defined three-dimensional neighborhood, because the location and order of functional groups are already fixed in one-dimension. Therefore, it can be said that the key is how to "encode" information into a three-dimensional matrix.

The final possibility, as present in natural enzymes or antibodies, has been termed the "discontinuate words" arrangement by R. Schwyzer (*Scheme 3D*).[24] The functional groups responsible for the catalytic activity are located at certain distances from each other along the main polymer chain, i.e. they are "decoded" one-dimensionally. At the same time, they can be brought into spatial relationship as a result of specific folding or binding between main chains. In other words, they are now "encoded" three-dimensionally. In this case, both the sequence
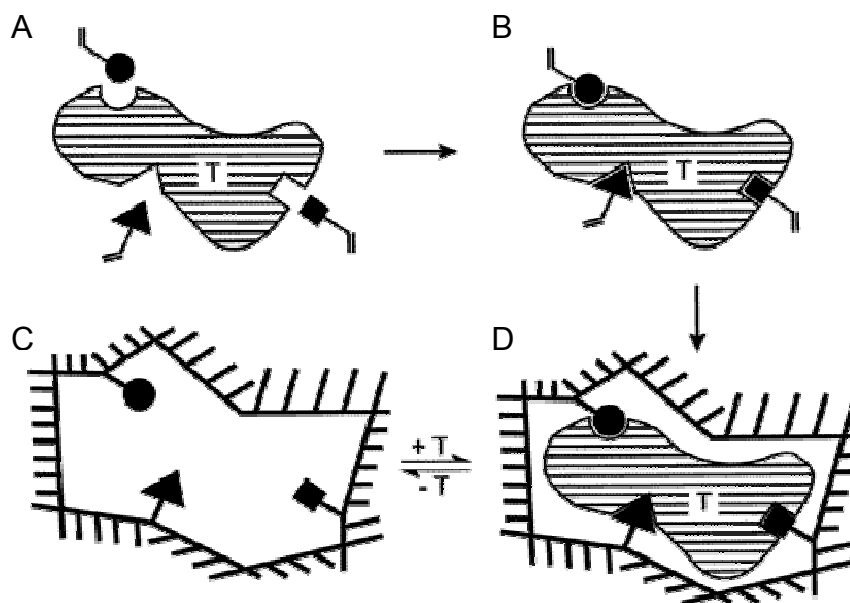
Scheme 4. Schematic representation of the imprinting of specific cavities in a cross-linked polymer by a template (T) with three different binding groups.

of functional groups in the chain and their topological orientation in space are newly defined. Improved polymeric enzyme mimics require the use of this approach and, furthermore, more of the other typical features of enzymes should be considered.

The concept of the molecular imprinting technique approaches the building of a structure similar to *D* in *Scheme 3*. A molecule that acts as a template (T) is brought in contact with functional monomers (*Scheme 4A*). The functional monomers interact with the template molecule through covalent or non-covalent binding (*Scheme 4B*), then a copolymerization is carried out with an excess of cross-linker to yield a highly cross-linked and rigid polymer (*Scheme 4D*). After removal of the template, a cavity containing functional moieties in certain positions and orientations remains in the polymer matrix (*Scheme 4C*). The resultant polymer provides specific binding cavities complementary to the structure of the template molecule used for imprinting (for reviews see [25,26]). In order to prepare an enzyme model by this method, in the preparation of the imprinted polymeric catalysts the functional groups to be introduced should act as binding sites and as catalytically active sites simultaneously.

15

Furthermore it is necessary to create a cavity with a shape that supports the catalysis, e.g. by stabilizing the transition state of the reaction.

This type of polymer was called "enzyme-analogue built polymer" and was suggested quite a long time ago by Wulff.[27,28] It had been demonstrated, using catalytic antibodies generated against stable analogues of the transition state of a reaction, that this concept is rather efficient.[29] Molecularly imprinted polymers have also shown significant enhancement in rate in quite some examples. Since most of the research in catalytic antibodies is concerned with ester hydrolysis, these were also the first reactions investigated in imprinting. The most serious problem to be solved in this case is to find a suitable template array containing both the stable transition state analogue as well as binding sites and catalytically active groups in the desired position.

To solve this problem, one can consider the use of non-covalent interactions with high association constants between template molecules and binding site monomers. This type of interaction is called "stoichiometric non-covalent interaction",[26] e.g. as observed in interactions of amidine groups with carboxylic acids, phosphonic esters or phosphoric diester groups. It is interesting to note that the most active esterase-type species among catalytic

1

2

3
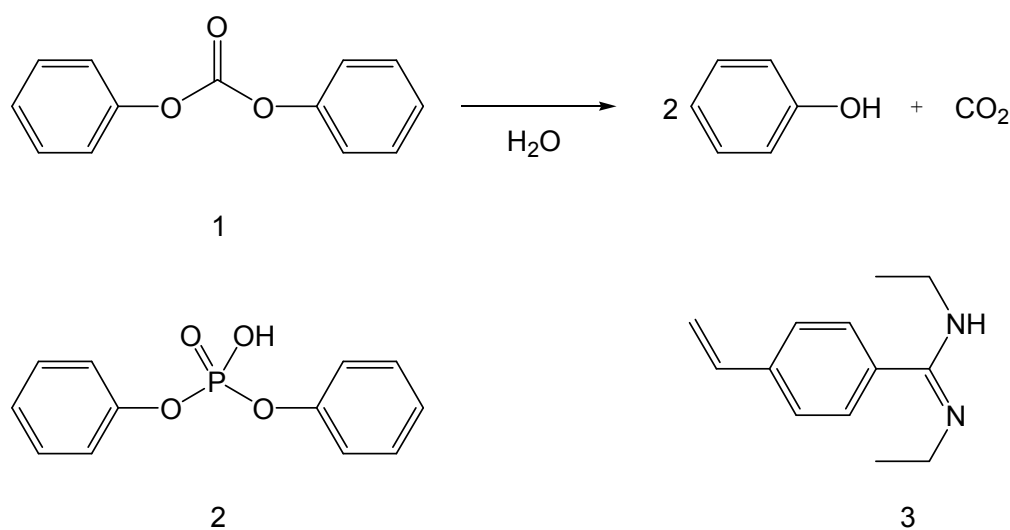
Scheme 5. The hydrolysis of diphenylcarbonate.

antibodies contain a guanidinium group (of the amino acid L-arginine), which plays an important role in catalyzing the basic hydrolysis of the ester.[30]

Inspired by this aspect, the functional monomer *N,N'*-diethyl(4-vinylphenyl)amidine (DEVPA) **3** was developed. It contains an amidinium group that is not only able to bind diphenylphosphate (DPP) **2** as a transition state analogue of the reaction, but also accelerates the catalytic action for the hydrolysis of esters, carbonates and carbamates (*Scheme 5*).[31]

The advantages of this system are a) there is no product inhibition of the catalyst, b) it is easy to modify due to its simplicity, and c) no synthesis is necessary for the starting reagents. These are the reasons why we decided to choose this system as a model reaction for developing a catalytically active imprinted microgel.

By bulk-type polymerization it was possible to obtain a molecularly imprinted polymeric catalyst showing a 588 times rate enhancement in the hydrolysis of diphenylcarbonate (DPC) **1** in comparison with the solution reaction. It was also demonstrated that this catalyst showed Michaelis-Menten kinetics, similar to enzymes.[32] For DPC hydrolysis with the imprinted polymer prepared in bulk, the kinetic constants were $K_m = 5.01$ mM, $V_{max} = 0.0227$ mM min^{-1}, $k_{cat} = 0.0115$ min^{-1}. These terms (e.g. K_m, k_{cat}) are all used in enzymology to indicate how strongly a substrate can bind to the active site of the enzyme and how efficient the enzyme is. In the next chapter these terms will be discussed in somewhat more detail.

Michaelis-Menten kinetics

In most cases, an enzyme converts one substrate into another one (the product). In a graph of product concentration *vs.* time three phases can be identified, as shown in the graph (*Figure 1*). In the very beginning (phase 1), the rate of product formation increases with time. Special
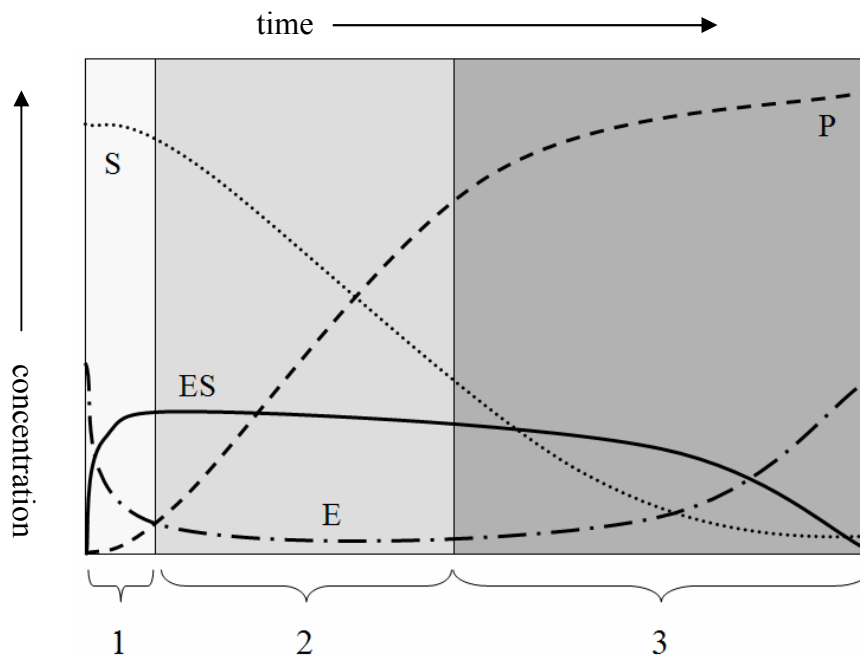
Figure 1. Diagram of three phases of the enzyme reaction. E: enzyme, S: substrate, P: product, ES: enzyme-substrate complex.[85]

techniques are needed to study the early kinetics of enzyme action, since this transient phase usually lasts less than a second. For an extended period of time (phase 2), the product concentration increases linearly with time. At later times (phase 3), the substrate is depleted, so the curve starts to level off. Eventually, the concentration of product reaches a plateau and no longer changes with time. It is difficult to fit a curve of the product concentration as a function over the whole time, even if one uses a simplified model that ignores the transient phase and assumes that the reaction is irreversible. Normal models simply cannot derive an

equation that expresses product concentration as a function of time. To fit these data - called an enzyme progress curve - one needs to use a program that can fit data to a mathematic model defined by differential equations or by an implicit equation. However, rather than fit the whole enzyme progress curve, most analyses of enzyme kinetics fit only the initial velocity of the enzyme reaction as a function of substrate concentration. The velocity of the enzyme reaction is the slope of the linear phase (phase 2), expressed as the amount of product formed per time. If the initial transient phase is very short, one can simply measure the product formed at a distinct time and define the velocity to be the concentration divided by the time interval. This method considers data collected only in the second phase. The terminology describing these phases can be confusing. The second phase is often called the "initial rate", ignoring the short transient phase that precedes it. It is also called the "steady state", because the concentration of enzyme-substrate complex does not change. However, the concentration of product accumulates, so the system is not truly at a steady state until, much later, the concentration of product *truly* does not change over time.
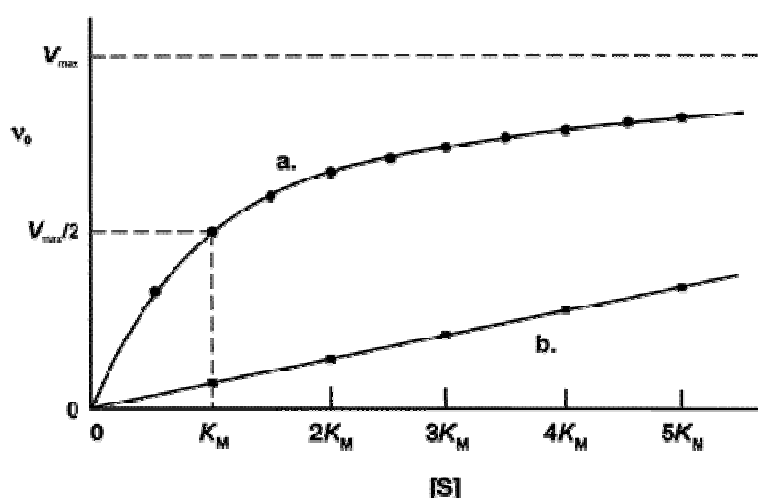
Figure 2. Schematic diagram of (a) Michaelis-Menten kinetics, in comparison with (b) simple catalysis, e.g., by protons.

19

As illustrated in *Figure 2*, by simple catalysis, e.g. by adding protons, the velocity of the reaction, v_o is accelerated in proportion to the amount of added catalyst (protons, *Figure 2b*). However, in the case of enzymes, it shows a somewhat different kinetic behavior, which is unlike that shown by most catalysts used in chemical laboratories or in industry. In *Figure 2a* the effect on v_0 with increasing [S] and constant enzyme concentration is shown.

At relatively low concentrations of substrate, v_0 increases almost linearly with increasing [S]. At higher substrate concentrations, the increase of v_0 becomes smaller and smaller. Finally, a point is reached beyond which there are only vanishingly small increases in v_0 with increasing [S]. This plateau is called the maximum velocity, V_{max}.

The enzyme-substrate complex is the key to the understanding of this kinetic behavior. Inspired by the kinetic pattern shown in *Figure 2a*, in 1903 Victor Henri proposed that an enzyme combines with its substrate molecule to form the ES complex as a necessary step in enzyme catalysis.[33] This idea was expanded into a general theory of enzyme action, particularly by Leonor Michaelis and Maud Menten, in 1913.[34] They postulated that the enzyme first combines reversibly with its substrate to form an enzyme-substrate complex in a relatively fast reversible step:

$$[E] + [S] \quad \underset{k_{-1}}{\overset{k_1}{\rightleftharpoons}} \quad [ES] \tag{1}$$

The ES complex then breaks down in a slower second step to yield first EP and then the free enzyme and the reaction product P:

$$[ES] \quad \rightleftharpoons \quad [EP] \quad \underset{k_{-2}}{\overset{k_2}{\rightleftharpoons}} \quad [E] + [P] \tag{2}$$
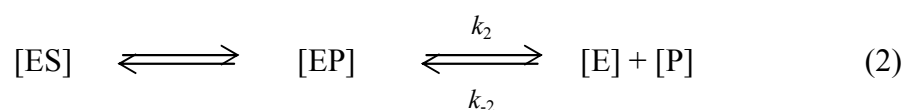
In this model, the second reaction (*Eqn. 2*) is slower and therefore limits the rate of the overall reaction. It follows that the overall rate of the enzyme-catalyzed reaction must be proportional to the concentration of the species that reacts in the second step, i.e. [ES].

At any given time in an enzyme-catalyzed reaction, the enzyme exists in two forms, the unoccupied form [E] and the occupied form [ES]. At low [S], most of the enzyme will be existent as the unoccupied form [E] and then the rate will be proportional to the amount of substrate, as the equilibrium in the *Equation 1* will be pushed towards the formation of more [ES] as [S] is increased. The maximum initial rate of the catalyzed reaction (V_{max}) can be observed if the entire enzyme is present as the ES complex and the concentration of "free" enzyme form [E] is vanishingly small. Under these conditions, the enzyme is completely "saturated" with its substrate, so that further increase in [S] has no effect on the rate. After the complex breaks down to yield the product P, the released enzyme directly makes complexes again to form [ES]. This peculiar behavior of enzymes is called the "saturation effect" or the "saturation kinetics", which is regarded as a distinguishing characteristic of enzyme catalysts and is responsible for the plateau observed in *Figure 2a*.

The most important achievement of Michaelis and Menten is that they proved that the relationship between substrate concentration and enzymatic reaction rate can be expressed quantitatively. Among the three phases in the enzyme-catalyzed reaction, they dealt with the steady-state rate and this type of analysis is referred to as steady-state kinetics. They derived the Michaelis-Menten equation by which the hyperbolic shape of the curve, as shown in *Figure 2a*, can be expressed algebraically. In this equation, the important terms are [S], v_0, V_{max} and a constant called Michaelis-Menten constant, K_m. All of these terms are readily measured experimentally.

$$v_0 = \frac{k_2[E_t][S]}{K_m + [S]} \qquad (3a) \qquad\qquad v_0 = \frac{V_{max}[S]}{K_m + [S]} \qquad (3b)$$

A simple case of the **Michaelis-Menten equation** is shown in *Equation 3*. This is the rate equation for a one-substrate, enzyme-catalyzed reaction. It is the description of the quantitative relationship between the initial velocity v_0, the maximum initial velocity V_{max}, and the initial substrate concentration [S], all related through the Michaelis-Menten constant K_m, which is defined as $(k_2 + k_{-1})/k_1$. [E_t] is the concentration of the total enzyme.

By considering the limiting situations where [S] is very high or very low, one can confirm that this Michaelis-Menten equation can fit the facts, as shown in *Figure 3*.[35] At low [S] and $K_m \gg$ [S], the [S] term in the denominator of the Michaelis-Menten equation (*Equation 3*) becomes insignificant and the equation simplifies to $v_0 = V_{max}[S]/K_m$, with v_0 exhibiting a linear dependence on [S], as observed (*Figure 3a*).
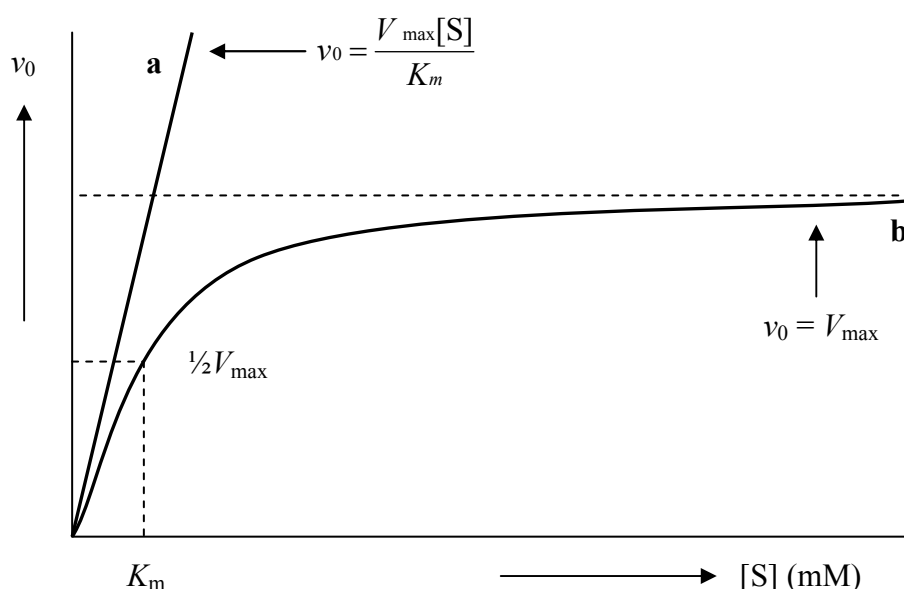
Figure 3. Dependence of the initial velocity on the substrate concentration [S], showing the kinetic parameters that define the limits of the curve at high and low [S].

On the other hand, at high [S], where [S] $\gg K_m$, the K_m term in the denominator of the Michaelis-Menten equation becomes negligible, so the equation simplifies to $v_0 = V_{max}$; this is consistent with the plateau observed at high [S] (*Figure 3b*). The Michaelis-Menten equation is therefore consistent with the observed dependence of v_0 on [S] and with the shape of the curve defined by the terms V_{max}/K_m at low [S] and V_{max} at high [S].

An important numerical relationship is derived from the Michaelis-Menten equation in the special case when v_0 is exactly one-half V_{max} (*Figure 3*). Then:

$$K_m = [S], \text{ when } v_0 = \tfrac{1}{2}V_{max} \tag{4}$$

This represents a very useful, practical definition of K_m. K_m is equivalent to that substrate concentration at which v_0 is one-half V_{max}. Note that K_m has units of molarity.

The Michaelis-Menten constant K_m can vary greatly from enzyme to enzyme and even for different substrates with the same enzyme (*Table 3*). K_m is often used as an indication of the affinity of an enzyme for its substrate.

Table 3. The Michaelis-Menten constant K_m for some enzymes.

Enzyme	Substrate	K_m (mM)
Catalase	H_2O_2	25
Hexokinase (brain)	ATP	0.4
	D-Glucose	0.05
	D-Fructose	1.5
Carbonic anhydrase	HCO_3^-	26
Chymotrypsin	Glycyltyrosinylglycine	108
	N-Benzoyltyrosinamide	2.5

The Michaelis-Menten equation can be algebraically transformed into forms that are more useful for plotting experimental data. One common transformation is derived simply by taking the reciprocal of both sides of the Michaelis-Menten equation to give, after transformation:

$$\frac{1}{v_0} = \frac{K_m}{V_{max}} \frac{1}{[S]} + \frac{1}{V_{max}} \qquad (5)$$

This equation is called the Lineweaver-Burk equation. For enzyme kinetics obeying the Michaelis-Menten relationship, a plot of $1/v_0$ versus $1/[S]$ (a "double-reciprocal" plot) yields a straight line (*Figure 4*).
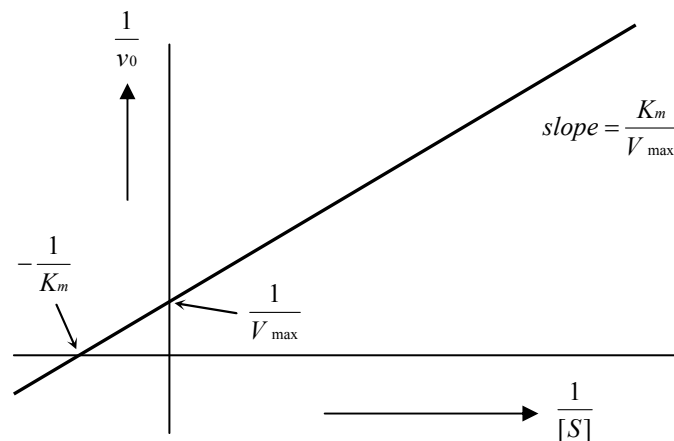
Figure 4. A double-reciprocal, or Lineweaver-Burk, plot.

This line will have a slope of K_m/V_{max}, an intercept of $1/V_{max}$ on the $1/v_0$ axis and an intercept of $-1/K_m$ on the $1/[S]$ axis. The double-reciprocal presentation, also called a Lineweaver-Burk plot, has the great advantage of allowing more accurate determination of V_{max}, which can only be approximated from a simple plot of v_0 versus [S] (see *Figure 3*).

V_{max} is also different from one enzyme to another one. As described previously, if an enzyme reacts by the two-step Michaelis-Menten mechanism, V_{max} is equivalent to $k_2[E_t]$, when k_2 is the rate-determining step and $[E_t]$ is the total concentration of enzyme. However, the number of reaction steps and the identity of the rate-limiting steps can vary from enzyme to enzyme. For example, consider the quite common situation where product releases, EP → E + P, is rate limiting. In this case, most of the enzyme is in the EP form at saturation, and $V_{max} = k_3[E_t]$.

$$E + S \underset{k_{-1}}{\overset{k_1}{\rightleftarrows}} ES \underset{k_{-2}}{\overset{k_2}{\rightleftarrows}} EP \overset{k_3}{\longrightarrow} E + P \tag{6}$$
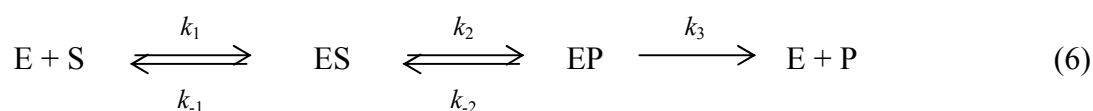
At this point, it is useful to introduce a more general rate constant, k_{cat}, to describe the limiting rate of any enzyme-catalyzed reaction at saturated conditions. If there are several steps in the enzyme-catalyzed reaction and one of them is clearly rate-limiting, k_{cat} is equivalent to the rate constant for that limiting step. For the Michaelis-Menten reaction (*Equation 3*), $k_{cat} = k_2$. For the reaction of the *Equation 6*, $k_{cat} = k_3$ if this is the rate determining step. When several steps are partially rate limiting, k_{cat} becomes a complex function of several of the rate constants that define each individual reaction step. In the Michaelis-Menten equation, $k_{cat} = V_{max} / [E_t]$, and *Equation 3* becomes,

$$v_0 = \frac{k_{cat}[E_t][S]}{K_m + [S]} \tag{7}$$

The constant k_{cat} is a first-order rate constant with units of reciprocal time and is called the **turnover number**. It is equivalent to the number of substrate molecules converted to product in a given unit of time on a single enzyme molecule when the enzyme is saturated with substrate. The turnover numbers of several enzymes are given in *Table 4*.

Table 4. Turnover numbers (k_{cat}) of some enzymes.

Enzyme	Substrate	k_{cat} (s⁻¹)
Catalase	H_2O_2	40,000,000
Carbonic anhydrase	HCO_3^-	400,000
Acetylcholinesterase	Acetylcholine	140,000
β-Lactamase	Benzylpenicillin	2,000
Fumarase	Fumarate	800
RecA protein (ATPase)	ATP	0.4

The kinetic parameters k_{cat} and K_m are generally useful for the study and comparison of different enzymes, regardless of whether their reaction mechanisms are simple or complicated. Each enzyme has optimum values of k_{cat} and K_m that reflect the cellular environment, the concentration of substrate normally encountered in vivo by the enzyme and the chemistry of the reaction being catalyzed.

Comparison of the catalytic efficiency of different enzymes requires the selection of a suitable parameter. The constant k_{cat} is not entirely satisfactory. Two enzymes catalyzing different reactions may have the same k_{cat} (turnover number), yet the rates of the uncatalyzed reactions may be different and thus the rate enhancement brought about by the enzymes may differ greatly. Also, k_{cat}, reflects the properties of an enzyme when it is saturated with substrate and is less useful at low [S].

The Michaelis-Menten constant K_m is itself also unsatisfactory. As shown by *Equation 4*, K_m must have some relationship to the normal [S]. An enzyme that acts on a substrate present at a very low concentration in the cell will tend to have lower K_m than an enzyme that acts on a substrate that is normally abundant.

The most useful parameter for a discussion of catalytic efficiency is one that includes both k_{cat}

and K_m. When [S] << K_m, *Equation 7* is reduced to the form

$$v_0 = \frac{k_{cat}}{K_m}[E_t][S] \qquad\qquad (8)$$

In this case v_o is dependent on the concentration of the two reactants, E_t and S, and, therefore,

this is a second-order rate law and the constant k_{cat}/K_m is a second-order rate constant. The

factor k_{cat}/K_m is generally the best kinetic parameter to use in comparisons of catalytic

efficiency. There is an upper limit to k_{cat}/K_m, imposed by the rate at which E and S can diffuse

together in an aqueous solution. This diffusion-controlled limit is 10^8 to 10^9 $s^{-1}M^{-1}$ and many

enzymes have a value of k_{cat}/K_m near this range (*Table 5*).

Table 5. Enzymes for which k_{cat}/K_m is close to the diffusion-controlled limit (10^8 to 10^9 $M^{-1}s^{-1}$).[36]

Enzyme	Substrate	k_{cat} (s^{-1})	K_m (M)	k_{cat}/K_m (s^{-1} M^{-1})
Acetylcholinesterase	Acetylcholine	1.4×10^4	9×10^{-5}	1.6×10^8
Carbonic anhydrase	CO_2	1×10^6	1.2×10^{-2}	8.3×10^7
	HCO_3^-	4×10^5	2.6×10^{-2}	1.5×10^7
Catalase	H_2O_2	4×10^7	1.1	4×10^7
Crotonase	Crotonyl-CoA	5.7×10^3	2×10^{-5}	2.8×10^8
Fumarase	Fumarate	8×10^2	5×10^{-6}	1.6×10^8
	Malate	9×10^2	2.5×10^{-5}	3.6×10^7
β-Lactamase	Benzylpenicillin	2.0×10^3	2×10^{-5}	1×10^8

Optimization of the polymer structure

The catalytic efficiency of an imprinted polymer can be affected by several factors, such as temperature, pH and chemical nature of the catalytic groups. The morphological status of the polymer structure is another factor. Thus, several attempts to optimize the polymer structure were carried out using a simple model reaction, the hydrolysis of diphenylcarbonate (DPC).

In the optimization procedure of the polymeric structure, two contradictory properties must be controlled: flexibility and rigidity. Furthermore, in case of macroreticular polymers, a high porosity is needed to guarantee ample surface area for good accessibility to as many cavities as possible. Flexibility in the polymer structure is necessary to facilitate release from and uptake into the specific cavities of templates and target molecules. On the other hand, sufficient rigidity is also essential to preserve the shape of the cavities for effective activity and selectivity. These two properties should be carefully adjusted each time to find a point of optimal performance.

Usually, with different degree of cross-linking during polymerization, these two properties
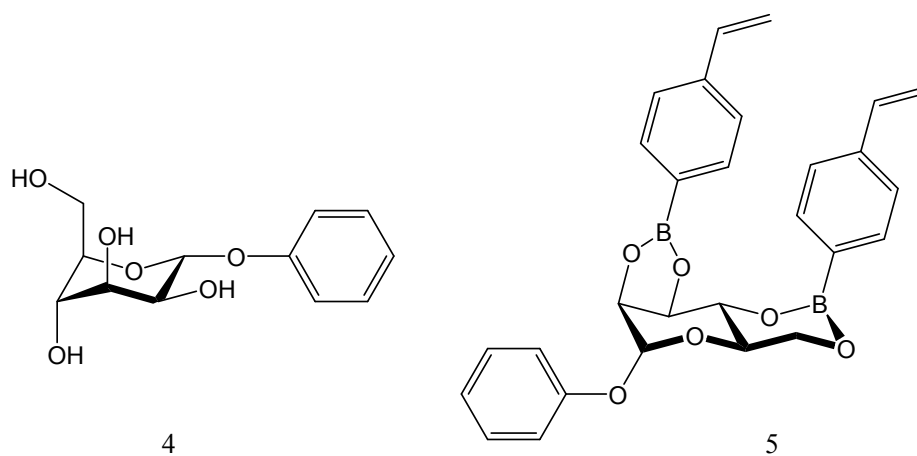
Scheme 6. Compounds for the selective recognition experiments with imprinted polymers.

can be controlled. Systematic investigations on the influence of the polymer structure were performed in early studies about the selective recognition of the sugar derivatives, phenyl-α-D-mannopyranoside **4** with imprinted polymers.[37,38] Two molecules of 4-vinylbenzeneboronic acid were bound to **4**, which acts as a template molecule, by covalent diester bonds to yield the polymerizable monomer **5** (*Scheme 6*).

For comparison this monomer was copolymerized with varying amounts of different kinds of cross-linker; namely ethylene dimethacrylate (EDMA), tetramethylene dimethacrylate, and divinylbenzene.[39] After splitting off the template molecule by the addition of water or methanol, the polymer was equilibrated in a batch procedure with a solution of the racemate of the template **4**. The enrichment of the antipodes on the polymer and in solution was determined and the separation factor α, i.e. the ratio the distribution coefficient of D- and L-compounds between polymer and solution, was calculated.

According to these results, it was found that below a certain amount of cross-linking (around 10%), no selectivity could be obtained because the cavities established in the polymer structure were not sufficiently stabilized. When the content of cross-linker was increased above 10%, however, selectivity is observed that increases steadily up to around 50% of cross-linker (*Figure 5*).

Remarkably, a strong increase in selectivity was observed between 50 and 66% crosslinker, especially with EDMA. The use of divinylbenzene as cross-linker led to lower selectivity, but this cross-linking agent has the advantage of higher chemical stability (bonds are not hydrolyzable) and less interaction with functional groups.[39]

These results have guided most research groups working in molecular imprinting field to use EDMA as a cross-linker at a concentration of 70 ~ 90% to obtain an effective imprinted polymer.

It has been discussed whether a similar trend with respect to the cross-linking degree is expected in the use of molecularly imprinted polymers for catalysis. For that purpose, a series of molecularly imprinted polymers with a low amount of crosslinker and DPP **2** as a template molecule was prepared (see *Scheme 5*). The results will be discussed later in the main section of this thesis.
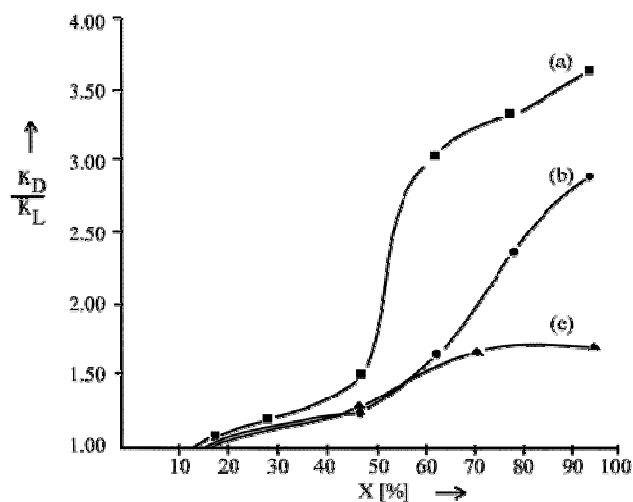
Figure 5. Selectivity dependence of imprinted polymers for racemic resolution of the racemate and amount (X) of the cross-linking agent. Crosslinker: (a) ethylene dimethacrylate, (b) tetramethylene dimethacrylate, (c) divinylbenzene.

The influence of the type of dispersion on the catalytic activity in DPC hydrolysis

In earlier investigations on the hydrolysis of DPC, several types of imprinted polymers were prepared and compared. These were irregular broken polymer particles from bulk polymerization, spherical beads via suspension polymerization and gel-type minigels via emulsion polymerization (*Figure 6*).[32,42]

Figure 6. Several types of catalytically active imprinted polymers for DPC hydrolysis.
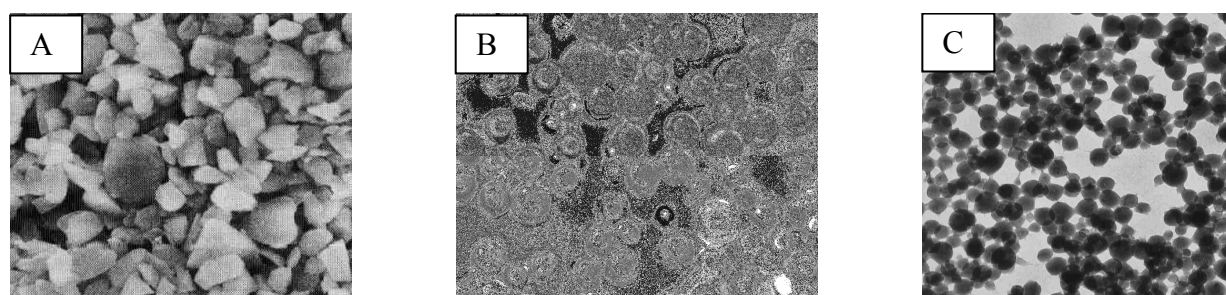
	Appearance	*Diameter size*	*Solubility*	*Polymerization Method*
A	Irregularly broken particles	$5 \sim 500$ μm	insoluble	Bulk polymerization
B	Spherical beads	$2 \sim 500$ μm	insoluble	Suspension polymerization
C	Spherical beads	$100 \sim 500$ nm	insoluble	Emulsion polymerization

For the bulk-type imprinted polymers, in most of cases macroporous polymer structures have been used for this purpose. To obtain macroporous polymers the polymerization is carried out with a relatively high content of cross-linking agent in the presence of inert solvents such as acetonitrile, toluene, etc. During the polymerization phase separation between insoluble polymer regions and the solvents, also known as porogens, takes place and, after removal of the porogen and drying, a permanent pore structure remains. The relatively high inner surface

31

area (50~600 m^2/g) and large pores (about 10~60 nm) ensure that the specific microcavities formed by the imprinting process are readily accessible and that small molecules can easily diffuse inside the pores.

However, there are still some drawbacks in preparing imprinted polymers by bulk polymerization. Usually the polymerization is carried out in ampoules to yield monoliths, which have to be crushed or milled and then sieved to obtain particles of the desired size. The preparation of these particles is a time-consuming and energy-wasteful process, which is also accompanied by large losses of materials. Furthermore, the resulting materials usually consist of irregular particles with a broad distribution range of particle sizes (5~500 μm) (see *Figure 2A*). Thus, the properties of the particles obtained by bulk polymerization may not be ideal with regard to flow, reproducibility and scale-up procedures.

On the other hand, suspension polymerization should be a better method to provide relatively uniform spherical beads that are far more suitable for the purpose (see *Figure 2B*). Although some research groups in the field have already considered this method for preparing molecularly imprinted materials,[40,41] there are problems. In many cases, relatively weak interactions between the template molecules and the binding site monomers are used. Under these circumstances simple suspension polymerization cannot be applied. Usual non-covalent interactions will be broken by the presence of water from the aqueous phase in the suspension polymerization. For this reason rather complicated inverse suspension polymerization has been used.

Another possibility is to use stronger interactions, *e.g.*, covalent bonds. However, in this case it is difficult to split off the imprint molecules from the binding monomers to make proper cavities.

To solve this problem, "stoichiometric non-covalent interactions" were suggested by G. Wulff *et al.*[26] The new DEVPA-functional monomer (**3** in *Scheme 5*) allows the use of well-

established suspension polymerization techniques, since the interaction between amidine and phosphonate, phosphate or carboxylate is very stable.

Classical aqueous suspension polymerization techniques proceeded smoothly to give beads of 8-~375 μm diameter, depending on the polymerization conditions used (e.g. mean diameter: 31.3 μm; index of polydispersity: 1.16; inner surface area: 277 m^2/g; mean pore radius: 6.3 nm; see also *Table 6*).[32] The DEVPA-DPP complex does not appear in the aqueous phase in the course of polymerization and the presence of this complex in the polymer matrix was confirmed by FT-IR and nitrogen elemental analysis. The free, imprinted active sites were obtained by removal of the template.

Table 6. Kinetic parameters for DPC hydrolysis with imprinted beads.[32,42]

Sample [a]	porogen	water phase composition	particle size (index of polydispersity)[43]	specific surface area (m^2/g)	hydrolysis of DPC relative reaction rate	
					k_{impr}/k_{sol}	k_{impr}/k_{stat}
DP1	acetonitrile	-	45~125 μm	232	588	7.8
SP2 [b]	cyclohexanol-dodecanol (9:1)	20% NaCl 8% starch	375 μm (1.16)	288	168	24
SP3	cyclohexanol-dodecanol (9:1)	2% PVA 1% PVP	31.3 μm (1.23)	234	168 [179] [c]	23
M1	-	2% PVA 1% PVP	149 nm	31	71	25
M2	-	2% PVA 1% PVP	230 nm	20	54	17

[a] The composition of the monomer mixture of all samples for the preparation of the imprinted polymers consisted of 79.6 wt % of EDMA, 10.4 wt % MMA, and 9.0 wt % of DEVPA-DPP-complex, and 1 wt % of azobis(isobutyronitrile), diluted by the same weight of the porogen, acetonitrile. In the control polymer the DPP-template was omitted.
[b] DP1 was prepared by bulk polymerization, whereas SP2 and SP3 by suspension polymerization; M1 and M2 by emulsion polymerization.
[c] In brackets the corresponding values for bulk polymers with the same porogen are given.

The imprinted beads displayed the same catalytic activity as bulk-type imprinted polymers if they were prepared with the same porogen, *e.g.*, cyclohexanol-n-dodecanol. Although the rate

constants of DPC hydrolysis are apparently higher for polymers prepared on the basis of acetonitrile as porogen, it is impossible to use it in suspension polymerization due to the miscibility of acetonitrile with water. As shown in *Table 6*, the enhancement with respect to non-imprinted polymers containing statistically distributed amidines is 7.8 for bulk polymers and up to 24 for imprinted polymer beads. Thus, the beads show a much higher selectivity than the bulk polymers.

Far smaller gel-type cross-linked particles could be obtained by an emulsion polymerization method first described by K. Landfester *et al.*[44] In this method, no porogen was used and, therefore, non-porous particles of about 100~500 nm in diameter were obtained, which are called minigels (see *Figure 2C*). It was found that the surface area of imprinted minigels is smaller ($15 \sim 35$ m^2/g) than that of particles prepared by bulk polymerization or suspension polymerization. As there are no mesoporous structures in these particles, only the outer surface is accessible. The imprinted minigels are generally insoluble in all solvents, but in some cases they are able to build up a colloidal form. Compared with the kinetic results of imprinted polymer beads, these minigels showed relatively low catalytic activity in the hydrolysis of DPC, with increases of about a half to one third. However, when the available surface is taken into account the situation is different. The surface area is only around one tenth of that of macroporous polymers or imprinted beads, thus the k_{impr}/k_{sol} value seems quite significant. Moreover, comparing to the selectivity (k_{impr}/k_{stat}), minigels show almost of the same order of magnitude as imprinted beads.

It might be that the better selectivity of imprinted polymer beads or minigels compared to imprinted bulk polymers may be due to better mass transfer properties. This idea encouraged us to prepare even smaller catalytically active particles for the DPC hydrolysis, which might also be soluble, as enzymes are.

Microgel

Insolubility is generally regarded as a characteristic property of cross-linked polymers. However, in the 1930s, Staudinger obtained soluble products during the polymerization of divinylbenzene (DVB) in presence of a solvent.[45] He could obtain crosslinked soluble polymers, named microgels, after heating a very dilute solution of DVB for several days to 100°C. From then on, a microgel was regarded as a fourth structural class of macromolecules. So to linear, branched, and cross-linked polymers, the intramolecularly crosslinked polymers were added (*Scheme 7*).
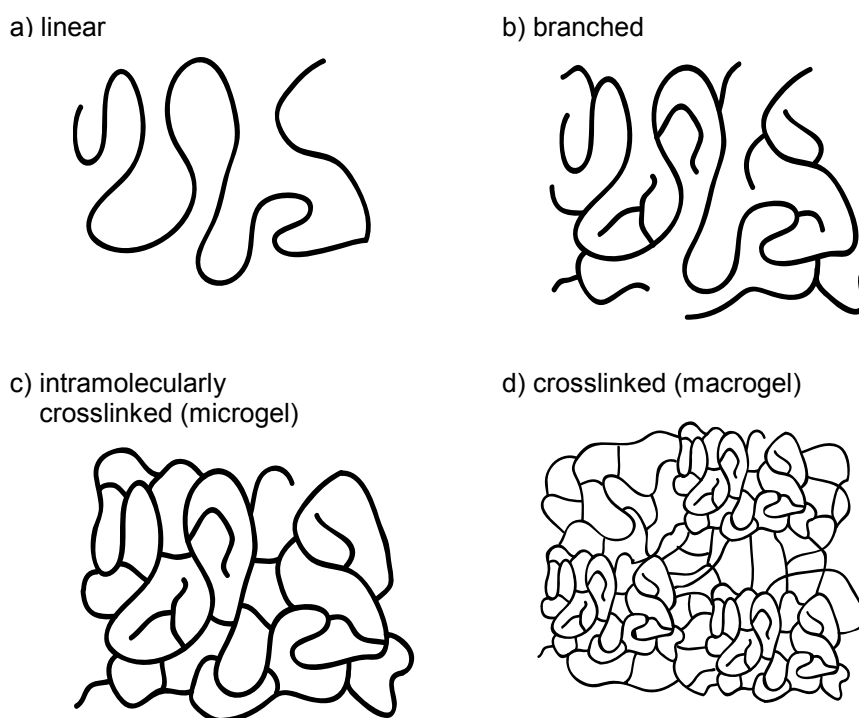
Scheme 7. Schematic representation of different types of macromolecules.

The applications of soluble, crosslinked microgels expanded into several directions, both for practical as well as academic applications. For example, they have been utilized as additives for coating[46] and printing[47] materials, as templates for syntheses,[48] as carriers for the delivery

of drugs,[49] catalysts,[50] and oligonucleotides[51] and as support materials for solid-phase synthesis.[52] Recently, there has been a growing interest in the synthesis and application of stimuli-sensitive microgels (i.e. temperature, pH).[53]

The term "microgel" was proposed by W. O. Baker[54] He defined microgels as intramolecularly crosslinked polymer particles possessing a size comparable to the statistical dimensions of non-crosslinked macromolecules (10^1~10^2 nm), which can exist as stable solutions in appropriate solvents. More simply, it is defined as a network of macromolecular dimension, thus also referred as micronetwork by IUPAC.[55,56] As this definition implies, the term "microgel" is for very small particles. They are usually reported to have a size ranging from a few to hundreds of nanometers; thus, the name "microgel" could be somehow misleading. In recent years, the term "microgel" has been replaced by "nanogel", because it directly indicates the size range of the particles.[57,58,59]

It was Carothers who first indicated that gelation is the result of an intermolecular linking process of monomeric molecules into a three-dimensional network of infinitely large size.[60] 10 years later, Flory defined that the term "infinitely large size" refers to a size of molecules having dimensions of an order of magnitude approaching that of the container vessel. However, every container vessel has a finite volume. Thus, such molecules are finite in size. However, in comparison to ordinary molecules, they may be considered infinitely large.[61] This implies that by decreasing the dimensions of the container vessel, the size of the macrogel formed can be minimized, even to a nanometer sized one.

Since microgels are intramolecularly crosslinked macromolecules of colloidal dimensions, it is necessary, for their synthesis, to control the size of the growing cross-linked molecules. This can be achieved by carrying out polymerization and crosslinking in a restricted volume, *i.e.* in a micelle or in a polymer coil. Thus, two general methods for microgel synthesis are available: a) emulsion polymerization and b) solution polymerization.

In emulsion polymerization, each micelle in an emulsion behaves like a separate micro-continuous reactor that contains all the components, such as monomers and radicals from the aqueous phase. Thus, analogous to the latex particles in emulsion polymerization, microgels formed by emulsion polymerization are distributed in the whole available volume. On the other side, a different type of particles is obtained by solution polymerization. Since an increase of dilution during crosslinking decreases the probability of the intermolecular binding, in an exceedingly diluted solution the growing polymer chains become intramolecularly crosslinked and their structure approaches that of the microgels formed within the micelles. Whereas the microgel particles, synthesized by emulsion polymerization with a sufficient amount of crosslinker, behave like a macroscopic globular gel and have a similar internal structure, microgels formed in solution may have various shapes depending on the relative contributions of intra- and intermolecular cross-linking. More efficient ways to synthesize microgels than with usual emulsion polymerization methods have been developed recently, which are called microemulsion,[62,63] and miniemulsion polymerizations.[64] There remain some drawbacks with these techniques, such as contamination of the microgel particles with the emulsifier and the relatively large particle size of the microgels. However, D. Zou and co-workers reported emulsifier-free emulsion polymerization in co-polymerizations with methacrylates and divinyl monomers.[65,66]

W. Funke *et al*. elucidated the process of the crosslinking copolymerization in microgels in detail and obtained various types of structures, from inhomogeneous gels to microgel particles.[67] He indicated that five different structural states may be distinguished when the degree of dilution and the amount of the crosslinking agent is varied (*Scheme 8*).

According to his explanations, three transitions states can be distinguished in the whole course of reaction. They are 1) macrophase separation, 2) solid-liquid transition and 3) macrogel-microgel transition. The "macrophase separation" is the transition process from
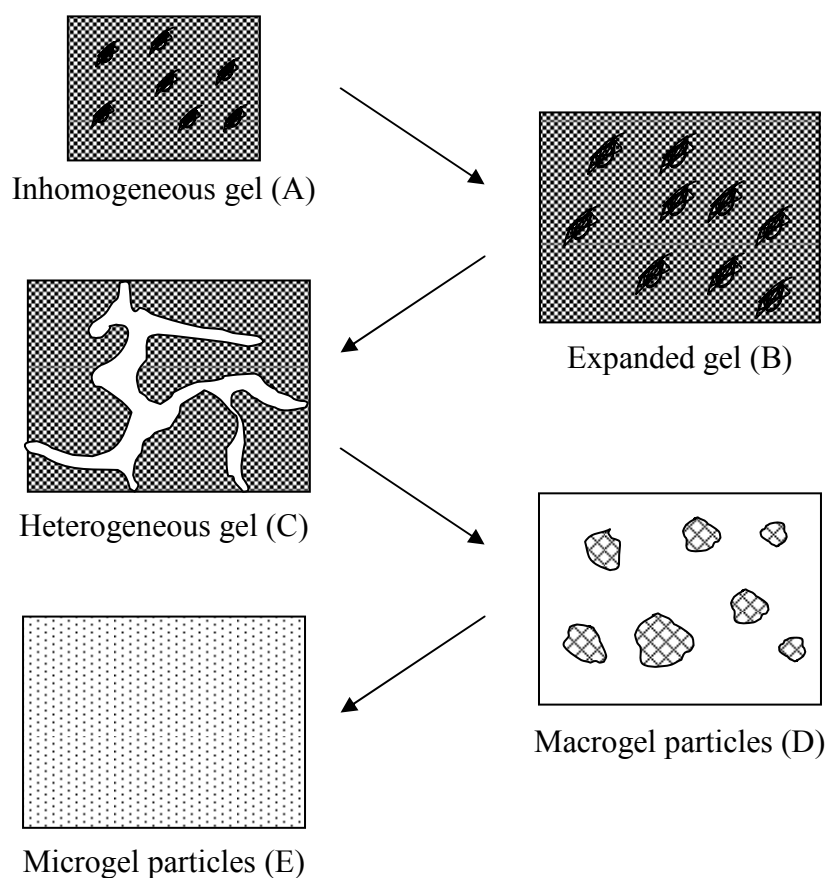
Scheme 8. Formation of various structures in radical crosslinking copolymerization of monovinyl-divinyl monomers with or without using a solvent (diluent).

inhomogeneous swollen gels (B) to heterogeneous gels (C), which takes place if the amount of the crosslinker is increased while that of solvent remains constant. This is due to the formation of a highly rigid polymer network that cannot absorb all the solvent molecules present in the reaction mixture. At this point, if the amount of solvent is increased, the whole system reaches a critical point, at which the system becomes discontinuous because the quantity of monomer is insufficient and the growing chains are not able to occupy the whole system volume available. This is the "solid-liquid transition", which results in a dispersion of macrogel particles (D) in the whole solvent domain. The next and final transition, which attracts considerable attention from us, is the "macrogel-microgel transition", which is observed when the amount of solvent is further increased to make the size of the gel particles

as small as ordinary macromolecules (E). This phenomenon can be explained by the probability of intermolecular binding of primary particles being dramatically reduced by infinite dilution. This is why microgelation in solution polymerization is regarded as an intermediate state of macrogelation.

At the very beginning stage of polymerization, primary microgel particles must be separate and possess a linear polymer backbone that have coiled up and crosslinked internally. As polymerization proceeds further, these primary particles combine to give covalently linked aggregates, finally leading to macrogelation.[68] However, the formation of macroscopic networks and premature gelation may be avoided when a suitable monomer-solvent system is selected.[69,70] The solvating power of the solvent strongly influences the onset of macrogelation and delayed gelation in a good solvent as was observed by A. Matsumoto in several polymerization systems.[71]
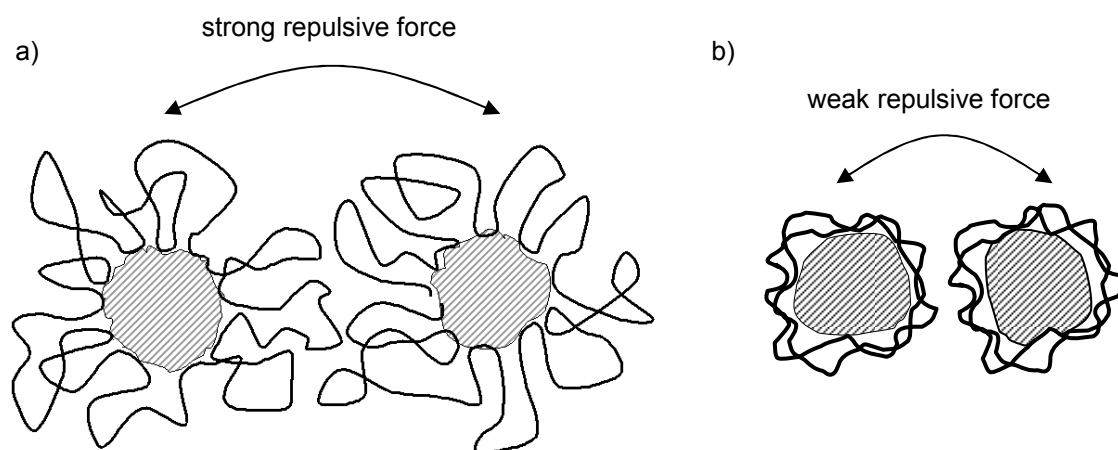
Scheme 9. Auto-steric stabilization effect between two illustrative particles in a) good solvent and b) poor solvent.

N. B. Graham et al. indicated that macrogelation can be avoided even at high monomer concentration, with almost complete conversion of monomers, in the presence of thermodynamically good solvents.[72,73] In this case, in the initial stage of the polymerization

there are some solvated short polymer chains on the surface of the particles. These chains act as barriers, providing repulsive forces between microparticles in solution that prevent further intermolecular reaction and, thus, form soluble microgels. This phenomenon is called the auto-steric stabilization effect.[74,75] As shown in *Scheme 9*, in a good solvent, polymer primary chains can be more effectively swollen, leading to strong repulsive forces between individual particles. Therefore the particles' growth will be restricted to a certain degree.

On the other hand, however, if the particles are growing in a poor solvent, the polymer chains around the particles will be shrunken (*Scheme 9b*), giving the opportunity for individual particles to contact with each other. This phenomenon will lead to more intermolecular binding to make bigger particles or even macrogelation.

This is the reason why the type of the solvent for solution polymerization should be carefully chosen. With the right choice of the solvent, even at relatively high concentration of monomers, the resulting polymer particles will remain soluble.

The monomer concentration should always be lower than the critical gelation concentration (CGC, critical monomer concentration, C_m) to avoid macrogelation. As a definition, the critical monomer concentration is the highest monomer concentration at which the microgels can be formed as a stable solution. To prepare soluble polymerized particles it is very important to know the value of C_m. This concentration should always be determined experimentally, so that the monomer concentration can be set below the C_m value. Otherwise, the resultant polymer would undergo macrogelation and non-soluble polymers would be formed.

It is known that the structure of the microgel particles is dependent on many factors, such as the crosslinker ratio, the polymerization temperature, the extent of the reaction, the nature of the crosslinker, the amount of initiator and the nature of the polymerization solvent. In the

same manner, C_m is strongly affected by these factors, especially by the kind of the polymerization solvent.

The nature of the solvent can be rationalized conveniently in terms of the solubility parameter δ. This value can be determined for both polymers and solvents.[76] As a first approximation, and in the absence of strong interactions such as hydrogen bonding (Hildebrand solubility parameter), good solubility can only be expected if the difference of $\delta_{solvent}$ and $\delta_{polymer}$ is less than 3.5~4.0. A few typical examples of δ values are shown in *Table 7*. Polymers that can be dissolved in these solvents are shown in the next column.

Table 7. Typical values of the solubility parameter δ for some common solvents.[77]

Solvent	$\delta[(J/cm^3)^{1/2}]$	Polymer class [a]	Solvent	$\delta[(J/cm^3)^{1/2}]$	Polymer class
decafluorobutane	10.6	-	methyl ethyl ketone	19.0	B C
neopentane	12.9	A	Acetone	20.3	B C
n-hexane	14.9	A	1,4-dioxane	20.5	B C
diethyl ether	15.1	-	dimethylformamide	24.8	B C (D)[b]
cyclohexane	16.8	A	*m*-cresol	27.2	B C D
carbon tetrachloride	17.6	A B	formic acid	27.6	B D
benzene	18.8	A B	Methanol	29.7	-
chloroform	19.0	A B C	Water	47.9	-

[a] Polymer classes that can be dissolved in this solvent. A: poly(isobutylene) δ=16.2, B: poly(methyl methacrylate) δ=18.6, C: poly(vinyl acetate) δ=19.2, D: poly(hexamethylene adipamide) δ=27.8.
[b] soluble only at high temperature.

This shows that the choice of the proper polymerization solvent is the most important factor for the preparing microgels via solution polymerization. In any case, the determination of C_m is also necessary since the δ values of the copolymers are not known exactly.

There are some advantages in using nanogels as catalytically active imprinted polymers. First of all, they are small, even comparable to the size of natural enzymes. The range of the particles size of bulk-type imprinted polymers after being crushed and sieved is from several tens to several hundreds of micrometers. From the point of view of enzyme mimicking, this size range is incomparably huge when matched against that of natural enzymes, whose radius of gyration is around 5~10 nm. However, the imprinted nanogels should have a size of around 10~20 nm, which is rather similar to that of natural enzymes. Due to their small size, the imprinted nanogels should exhibit better mass transfer properties in comparison to macroporous imprinted polymers, as described above.

Secondly, the nanogels are soluble. Soluble enzyme mimics can be characterized using standard techniques for the investigation of soluble macromolecules, such as GPC, NMR and membrane osmometry. Such investigations are not available with insoluble imprinted polymers.

Finally, they are still as stable as the insoluble imprinted polymers. Whereas natural enzymes or antibodies degrade under harsh conditions, such as high temperature, chemically aggressive media and high and low pH, imprinted polymers show better behavior in most cases. They have both good mechanical and thermal stability.

The first experiments with a catalytically active imprinted microgel were performed by M. Resmini et al.,[78] who reported that they used polymerisable amino acid derivatives, derived from tyrosine and arginine, to produce a stable complex with a phosphate template molecule. This system is very similar to a system that has been used before with macroporous polymers.[32] The results showed k_{cat}/k_{uncat} value of 530 by considering just 1% of the estimated arginine residues present to be catalytically active.

In this thesis, catalytically active imprinted nanogels for the DPC hydrolysis are reported. For the first time, direct proof of the size and shape of the individual nanogel particles is

presented, obtained via gel permeation chromatography and microscopic methods. The newly prepared nanogels show significant catalytic activity for the hydrolysis of DPC and, after optimization of the polymeric structure, display even much better performance. In the best result, the rate constant is about 290 times higher than the reaction in buffer solution and an 18.5 fold enhancement in selectivity is obtained.

Results and Discussion

A. The methodology of the preparation and the characterization of nanogels

Determination of the critical monomer concentration (C_m)

It has been reported to date that there are several methods available for preparing nanogel particles. These are emulsion polymerization, precipitation polymerization and solution polymerization. Unlike the other methods, solution polymerization can provide resultant particles that are still soluble in the polymerization solvent even after the completion of the reaction. This is a very distinctive feature of solution polymerization and is the reason why this method was selected to prepare catalytically active nanogels.

As discussed earlier, in order to obtain soluble polymer particles, despite a high degree of cross-linking, it is very important to choose the right polymerization solvent as well as the right monomer concentration.

The critical monomer concentration C_m is defined as the highest monomer concentration at which the nanogels can be formed as a stable solution. C_m should always be determined experimentally for the experimental conditions to be used so that the monomer concentration can be set below C_m. Otherwise the resultant polymer would undergo macrogelation and non-soluble polymers would be formed.

With the polymerization condition of 8:2 wt% of EDMA and MMA, with 3 wt% of AIBN as an initiator and polymerized at 80°C for 4 days, it was found that the C_m values were 2%, 1.5% and 1.5% in cyclopentanone (CyP), cyclohexanone (CyH), and *N,N'*-dimethylformamide (DMF), respectively. These solvents were employed because their δ values are similar to that of methacrylate-based polymers (21.3, 20.3 and 24.8 for CyP, CyH

and DMF, respectively; 18.6 for poly(methyl methacrylate). Unit: $(J/cm^3)^{1/2}$). The resultant polymers were characterized using GPC (*Table 8*).

Table 8. Highly crosslinked microgels by radical polymerization in different solvents. [a]

Monomer conc. wt.-%	Product	Conversion %	M_w [b]	M_n [c]	M_w/M_n
cyclopentanone					
0.5	Microgel	70.1	5.91×10^3	2.09×10^3	2.83
1.0	Microgel	92.2	3.63×10^4	5.21×10^3	6.97
1.5	Microgel	>99.9	1.20×10^5	5.86×10^3	20.48
- 2.0 -	Microgel	>99.9	9.31×10^5	9.76×10^3	95.33
2.5	microgel [d]	>99.9	-	-	-
3.0	microgel [d]	>99.9	-	-	-
4.0	Macrogel	-	-	-	-
5.0	Macrogel	-	-	-	-
cyclohexanone					
0.5	Microgel	>99.9	8.46×10^3	3.01×10^3	2.81
1.0	Microgel	>99.9	4.75×10^4	4.51×10^3	10.52
- 1.5 -	Microgel	>99.9	4.15×10^5	7.67×10^3	54.10
2.0	microgel [d]	>99.9	-	-	-
2.5	Macrogel	-	-	-	-
3.0	Macrogel	-	-	-	-
4.0	Macrogel	-	-	-	-
5.0	Macrogel	-	-	-	-
N,N-dimethylformamide					
0.5	Microgel	62.7	- [e]	-	-
1.0	Microgel	74.0	7.91×10^4	1.59×10^4	4.98
- 1.5 -	Microgel	86.9	3.62×10^5	1.45×10^4	24.98
2.0	microgel [d]	97.6	-	-	-
2.5	microgel [d]	98.8	-	-	-
3.0	Macrogel	-	-	-	-
4.0	Macrogel	-	-	-	-
5.0	Macrogel	-	-	-	-

[a] Polymerization condition: EGDMA:MMA=8:2 (wt.-%), 3% AIBN, 80°C, 4 days.
[b] Weight-averaged apparent molecular weight from GPC.
[c] Number-averaged apparent molecular weight from GPC.
[d] Partially soluble after isolation.
[e] No precipitation was observed when isolated.

It is worth noting that the value of C_m is sensitive to several factors, such as crosslinker ratio, polymerization temperature, length of reaction time, nature of crosslinker, amount of initiator and the nature of the polymerization solvent, etc. For example, in previous work by A. Biffis *et al.*,[79] whose investigations were focused on the synthesis of imprinted nanogels for

selective molecular recognition, the determination of C_m was carried out under the polymerization condition of 7:3 -wt% of EDMA and MMA, while the other experimental conditions were exactly as for the nanogels shown in *Table 8*. Under these conditions, it turned out that the C_m values were 4%, 3% and 3% for CyP, CyH and DMF, respectively. *Figure 7* shows the dependence of the weight-averaged molecular weight of the nanogels on the initial monomer concentration, as shown in *Table 8*.
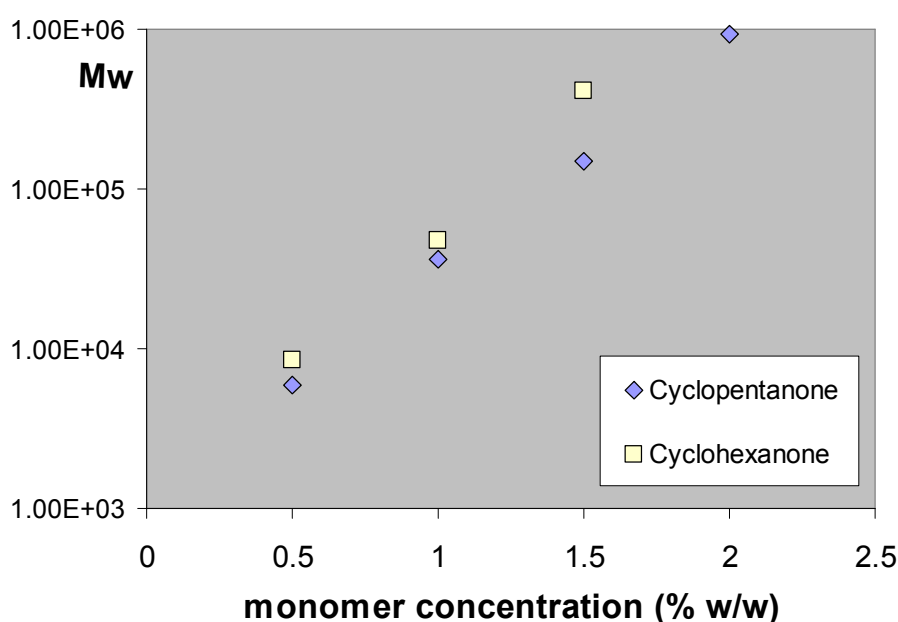
Figure 7. Dependence of the weight-averaged molecular weight on monomer concentration for highly crosslinked nanogels in CyP and CyH. See *Table 8* for the molecular weight data.

As also shown in Ref. 79, a simple exponential dependence was observed for CyP and CyH. It is apparent that the nanogels prepared in CyP possess lower molecular weight than those prepared in either CyH or DMF. The less steep curve of CyP represents the better stabilization exerted by this solvent.

It was found that CyP always gave a higher C_m value than the other solvents; therefore, it was selected as the polymerization solvent for further investigations. Moreover, CyP is generally

easier to handle in laboratory work, as its boiling point is relatively low vompared to CyH or DMF.

It is noteworthy that at C_m values, there exist some insoluble or only partially soluble polymers after work-up, even though these polymers *were* completely soluble at the end of the polymerization. It seems that these polymers are at the border between nanogel and macrogel. If the monomer concentration is increased over this point, macrogelation has been observed clearly. It is not suitable to use the polymers at this monomer concentration for further investigations.

The overall yields of nanogels prepared in DMF were always lower than those of the nanogels synthesized in CyP or CyH. The same tendency was also reported in the above-cited investigation.

Preparation of the Imprinted Nanogels

- General Preparation

The results for the determination of C_m in the model systems were used to set the conditions for the preparation of the imprinted nanogels. It should be noted that the C_m was obtained in a system without the binding monomer-template complex. It was observed that with addition of the DEVPA-DPP complex, the C_m value in CyP slightly decreased to 1.5%. The nanogel particles prepared with 2.0% monomer concentration were only partially soluble after isolation. The lower solubility can be explained due to the ion pair between binding monomer and template molecule.

It is known that the functional monomer, *N,N´*-diethyl-(4-vinylphenyl)amidine (DEVPA, **3**)[80,81] can form stable complexes with a number of compounds, such as carboxylic acids, phosphonates or phosphates, with relatively high association constants (*Table 9*).[82] Such

stoichiometric non-covalent interactions have been shown to provide strong complexation between the functional monomer and the derived template molecules.

Table 9. Association constants of different acids with amidine **3**.[81,83,84]

	solvent	K_{ass}[a] (M^{-1})	complexation (%) [b]
carboxylic acid [c]	chloroform	3.4×10^6	99.9
carboxylic acid [c]	acetonitrile	1.2×10^4	97.2
phosphonate [d]	acetonitrile	8.7×10^3 (25°C)	97.7
		7.6×10^3 (60°C)	96.4
phosphate [e]	acetonitrile	4.6×10^3	95.4

[a] Determined by ^{1}H NMR spectroscopy at 25°C.
[b] Complexation percentage at equimolar concentrations (0.1 mol L^{-1}) of acids and amidine **3**.
[c] 3,5-Dimethylbenzoic acid.
[d] 3,5-Dimethylbenzylphosphonic mono(3,5-dimethylphenyl) ester.
[e] Bis(3,5-dimethylphenyl) phosphate.

In this thesis diphenylphosphate (DPP, **2**) was chosen as the template molecule, to form a cavity mimicking the transition state of the hydrolysis of the substrate diphenylcarbonate (DPC, **1**) (see *Scheme 5*). This system showed some advantages.[85] For example, there is no need to synthesize the functional monomer, the template or the substrate because they are all commercially available. This saves time in the optimization of the reaction conditions. Furthermore, the hydrolysis of carbonates results in CO_2 and phenol as reaction products. This makes it possible to avoid product inhibition, which is observed in the hydrolysis of esters.[31]

At the start of my investigations on imprinted nanogels with catalytic activity with the system mentioned in *Scheme 5*, one standard imprinted nanogel **ING1** was prepared. In parallel, a corresponding control polymer **CNG1**, without the template DPP 2, but with formic acid as the counter ion, was also prepared. These two nanogels were investigated and characterized with all available methods. Thus, a lot of experience could be gained. It was found that the

catalytic properties of this first example were not sufficient. Therefore, after these first results, presented in this section (A), a very thorough optimization of the nanogel structure was undertaken, as is presented in section (B). Fortunately, a large improvement of the catalytic activity could be obtained. The present section (A) now gives an introduction into the methodology of the preparation and characterization of nanogels, with **ING1** and **CNG1** as the examples (*Table 10*).

Table 10. Preparation of molecularly imprinted nanogels for catalysis of DPC hydrolysis.

Nanogel [a]	EDMA (g)	MMA (g)	DEVPA (g)	Template (g)	Initiator (-wt.%)	Solvent (g)	Monomer concentration	Crosslinking ratio
ING1	4.00	0.55	0.20	DPP 0.25	AIBN 3.0	CyP 495.00	1.0%	80.0%
CNG1	4.00	0.75	0.20	formic acid 0.05	AIBN 3.0	CyP 495.00	1.0%	80.0%

[a] ING: Imprinted nanogel, CNG: Control nanogel. Polymerization was carried out at 80°C for 4 days.

The ratio of monomers and the degree of cross-linking were exactly the same as in earlier investigations to prepare imprinted macroporous polymers and imprinted beads[32] for the same purpose, with only the amount of solvent and initiator being different. The normal ratio of monomers to solvent used for the preparation of macroporous polymers is 1:1. However, in the synthesis of imprinted nanogels, this ratio should be kept under the C_m, so a ratio of 1:99 (monomer : solvent) was used. Meanwhile, the content of initiator should be increased accordingly due to the high dilution of the system. Therefore, 3 wt.% of initiator in relation to the sum of the monomers was added, whereas only 1 wt.% is used for the preparation of "traditional" imprinted polymers.

The degree of monomer conversion was determined by drying of aliquots of the polymerization mixture. After evaporating off the solvent in a vacuum oven, the residue was weighed to determine the amount of nanogel formed in the polymerization solution sample. Alternatively, the degree of conversion was also determined directly from the weight of the nanogels isolated by precipitation (*Table 11*). These two values did not show great differences but, in general, the conversion calculated after evaporation is higher than that after precipitation. This tendency can be explained by the possibility of material loss during the nanogel separation process. It was also found that the imprinted nanogel **ING1** showed the higher degree of conversion, around twice as high as the corresponding control nanogel **CNG1**.

Table 11. The degree of monomer conversion determined by evaporation or precipitation.

Nanogel	Conversion by evaporation (%)	Conversion by precipitation (%)
ING1	63.5	53.6
CNG1	31.4	24.7

- Isolation of Imprinted Nanogels

As the polymerization in CyP was proceeding, it was usually observed that the color of the solution darkened slightly. This observation was more prominent when the polymerization took place at a higher temperature and for a longer period. It is suspected that this color originates from byproducts of CyP since, after careful purification of CyP, the color change was less pronounced.

The solution at the end of the polymerization was completely transparent, providing evidence for the solubility of the macromolecules formed. After completion of the polymerization the

imprinted nanogel was isolated via precipitation, using petroleum ether (bp 60-80°C) as the precipitating solvent..

The polymerization solution was first cooled to ambient temperature and subsequently evaporated under vacuum up to around one-third of its original volume. It was then dropped into about five times its volume of the vigorously stirred precipitating solvent. Cloud-like particles were observed in the precipitating solvent, which were isolated by ultracentrifugation or ultrafiltration.

- Removal of the Template from the Imprinted Nanogels

The template molecules must be removed from imprinted nanogels in order to obtain free, specific cavities for catalysis. This was achieved by liquid-liquid phase extraction. This is a very special methodology since the molecularly imprinted nanogels are *soluble*. Traditionally, the template molecules are extracted from the *insoluble* imprinted polymers via liquid-solid extraction using a suitable solvent, *e.g.* using 0.1N sodium hydroxide (aqueous) and acetonitrile (1:1, *v/v*), followed by shaking in an ice bath over 8 hours. This procedure is repeated several times until no trace of template molecule can be detected in the extraction solvent by TLC or HPLC. Subsequently, the extracted polymers are neutralized with pH 7.0 buffer and acetonitrile (1:1, *v/v*), filtered and finally dried.

This method has been found to be a quite effective way to remove the templates, because it has been consistently reported that around 70~90% of the template molecules can be removed by this manner. However, this procedure seems somewhat cumbersome due to the relatively long period of time required.

The soluble imprinted nanogels can be extracted more easily, as described before, in a homogeneous system. A definite amount of imprinted nanogel **ING1** was completely dissolved in chloroform and shaken rapidly with an ice-cooled aqueous NaOH solution. This

was done three times. The organic layer was subsequently washed with neutral water and thereafter added dropwise to a precipitating solvent, *i.e.* petroleum ether 60/80. After isolation by ultracentrifugation, the extracted nanogel was collected for further investigations. The corresponding control nanogel **CNG1** was extracted in the same manner. The amount of the released template molecules was determined by HPLC.

At the start of the investigation, 0.2N aqueous NaOH solution was used, compared to 0.1N solution in the heterogeneous system. However, after trace amounts of hydroxide ion were found in the extracted nanogels, lower concentrations were tried. Therefore, 0.05N NaOH solution was selected and it was found that this reagent is sufficient to extract the template.

Further, if the nanogel solution in chloroform is too concentrated, on addition of the NaOH solution emulsions can form, resulting in considerable loss of sample. To improve the situation, the polarity of the aqueous layer was increased, *e.g.* with saturated NaCl solution. Later on, imprinted nanogels were always dissolved in chloroform at a lower concentration (1.0mg/mL).

Generally speaking, natural enzymes possess, with high homogeneity, only one active site per each individual unit. However, with respect to the artificial enzymes, *i.e.* molecularly imprinted polymers, heterogeneity is inevitable. Therefore, the active sites in the polymers possess different binding ability, selectivity and catalytic activity from each other. While the number of active sites of a natural enzyme can be easily calculated from its concentration due to the mono-clonality, the number of active sites of artificial imprinted polymer has to be determined by experimental methods. Polymer titration is one of the direct ways in which to determine the number of free cavities.[86]

Scheme 10 is a representation of the whole processes of preparing the imprinted polymers. The scheme was systematically designed for showing the amount of the template at each

A. Polymerization solution

- EDMA (*a*)
- MMA (*b*)
- *DEVPA-DPP* (*c*)
- AIBN

→ polymerization →

B. After Polymerization

- unreacted EDMA (*a'*)
- unreacted MMA (*b'*)
- unreacted *DEVPA-DPP (c')*
- *Polymer* (*d*) (*containing DPP (c'')*)
- *Oligomer* (*e*) (*containing DPP (c''')*)

$$c = c' + c'' + c'''$$

precipitation ↓

C. After Precipitation

- *DEVPA-DPP (c*)* (unreacted-precipitated)
- *Polymer* (*d*) (*containing DPP (c'')*)

$$c' \geq c^*$$

→ extraction →

DPP (*f*)
($f = c^* + c''$)

D. After Extraction

- Free Polymer (*d'*) (containing (n_{cav}))

if $c^* \neq 0$, $n_{cav} < f$
$$n_{cav} = f - c^*$$

Scheme 10. A Schematic representation of determining n_{cav}. Template DPP containing entities are highlighted in italic. Note that c'', c''', and n_{cav} are in concentration unit (*i.e.*, mmol/g) calculated according to *c*, while others are in molar unit (*i.e.*, mmol).

process. At each step of the preparation the substances are indicated and, especially, the template containing materials are marked in *italics*. By applying this scheme, we can determine the amount of added template that has been extracted and the amount still in the polymers.

The number of available cavities (n_{cav}) formed in the molecularly imprinted polymers is directly associated with the amount of template molecules involved in the reaction. The template DPP **2** forms complexes (*c*) with the functional monomer DEVPA **3** and is

incorporated into the polymer network during the reaction. Afterwards, the templates are removed by extraction, leaving behind the cavities with free amidine groups.

In highly crosslinked, insoluble imprinted polymers prepared by bulk polymerization, almost 100% of the template molecules are included in the polymer matrix due to the high degree of monomer conversion (*i.e.*, $c'=0$ and $e=0$, thus $c=c''$). As mentioned before, it is reported that around 70~90% of the templates have been detected in the extraction solution ($f=0.7c \sim 0.9c$). This was ascertained by potentiometric titration of the number of available cavities ($n_{cav} \approx f = 0.7c \sim 0.9c$). Thus, the overall incorporation of template molecules for making cavities in the polymer can be regarded as 70~90% in this case. Please note that there is no precipitation step in the preparation of bulk-type imprinted polymers.

On the other hand, for the soluble imprinted nanogels the situation seems somewhat complicated. Not all of the added template molecules (c) can be incorporated into the nanogel particles, since the conversion of monomers is lower due to the higher dilution (*i.e.*, $c' \neq 0$ and $e \neq 0$, thus $c > c''$). This was confirmed by the results shown in *Table 11*. After precipitation (B → C) the unreacted monomers and the oligomers would be removed completely. However, part of the non-polymerized DEVPA-DPP complex could remain in the precipitate, because the complex was found to be incompletely soluble in the precipitating solvent, petroleum ether 60/80 (thus, $c' \geq c^*$). When this precipitate is extracted with NaOH solution (C → D), not only DPP from the nanogels (c'') is split off, but also DPP from the complexes (c^*) is extracted. Finally, the whole amount of extracted DPP (f) is detected by HPLC to determine the quantity. Hence, it is not surprising that the number of available cavities determined by titration (n_{cav}) is lower than the amount of DPP (f) analyzed by HPLC (if $c^* \neq 0$, $n_{cav} < f$).

The difference between the number of cavities (n_{cav}) and the amount of DPP in the extracting solution (f) corresponds to the amount of DEVPA-DPP complex not polymerized and precipitated with the polymer nanogel. Therefore it is not known exactly how much of the

incorporated templates (c'') can be removed by extraction to yield the available cavities (n_{cav}). However, if the relatively flexible polymeric structure of nanogels is taken into account, it is expected that almost all of the template molecules can be removed easily ($n_{cav} = f - c^*$).

In *Table 12* the results of extraction and potentiometric titration of imprinted nanogel **ING1** and the corresponding control nanogel **CNG1** are shown.

Table 12. The results of extraction and potentiometric titration.

Nanogel	The amount (%) [a]		Available cavities after extraction (mmol/g)	pK$_a$ range
	of DPP determined by HPLC (f)	of amidine determined by titration (n_{cav})		
ING1	67.1	33.5	0.0670	8.68 ~ 8.96
CNG1	74.3	44.7	0.0927	8.52 ~ 8.67

[a] They are expressed in percentages as a proportion to the amount of DPP added in the beginning of the polymerization (c). See *Scheme 10* for detail.

At a first glance, it can be noticed that the percentage of DPP determined by HPLC is generally *ca.* twice as high as the amount of amidine groups determined by titration. In case of **ING1**, 67.1% were obtained by HPLC, whereas only 33.5% were determined by potentiometric titration. A similar tendency was observed with **CNG1**, with 74.3% and 44.7%. It simply indicates that around 30% of the starting DPP (c) has not been included in the polymers. However, in the case of insoluble imprinted polymers, it has been reported that these two values for the determination of template splitting percentages do not show such a big difference; in both cases they are usually over 70%. Furthermore, as seen in later investigations, this difference becomes much smaller in optimized nanogels.

It is expected that there are active sites of very different specificity. *Figure 8* is a typical acid-base titration curve of imprinted nanogels after extraction (dots). As noticed, the curve shows a slow decrease over the range as strong acid is added. This implies that there are many amidinium sites with different pK_a values to yield such a curve. On the other hand, when only one chemical species is titrated, *e.g.* hydroxide ion, the titration would give a very distinct curve (*Figure 8*, solid line). Further, it was observed that the average of the pK_a values of the amidine groups in the polymer are lower compared to those in solution (pK_a=11.6).
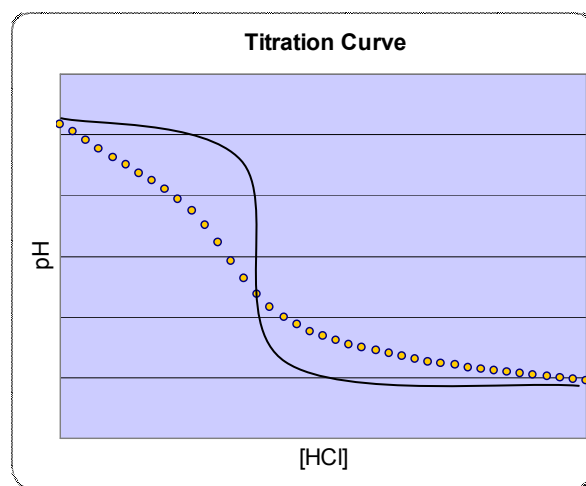
Figure 8. A typical potentiometric titration curve for the imprinted nanogel after extraction (dots). Solid line curve represents titration of strong base with strong acid.

Characterization of the imprinted nanogels

- Gel permeation chromatography (GPC)

The measurement of the molecular weights of the imprinted nanogels can give important information. Using gel permeation chromatography (GPC) and membrane osmometry, the imprinted nanogels were characterized to obtain their molecular weights. Because of their good solubility, the characterization of the imprinted nanogels becomes possible, unlike the insoluble imprinted polymers. In *Table 13* the results of GPC measurements for both **ING1** and **CNG1** are shown. These values are relative molecular weights compared to polystyrene standards. From the chromatograms, both weight-averaged and number-averaged molecular weights, as well as the polydispersity, can be derived.

Table 13. Characterization of **ING1** and **CNG1** by GPC.

Nanogel	before extraction			after extraction		
	M_w [a]	M_n [b]	polydispersity	M_w	M_n	polydispersity
ING1	2.18×10^5	2.56×10^4	8.5	1.97×10^5	2.31×10^4	8.5
CNG1	1.30×10^4	4.55×10^3	2.9	1.09×10^4	4.05×10^3	2.7

[a] Weight-averaged molecular weight by GPC.
[b] Number-averaged molecular weight by GPC.

The molecular weight of the imprinted nanogel **ING1** was found to be higher than that of the corresponding control nanogel **CNG1** by around one order of magnitude. This relation has been repeatedly observed for all cases of nanogel characterizations. Therefore, it can be assumed that the interparticle bonding takes place more frequently during the preparation of the imprinted nanogel **ING1** than in the corresponding control nanogel **CNG1**. The polydispersities **ING1** and **CNG1** are 8.5 and 2.9, respectively. An around three times larger value for **ING1** than **CNG1** indicates that the nanogel particles have been aggregated to yield higher molecular weights and a broader polydispersity. Actually, the GPC chromatogram of **ING1** appeared bimodal, whereas that of **CNG1** is rather monomodal. The conversion for **CNG1** was around half of that of **ING1** (see *Table 11*). It was observed that the polydispersity did not change significantly after extraction for either polymer.

- Membrane Osmometry

Osmotic pressure is one of the four colligative properties that provide a practical method for the measurement of the average molecular weights of polymers. In this case, unlike GPC, absolute molecular weights are obtained. The other colligative properties are vapor-pressure lowering, boiling point elevation and freezing point depression.[87] There are two general

methods for measuring the osmotic pressure: membrane osmometry and vapor-pressure osmometry. For the investigation in the present thesis, membrane osmometry was chosen.

For correct measurements, the proper semi-permeable membrane must be chosen. If the pore size of the membrane is larger than that of the imprinted nanogels, reliable measurements cannot be achieved because the nanogels can permeate completely. Therefore, a membrane with a pore size smaller than the nano particles is essential.

The choice of membrane is also dependent on the solvent used. Methacrylate-based imprinted nanogels were found to be soluble in chloroform, dichloromethane, dimethylformamide (DMF) and dimethylsulfoxide (DMSO). However, it was observed that DMSO solidified when it was under higher pressure during the course of measuring because of its relatively high melting point. The use of DMF in early experiments led to results that were rather unreliable.

The stability of the membranes presents another problem. Only a few series of membranes are available for the solvents discussed above. Unfortunately, cellulose triacetate membranes, which are commonly used for this purpose, were found to be incompatible with chloroform or dichloromethane. Therefore, regenerated cellulose membranes, resistant against chloroform and with a pore size 5 nm and 10 nm (cutoff 10K and 20K Dalton, respectively) from Knauer, were selected for the measurement.

The density of the nanogel particles can be expressed by the factor M_{abs}/M_n, where M_{abs} is the absolute number-averaged molecular weight determined by membrane osmometry and M_n is the relative number-averaged molecular weight by GPC. The M_n value in GPC is calculated by a comparison with polymer standards of known molecular weights, *e.g.* linear polystyrene. However, highly cross-linked nanogel particles are expected to have a sphere-like form and therefore yield a relatively smaller radius of gyration compared to statistical coils of linear polymer standards of the same molecular weight. Thus, as will be clearly shown, the nanogel

particles with the same hydrodynamic volume possess much higher molecular weights than the traditional linear polymer standards.

This is the reason why, for nanogels, the absolute number-averaged molecular weight M_{abs} is always greater than the relative number-averaged molecular weight M_n obtained from GPC. In previous investigations[79] with imprinted nanogels for selective molecular recognition, the factor M_{abs}/M_n has been reported to be around 20.

Table 14. Characterization of the imprinted nanogels by membrane osmometry.

Nanogel	before extraction			after extraction		
	M_{abs}[a)	M_n[b)	M_{abs}/M_n	M_{abs}	M_n	M_{abs}/M_n
ING1	4.39×10^5	2.56×10^4	17.1	3.81×10^5	2.31×10^4	16.5
CNG1	8.14×10^4	4.55×10^3	17.9	6.98×10^4	4.05×10^3	17.2

[a) Absolute number-averaged molecular weight by membrane osmometry.
[b) Number-averaged molecular weight by GPC.

The results of the characterization of **ING1** and **CNG1** by membrane osmometry are shown in *Table 14*. Values of around 16.5 ~ 17.9 were calculated for M_{abs}/M_n in all cases. This is quite similar compared with the imprinted nanogels for selective molecular recognition, although the values are somewhat lower. The values for the extracted nanogels are slightly lower again.

General Procedure for the kinetic measurements

In the beginning of the kinetic investigations a serious problem had to be solved, namely the solubility of the nanogels in a solvent suitable for the catalytic hydrolysis of carbonates. The main advantage of nanogels is their good solubility, by which a better mass transfer is achieved compared to the normal insoluble bulk polymer particles. The solubility of imprinted and control nanogels in several solvents was thus checked, as reported in *Table 15*.

Table 15. The solubility test of imprinted nanogels before and after extraction. [a]

	ING1	ING1-Ex [b]	CNG1	CNG1-Ex [b]
THF	X [c]	O	O	O
CHCl3	O	O	O	O
DMF	O	O	O	Δ
1,4-dioxane	X	Δ	O	O
CH2Cl2	O	O	O	O
DMSO	O	O	O	O
acetone	X	X	O	O
EtOAc	X	X	X	X
MeOH	X	X	X	X
EtOH	X	X	X	X
toluene	X	X	X	X
CCl4	X	X	X	X
ACN	X	X	X	X
H_2O	X	X	X	X
ACN : HEPES = 1 : 1(v/v) [d]	O	O	O	O

[a] Carried out at 25°C overnight. 1mg/1ml.
[b] Nanogel after extraction.
[c] **X** = insoluble, **O** = soluble, **Δ** = partially soluble.
[d] 0.1N of HEPES in H_2O was mixed with the same volume of acetonitrile, subsequently set pH value at 7.3. 0.05N HEPES : ACN = 1 : 1 (v/v) solution was also tested and proved to be capable of dissolving nanogels.

Chloroform, dichloromethane, DMF and DMSO are good solvents in all cases. With tetrahydrofuran (THF), it was observed that the imprinted nanogels were only slightly soluble.

However, after removal of the template they become soluble again. This was a severe disadvantage for the GPC investigation.

Traditionally, a mixed solvent of acetonitrile and buffer solution has been employed in our group for the kinetic experiments involving the hydrolysis of diphenylcarbonate (DPC) in the presence of imprinted macroporous polymers. Thus, the insolubility of the imprinted nanogels in acetonitrile appeared to be a severe disadvantage. As expected, it was observed that the nanogel was also insoluble in HEPES buffer solution (0.05N, pH=7.3). Fortunately, however, when these two different solvents were mixed, the nanogel particles were dissolved completely. This behavior can be explained by the polyelectrolyte effect.[88,89] This explanation is supported by the observation of precipitation of the nanogels by adding of HCl or NaOH to such a solution. This means that the solubility of the nanogels in this acetonitrile:buffer mixed system is dependent on the pH value of the solution.

Therefore, the kinetic experiment in 0.05N HEPES (pH=7.3):acetonitrile (1:1 (v/v)) mixed solvent became possible, allowing a direct comparison with the kinetic parameters obtained using insoluble imprinted polymers. A general protocol was followed for the kinetic experiments (see Experimental section). The rate of the reaction of DPC hydrolysis was monitored by HPLC. Aliquots from the reaction were collected at regular intervals and the reaction rate constant was calculated after quantification of the chromatogram. The reaction could be treated as a pseudo first-order reaction because the reaction was only monitored during the initial stage. To follow the reaction rate, the reaction product phenol was determined quantitatively, using acetophenone as an internal standard. The results of the kinetic experiments using **ING1** and **CNG1** are shown in *Table 16*. **ING1** acts as a first model for optimization of the conditions to be modified later in further investigations.

Table 16. Results of kinetic experiments of imprinted nanogels.[a]

Nanogel	k_{impr} (min^{-1})	k_{impr} / k_{soln}	k_{impr} / k_{contr}
ING1	3.59 × 10^{-7}	14.8	1.4
CNG1	2.52 × 10^{-7}	10.4	-

[a] Experimental condition: 0.05N HEPES (pH=7.3) + MeCN = 1 : 1 (v/v), at 10°C. 2eq. of cavities to 1eq. of substrate. Acetophenone as internal standard.

The results of kinetic experiments with **ING1** revealed an enhancement of the rate constant by a factor of 14.8 compared with the results obtained in buffer solution without catalyst. **CNG1** also showed a significant catalytic activity, with a factor of 10.4. Thus, the selectivity of this system (k_{impr} / k_{contr}) was only 1.4.

Although some catalytic activity was obtained, the result was somewhat disappointing. In experiments with insoluble macroporous polymers, the relative enhancement for the hydrolysis of diphenylcarbonate was considerably better, with 588-fold and even bulk imprinted beads gave an enhancement of 168-fold under comparable experimental conditions (see *Table 6*).

The reason for the relatively low catalytic activity of **ING1** might originate from the lack of stiffness in the polymeric structure. The high dilution of the polymerization solution may cause the cavities in the nanogels to be too flexible. Therefore, proper catalytic activity cannot be expected.

To improve the properties of the imprinted nanogels, some ideas to make more rigid nanogels were considered. They are 1) increasing the cross-linker ratio, 2) modification of the polymerization temperature, 3) using more active cross-linkers, 4) increasing the monomer concentration, 5) the post-dilution method, and 6) stepwise polymerization.

B. Optimization of the nanogel structure

1) The influence of the crosslinker ratio on the catalytic activity

It was strongly suspected that the relatively low catalytic activity of **ING1** was due to the lack of rigidity of the nanogel structure. To increase the stiffness of the nanogel structure, the variation of the amount of crosslinker was checked first; **ING2**, **ING3**, **ING4** and **ING5** (containing 60, 70, 85 and 90% of EDMA as a crosslinker, respectively) were synthesized similarly to **ING1**, but with varying crosslinker contents (***Table 17-1***).

Table 17-1. Preparation of molecularly imprinted nanogels with varying crosslinking ratio.[a]

Nanogel	EDMA (g)	MMA (g)	DEVPA (g)	Template (g)	Initiator (-wt.%)	Solvent (g)	Monomer concentration	Crosslinking ratio
ING2	1.20	0.62	0.08	DPP 0.10	AIBN 3.0	CyP 198.00	1.0%	60.0%
ING3	1.40	0.42	0.08	DPP 0.10	AIBN 3.0	CyP 198.00	1.0%	70.0%
ING4	1.70	0.12	0.08	DPP 0.10	AIBN 3.0	CyP 198.00	1.0%	85.0%
ING5	1.80	0.02	0.08	DPP 0.10	AIBN 3.0	CyP 198.00	1.0%	90.0%

[a] Polymerization was carried out at 80°C for 4 days as done for **ING1**.

For the preparation of the series **ING2** ~ **ING5**, the polymerization conditions and work-up were exactly the same as for **ING1**. The results of the characterization for **ING2** - **ING5** are reported in *Table 17-2*.

Table 17-2. Properties of molecularly imprinted nanogels with varying of crosslinking ratio.

Nanogel	Conversion (%)		The amount of DPP (%) [a]		Available cavities (mmol/g)	pK_a range
	by evaporation	by precipitation	by HPLC	by titration		
ING2	36.2	33.0	63.1	36.9	0.0737	8.73~8.98
ING3	38.8	41.6	66.8	41.5	0.0822	8.38~8.62
ING4	45.2	44.2	65.2	45.9	0.0897	8.48~8.64
ING5	84.6	81.3	71.4	49.1	0.0970	8.15~8.32

[a] They are expressed in percentages as a proportion to the amount of DPP added in the beginning of the polymerization (*a*). See *Scheme 10* for detail.

The degree of conversion, determined by evaporation or precipitation, seems quite similar in this series of nanogels. They are all below 50% except for **ING5**. This nanogel, possessing the most cross-linker, showed a significantly higher conversion (over 80%). The amount of the incorporated DPP was 71.4%, as determined by HPLC. It also showed the highest content of available cavities among the other nanogels (0.0970 mmol/g). The results of characterization of this series by GPC and membrane osmometry are listed in *Table 17-3*.

Table 17-3. Characterization of the imprinted nanogels by GPC and membrane osmometry.

Nanogel		M_w	M_n	polydispersity	M_{abs}	M_{abs}/M_n
ING2	non-extracted	7.07×10^4	1.98×10^4	3.57	3.27×10^5	16.5
	extracted	6.26×10^4	1.78×10^4	3.52	2.82×10^5	15.9
ING3	non-extracted	1.31×10^5	2.27×10^4	5.77	3.96×10^5	17.4
	extracted	1.11×10^5	2.11×10^4	5.27	3.48×10^5	16.5
ING4	non-extracted	2.78×10^5	2.89×10^4	9.62	5.18×10^5	17.9
	extracted	2.18×10^5	2.41×10^4	9.07	4.32×10^5	17.9
ING5	non-extracted	3.41×10^5	3.20×10^4	10.66	5.36×10^5	16.8
	extracted	3.05×10^5	2.95×10^4	10.35	4.92×10^5	16.7

It can be seen that **ING5** has the highest molecular weight. As the degree of crosslinking increases, both of the weight-averaged molecular weight and number-averaged molecular weight go up accordingly. The same tendency was observed in the polydispersity. *Figure 9* shows the dependence of the weight-averaged molecular weight and the polydispersity of the nanogels on the degree of crosslinking. With regard to the weight-averaged molecular weight and the degree of crosslinking, a simple exponential dependence was observed.

a)

b)
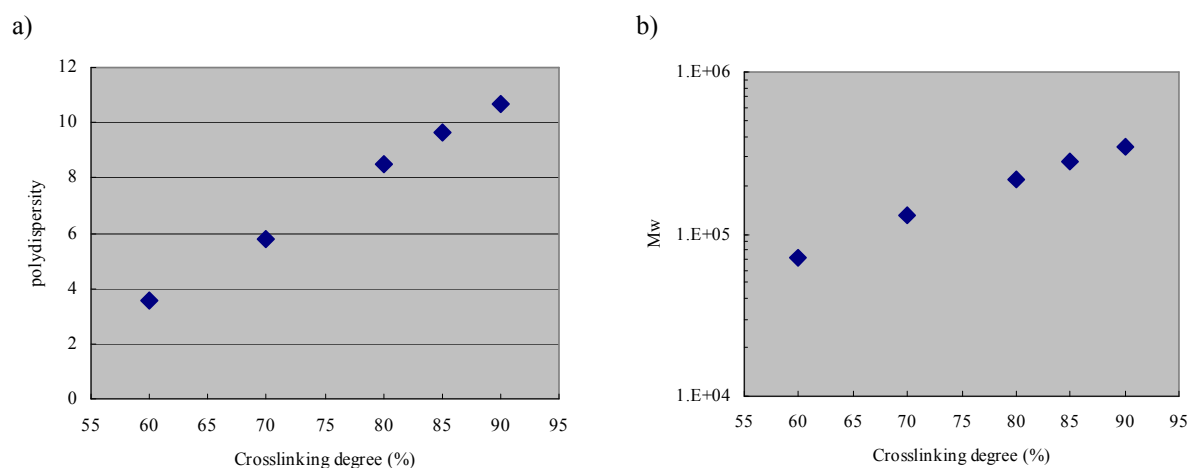
Figure 9. Dependence of a) the polydispersity of the nanogels and b) the weight-averaged molecular weight on the degree of crosslinking.

Kinetic experiments using each imprinted nanogel in this series were carried out to check the influence of the catalytic activity on the degree of crosslinking. The results of the kinetic experiments using **ING2** - **ING5** are shown in *Table 17-4*. Since this series of imprinted nanogels were prepared only for the investigation of the dependence of the catalytic activity on the crosslinking degree, no corresponding control nanogel was synthesized in parallel.

Table 17-4. Results of kinetic experiments of imprinted nanogels.[a]

Nanogel	Crosslinking ratio (%)	k_{impr} (min^{-1})	k_{impr} / k_{soln}	Enhancement factor compared to ING1 [b]
ING2	60.0	2.29 X 10^{-7}	9.4	0.6
ING3	70.0	2.89 X 10^{-7}	11.9	0.8
ING1	80.0	3.59 X 10^{-7}	14.8	1.0
ING4	85.0	4.76 X 10^{-7}	19.5	1.3
ING5	90.0	6.16 X 10^{-7}	25.3	1.7

[a] Experimental condition: 0.05N HEPES (pH=7.3) + MeCN = 1 : 1 (v/v), at 10°C. 2eq. of cavities to 1eq. of substrate. Acetophenone as internal standard.
[b] Relative enhancement factor with comparing the rate constant measured by **ING1**.

A strong dependence of the amount of crosslinker on the relative enhancement was observed (*Figure 10*), with an especially significant rise above 80% crosslinker. This implies that the more rigid polymeric structure can lead to more stabilized cavities and, thus, to better rate enhancements. **ING5** showed a relative enhancement factor of 25.3, which was the best result up to this point. However, this value is still quite low when compared with the results using insoluble macroporous polymers. Apparently, the rigidity of the imprinted nanogel is still low,

Figure 10. Relative enhancements in rate constant with varying of crosslinker contents

because the M_{abs}/M_n values are quite similar to that of **ING1**. Therefore it is necessary to find another strategy for obtaining more rigidly structured nanogel particles.

Actually, the dependence of the crosslinker ratio on the catalytic activity in the imprinted polymers was also observed with a series of slightly crosslinked polymers. This series of polymers was prepared using very low degrees of crosslinking, *i.e.* with 10%, 5%, 2% and even with no crosslinker. The polymers with 2%, 5%, and 10% crosslinking ratio were prepared via suspension polymerization. Traditional bulk polymerization could not be applied for these polymers. If these slightly crosslinked polymers are prepared by bulk polymerization, then the resultant polymers are too elastic to be crushed. Thus, it is not possible to obtain particles with the desired size. The results of the kinetic experiments are listed in *Table 17-5*.

Table 17-5. Results of kinetic experiments of slightly crosslinked imprinted polymers.

Entry	Crosslinking ratio (%)	Polymerization method	k_{impr} / k_{soln}
S-IP	0.0	bulk	3.3
2%-IP	2.0	suspension	9.9
5%-IP	5.0	suspension	21.1
10%-IP	10.0	suspension	54.8
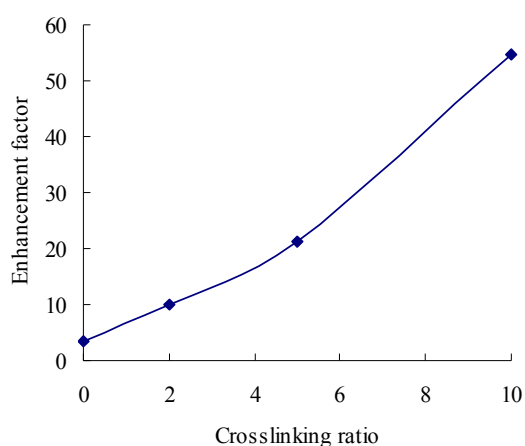
As the crosslinking ratio increased, increase of the enhancement factor was observed. Even with 10% crosslinking, the imprinted polymer exhibited higher catalytic activity than the nanogel with 90% crosslinking. This indicates that the structure of nanogels is not sufficiently rigid.

2) The influence of the polymerization temperature

A wide range of thermal initiators are available with appropriate half-lives at various polymerization temperatures. For example, 2,2'- azobisisobutyronitrile (AIBN) has a half-life of 74 hours at 50°C, 4.8 hours at 70°C, and 7.2 minutes at 100°C.[90,91] Upon heating, the thermal initiator forms free radicals, which initiate the polymerization.

In most cases published up to now for preparing imprinted microgels, AIBN was used as initiator at 80°C with a reaction time of 4 days. However, the half-life of AIBN at 80°C is around 90 minutes, which implies that around 95% of the initiator would be consumed in just 6 hours. Therefore the polymerization temperature and period should be adjusted to provide enough chance for the complete consumption of polymerisable double bonds.

Thus, a new pair of imprinted nanogels was polymerized under variation of the polymerization temperature from 60°C to 70°C and, finally, 80°C (*Table 18-1*). It was hoped that this multi-stage polymerization would give a better chance for obtaining more rigid polymeric structures. **CNG2** is the corresponding control nanogel for **ING6**.

Table 18-1. Preparation of molecularly imprinted nanogels with varying of polymerization temperature.[a]

Nanogel	EDMA (g)	MMA (g)	DEVPA (g)	Template (g)	Initiator (-wt.%)	Solvent (g)	Monomer concentration	Crosslinking ratio
ING6	1.60	0.22	0.08	DPP 0.10	AIBN [b] 3.0 / 1.0 / 1.0	CyP 198.00	1.0%	80.0%
CNG2	1.60	0.22	0.08	formic acid 0.02	AIBN 3.0 / 1.0 / 1.0	CyP 198.00	1.0%	83.4%

[a] Polymerization was carried out at 60°C, 70°C, and 80°C for periods of demanding (see *Table 18-2*).
[b] Initiator was added three times for each polymerization phase.

At every intermission, the conversion ratio of the monomers was determined and the results are shown in *Table 18-2*.

Table 18-2. Characterization of the intermediates of the imprinted nanogels prepared by polymerization at different temperatures.

Nanogel		Polymerization condition [a]			Properties of intermediates			
		Temp. (°C)	Time (hours)	AIBN (-wt.%)	Conversion (%) [b]	M_w [c]	M_n [d]	M_w/M_n
ING6	phase 1	60	144	3.0	64.9	7.61×10^4	1.54×10^4	4.9
	phase 2	70	96	1.0	82.1	1.38×10^5	2.47×10^4	5.6
	phase 3	80	96	1.0	85.3	1.63×10^5	2.71×10^4	6.0
CNG2	phase 1	60	132	3.0	32.1	6.37×10^3	3.12×10^3	2.0
	phase 2	70	90	1.0	35.6	8.11×10^3	3.92×10^3	2.1
	phase 3	80	90	1.0	45.6	1.48×10^4	5.76×10^3	2.6

[a] Each probe was collected at the end of the corresponding polymerization phase.
[b] Determined by evaporation of the resultant polymerization solution.
[c] Weight-averaged apparent molecular weight from GPC.
[d] Number-averaged apparent molecular weight from GPC.

The half-life of AIBN at 60°C is around 20 hours, at 70°C is 4.8 hours, and at 80°C is 1.5 hours. In the gap between each phase, a portion of additional initiator was introduced. This newly adjusted polymerization condition resulted in a higher degree of monomer conversion. It becomes even clearer when **ING1** and **ING6** are compared. The degree of conversion of **ING6** was 85.3%, increased from 63.5% for **ING1**, which was prepared at 80°C for 4 days (see *Table 11*).

Increase in the conversion percentage was also observed in the same nanogel as the reaction proceeded. The overall yields were consistently raised during the different phases, as along with the molecular weights and the polydispersity. Especially in the case of the imprinted nanogel **ING6**, this increase was most remarkable between 60°C and 70°C (from 64.9% to 82.1%), while in the case of the control nanogels, in which the template molecule is formic acid, between 70°C and 80°C the increase is strongest (from 35.6% to 45.6%).

After completion of the three-step polymerization, the resulting particles were characterized as shown in *Table 18-3*. The values of **ING1** are added together for easier comparison.

Table 18-3. Properties of molecularly imprinted nanogels prepared by polymerization at different temperatures.

Nanogel	Conversion (%)		The amount of DPP (%) [a]		Available cavities (mmol/g)	pK_a range
	by evaporation	by precipitation	by HPLC	by titration		
ING6	85.3	77.0	87.9	62.0	0.1240	8.48~8.81
CNG2	45.6	30.2	61.3	42.0	0.0864	7.97~8.01
ING1	*63.5*	*53.6*	*67.1*	*33.5*	*0.0670*	*8.68~8.96*

[a] They are expressed in percentages as a proportion to the amount of DPP added in the beginning of the polymerization (*a*). See *Scheme 10* for detail.

As mentioned before, the most impressive feature of **ING6** is an increase in the conversion percentage. Moreover, the difference between the amount of the incorporated DPP determined by HPLC and titration becomes smaller than that with **ING1**. This indicates that the more rigid structure may be built in **ING6**. The amount of available cavities of 0.124 mmol/g is also double that of **ING1**. The corresponding control nanogel showed around half the degree of conversion of **ING6**, which has been also shown in the relation between **ING1** and **CNG1**.

Table 18-4. Characterization of the imprinted nanogels prepared by polymerization at different temperatures by GPC and membrane osmometry.

Nanogel		M_w	M_n	polydispersity	M_{abs}	M_{abs}/M_n
ING6	non-extracted	1.63×10^5	2.71×10^4	6.01	4.66×10^5	17.2
	extracted	1.45×10^5	2.55×10^4	5.69	4.33×10^5	17.0
CNG2	non-extracted	1.48×10^4	5.76×10^3	2.57	1.00×10^5	17.4
	extracted	1.12×10^4	5.19×10^3	2.16	8.75×10^4	16.9
ING1	*non-extracted*	2.18×10^5	2.56×10^4	*8.52*	4.39×10^5	*17.1*
	extracted	1.97×10^5	2.31×10^4	*8.53*	3.81×10^5	*16.5*

The GPC and membrane osmometry measurements on ING6 revealed that the overall molecular weights have not been changed significantly by the change of polymerization temperature. When M_n and M_w for **ING1** and **ING6** are compared, they both decreased, from 2.56×10^4 to 2.17×10^4 for M_w, and from 2.56×10^4 to 2.17×10^4 for M_n. Furthermore, the polydispersity also decreased from 8.52 to 6.01. However, M_{abs} slightly increased resulting in the comparatively similar value of M_{abs}/M_n of 17.1 and 17.2. From these observations it can be concluded that only the modification of the polymerization temperature is not sufficient to build up rigid polymeric structures.

The results of kinetic experiments support this conclusion (*Table 18-4*).

Table 18-4. Results of kinetic experiments of imprinted nanogels prepared by polymerization at different temperatures.[a]

Nanogel	k_{impr} (min^{-1})	k_{impr} / k_{soln}	k_{impr} / k_{contr}	Enhancement factor compared to **ING1** [b]
ING6	7.64×10^{-7}	31.4	2.46	2.1
CNG2	3.10×10^{-7}	12.7	-	-
ING1	*3.59×10^{-7}*	*14.8*	*1.42*	-

[a] Experimental condition: 0.05N HEPES (pH=7.3) + MeCN = 1 : 1 (v/v), at 10°C. 2eq. of cavities to 1eq. of substrate. Acetophenone as internal standard.
[b] Relative enhancement factor with comparing the rate constant measured by **ING1**.

As shown in *Table 18-4*, the relative enhancement of the rate DPC hydrolysis with **ING6** was 31.4. This is around twice the rate enhancement obtained with **ING1**. The substrate selectivity with **ING6** was calculated to be 2.46, which is also almost twice that of **ING1**.

This is an improvement, but the values are still lower than those of insoluble macroporous polymers. Thus, a further attempt was made to prepare more rigid imprinted nanogel structures.

3) The influence of the type of crosslinker

To increase the structural rigidity, a different imprinted nanogel was synthesized under similar conditions to **ING6**, except that another type of crosslinker was used. The polyfunctional crosslinker trimethylolpropane trimethacrylate (TRIM) **6** was used for nanogel **ING7** (*Figure 11*).

TRIM is nowadays a quite popular crosslinker, employed in many laboratories, and frequently offers a more rigid crosslinked polymer backbone (compared to EDMA).[92,93]

In *Table 19-1*, the composition for the preparation of **ING7** is shown. **CNG3** is the corresponding control nanogel, imprinted with formic acid.
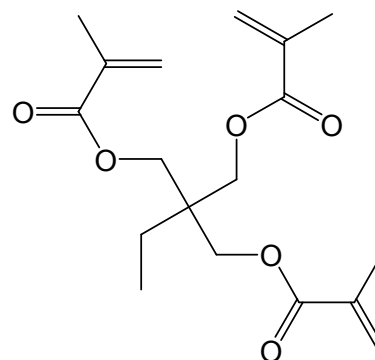
Figure 11. Polyfunctional crosslinker trimethylolpropane trimethacrylate (TRIM) **6**

Table 19-1. Preparation of molecularly imprinted nanogels with TRIM as a crosslinker.[a]

Nanogel	TRIM (g) [b]	MMA (g)	DEVPA (g)	Template (g)	Initiator (-wt.%)	Solvent (g)	Monomer concentration	Crosslinking ratio
ING7	1.28	0.17	0.07	DPP 0.08	AIBN [c] 3.0 / 1.0 / 1.0	CyP 160.50	1.0%	80.0%
CNG3	1.60	0.22	0.08	formic acid 0.02	AIBN 3.0 / 1.0 / 1.0	CyP 196.00	1.0%	83.4%

[a] Polymerization was carried out at 60°C, 70°C, and 80°C (see *Table 19-3*).
[b] TRIM was used as crosslinker instead of EDMA.
[c] Initiator was added three times for each polymerization phase.

Since the modification of the polymerization temperature from 60°C to 80°C turned out to be an effective way to obtain catalytically more active imprinted nanogels, this method was applied for the preparation of **ING7**. In *Table 19-2*, the properties of **ING7** and **CNG3** are given.

Table 19-2. Properties of molecularly imprinted nanogels with TRIM as a crosslinker.

Nanogel	Conversion (%)		The amount of DPP (%) [a]		Available cavities (mmol/g)	pK$_a$ range
	by evaporation	by precipitation	by HPLC	by titration		
ING7	100.0	67.9	77.2	55.4	0.1097	8.60~8.72
CNG3	99.3	34.8	59.3	33.2	0.0841	8.24~8.46
ING1	*63.5*	*53.6*	*67.1*	*33.5*	*0.0670*	*8.68~8.96*

[a] They are expressed in percentages as a proportion to the amount of DPP added in the beginning of the polymerization (*a*). See *Scheme 10* for detail.

Both **ING7** and **CNG3** were prepared by a multi-phases polymerization procedure at different temperatures. The intermediate conversion percentages were also determined, as in case of **ING6** and **CNG2** described previously (*Table 19-3*).

Table 19-3. Properties of molecularly imprinted nanogels with TRIM as a crosslinker.

Nanogel		Polymerization condition [a]			Properties of intermediates
		Temp. (°C)	Time (hours)	AIBN (-wt.%)	Conversion (%) [b]
ING7	phase 1	60	132	3.0	95.2
	phase 2	70	90	1.0	96.7
	phase 3	80	90	1.0	100.0
CNG3	phase 1	60	132	3.0	95.1
	phase 2	70	90	1.0	97.6
	phase 3	80	90	1.0	99.3

[a] Each probe was collected at the end of the corresponding polymerization phase.
[b] Determined by evaporation of the resultant polymerization solution.

It can be seen that the degree of conversion determined by evaporation for **ING7** or **CNG3** is exceptionally high, since there was almost complete conversion. However, after precipitation, they showed only 67.9% and 34.8% yield, respectively. This can be explained by the relatively high boiling point of TRIM. Even though it was evaporated under high vacuum and

temperature, TRIM might have remained in the residue, thus simulating a higher degree of conversion.

Table 19-4. Characterization of the imprinted nanogels with TRIM as a crosslinker by GPC and membrane osmometry.

Nanogel		M_w	M_n	polydispersity	M_{abs}	M_{abs}/M_n
ING7	non-extracted	4.17×10^5	3.02×10^4	13.8	4.99×10^5	16.5
	extracted	3.98×10^5	3.13×10^4	12.7	4.72×10^5	15.1
CNG3	non-extracted	5.39×10^4	7.48×10^3	7.21	1.26×10^5	16.8
	extracted	4.80×10^4	7.52×10^3	6.38	1.12×10^5	14.9
ING1	*non-extracted*	2.18×10^5	2.56×10^4	*8.52*	4.39×10^5	*17.1*
	extracted	1.97×10^5	2.31×10^4	*8.53*	3.81×10^5	*16.5*

In *Table 19-4*, the results of the characterization of **ING7** and **CNG3** by GPC and membrane osmometry are reported. Most remarkable are the high values for the polydispersity. **ING7** showed a polydispersity of 13.8 before extraction and 12.7 after extraction. Unlike other control nanogels, **CNG3** also displayed high polydispersity, with 7.21 before extraction and 6.38 after extraction. This tendency can be explained by the fact that TRIM is a very active functional monomer. Three polymerisable methacrylate functional groups in one molecule make it easier to interact with other particles, even after the polymerization has proceeded to some extent. If just one of the methacrylate functional groups survives during the polymerization, an agglomeration of the particles will be possible. Therefore, when using TRIM or more functionalized monomers as crosslinkers, the full conversion should be carefully controlled to avoid unexpected agglomeration.

The M_w, M_n, and M_{abs} were also found to increase significantly when compared with the values for **ING1**. In particular, the M_w was increased almost 2 times, from 2.18×10^5 to 4.17

$\times$ 10^5, whereas the M_n or M_{abs} showed lower increment factors of 1.18 and 1.14, respectively. This shows that **ING7** possesses broader polydispersity than **ING1**.

In the investigation of imprinted nanogels for selective molecular recognition, a similar phenomenon was observed when using TRIM as the crosslinker.[79] Biffis *et al.* reported that the M_w was 1.21 $\times$ 10^5 for the imprinted microgel prepared with EDMA using 80% crosslinking ratio. Under the same polymerization conditions, except that TRIM was used as a crosslinker at a lower crosslinking ratio (70%), another imprinted microgel was synthesized. The weight-averaged molecular weight of the microgel was 2.03 $\times$ 10^5, which was found to be around twice as large as that of the EDMA-based microgel particles with a higher crosslinking degree. With respect to the number-averaged molecular weight, however, they gave quite similar numbers, 1.42 $\times$ 10^4 for EDMA-based microgel and 1.45 $\times$ 10^4 for TRIM-based microgel. Therefore, the polydispersity of the TRIM-based microgel showed a value of 14.0, which is consistent with that of **ING7**.

The M_{abs}/M_n values of **ING7** and **CNG3** did not meet my expectations. They are around 15 - 17, which are lower than that of **ING1**. This phenomenon can be explained by nanogel agglomeration, as indicated above. The use of TRIM induces a higher probability of particle aggregations. When an individual nanogel particle interacts with another one, they form agglomerates comprising highly crosslinked dense cores, as well as loosely crosslinked regions between the cores. If the aggregation events occur more frequently, the broader portion of the looser regions between cores would be expected, resulting in the larger average swelling volume. Thus, larger M_n values by GPC due to the higher hydrodynamic volume of the agglomerates bring about the lower M_{abs}/M_n values.

Table 19-5. Results of kinetic experiments of imprinted nanogels with TRIM as a crosslinker.[a]

Nanogel	k_{impr} (min^{-1})	k_{impr} / k_{soln}	k_{impr} / k_{contr}	Enhancement factor compared to ING1 [b]
ING7	1.36×10^{-6}	55.8	2.88	3.8
CNG3	4.71×10^{-7}	19.4	-	-
ING1	*3.59×10^{-7}*	*14.8*	*1.42*	-

[a] Experimental condition: 0.05N HEPES (pH=7.3) + MeCN = 1 : 1 (v/v), at 10°C. 2eq. of cavities to 1eq. of substrate. Acetophenone as internal standard.
[b] Relative enhancement factor with comparing the rate constant measured by **ING1**.

However, the kinetic experiments showed somewhat more encouraging results, as can be seen in *Table 19-5*. The relative enhancement in the rate of DPC hydrolysis with **ING7** was 55.8. This number provided an enhancement factor in rate constant of 3.8 compared with that of **ING1**. Further, the selectivity factor was 2.88, i.e. a better result than the pair **ING1** and **CNG1** or even **ING6** and **CNG2**.

If the influence of TRIM on the catalytic activity is looked at, one should compare the kinetic result of **ING7** with that of **ING6**, not with **ING1**, since **ING1** was not prepared with the variation of the polymerization temperature. TRIM improved the catalytic activity by a factor of 1.78, comparing the k_{impr} / k_{soln} values of **ING7** and **ING6**.

This is a quite interesting result because, in the investigation of imprinted nanogels for selective molecular recognition, the use of TRIM did not bring any improvement in selectivity compared to other series of nanogels prepared with EDMA as a crosslinker.

4) The influence of the monomer concentration

Among the factors that can have an effect on the morphology of the nanogel structure, the monomer concentration is certainly a very important one. The monomer concentration should be very carefully controlled to be below the critical monomer concentration C_m. Above this point, macrogelation would occur and no soluble nanogel will be obtained.

It was reported in the investigations on imprinted nanogels to be used for selective molecular recognition, that increasing the monomer concentration induced an appreciable rise in molecular weight and in polydispersity.[79] A pair of microgels with 70% crosslinking, was prepared under the conditions of 1% and 2% of monomer concentration, respectively. While the former showed $M_w = 3.96 \times 10^4$, the latter showed 5.12×10^5. For the polydispersity, the former had 4.3 only, whereas the latter showed as much as 23.1. This quite significant increase in both molecular weight and polydispersity indicates that the change of monomer concentration can affect the morphology of nanogels critically.

According to the results in determining C_m (*Table 8*), 2.0% is the highest monomer concentration possible in CyP. This value is only under the condition of 80% of crosslinker at 80°C for 4 days polymerization. As proposed in the previous section, the new polymerization temperature procedure was applied. Thus, C_m was determined under this condition. As a result, 1.5% monomer concentration was appropriate, whereas the polymer prepared at 2.0% monomer concentration was found to be only partially soluble after isolation.

In *Table 20-1* are shown the components ratio for **ING8**, prepared with a monomer concentration of 1.5%. The corresponding control nanogel was not synthesized in this case.

Table 20-1. Preparation of molecularly imprinted nanogels with 1.5% of monomer concentration.[a]

Nanogel	EDMA (g)	MMA (g)	DEVPA (g)	Template (g)	Initiator (-wt.%)	Solvent (g)	Monomer concentration	Crosslinking ratio
ING8	1.20	0.17	0.06	DPP 0.07	AIBN [b] 3.0 / 1.0 / 1.0	CyP 98.50	1.5%	80.0%

[a] Polymerization was carried out at 60°C, 70°C, and 80°C for 133, 112, and 96 hours, respectively.
[b] Initiator was added three times for each polymerization phase.

At each intermission of the polymerization, the intermediate conversion was determined as in the previous investigations (*Table 20-2*). Similarly to **ING6** (see *Table 18-2*), a remarkable increase in conversion was detected between 60°C and 70°C (from 67.4% to 90.4%).

Table 20-2. Properties of molecularly imprinted nanogels with 1.5% monomer concentration.

Nanogel		Polymerization condition [a]			Properties of intermediates
		Temp. (°C)	Time (hours)	AIBN (-wt.%)	Conversion (%) [b]
ING8	phase 1	60	133	3.0	67.4
	phase 2	70	112	1.0	90.4
	phase 3	80	96	1.0	> 100.0

[a] Each probe was collected at the end of the corresponding polymerization phase.
[b] Determined by evaporation of the resultant polymerization solution.

After completion of the polymerization, **ING8** was separated and extracted for further investigation. The results of potentiometric titration and determination of the splitting percentage are listed below in *Table 20-3*.

Table 20-3. Properties of molecularly imprinted nanogels with 1.5% monomer concentration.

Nanogel	Conversion (%)		The amount of DPP (%) [a]		Available cavities (mmol/g)	pK$_a$ range
	by evaporation	by precipitation	by HPLC	by titration		
ING8	> 100.0	79.9	92.5	91.9	0.1849	8.35~8.41
ING1	*63.5*	*53.6*	*67.1*	*33.5*	*0.0670*	*8.68~8.96*

[a] They are expressed in percentages as a proportion to the amount of DPP added in the beginning of the polymerization (*a*). See *Scheme 10* for detail.

Considerably higher values for conversion and the amount of incorporated DPP were obtained. Around 80% conversion determined by precipitation was a very positive result. Furthermore, the amount of incorporated DPP calculated from the potentiometric titration was 91.9% and shows only a small difference with the value determined by HPLC. Consequently, the number of available cavities is found to be 0.1849 mmol/g, indicating that more than 90% of the added template survived during the polymerization and work-up process.

This was quite encouraging, since all the preceding imprinted nanogels showed relatively large differences between the values of incorporated DPP, as measured by HPLC and titration. As pointed out before, these differences indicate the amount of DEVPA-DPP complex not incorporated into the polymer network. For example, **ING1** showed a difference of 33.6% and **ING5** a difference of 22.3%. Even TRIM-based nanogel **ING7** exhibited a difference of 21.8%. These numbers all indicate the insufficiency of structural rigidity in the previous polymers. In this respect, it might be considered that **ING8** has the most rigid morphological status among the imprinted nanogels described up to this point.

In *Table 20-4*, the results of the characterization of **ING8** by GPC and membrane osmometry are given. As predicted by the results of Ref. 79, the polydispersity of **ING8** was more than 20, both before and after extraction. It was rather surprising that a crosslinked macromolecule with the molecular weight of almost one million is still soluble in appropriate solvents.

Table 20-4. Characterization of the imprinted nanogels prepared with 1.5% monomer concentration by GPC and membrane osmometry.

Nanogel		M_w	M_n	polydispersity	M_{abs}	M_{abs}/M_n
ING8	non-extracted	9.86×10^5	4.76×10^4	20.71	7.18×10^5	15.1
	extracted	8.52×10^5	4.21×10^4	20.24	6.23×10^5	14.8
ING1	*non-extracted*	*2.18×10^5*	*2.56×10^4*	*8.52*	*4.39×10^5*	*17.1*
	extracted	*1.97×10^5*	*2.31×10^4*	*8.53*	*3.81×10^5*	*16.5*

Membrane osmometry showed a M_{abs} for **ING8** of 7.18×10^5 before extraction and 6.23×10^5 after extraction. Accordingly, low values of M_{abs}/M_n, 15.1 and 14.8, were obtained.

M_n is usually determined using gel permeation chromatography (GPC), while M_{abs} is calculated from osmotic pressure measurements to give the absolute number-averaged molecular weight of the macromolecules. For the GPC measurements, it is always necessary to calibrate the chromatograms with polymer standards of known molecular weights. In most cases, linear polystyrenes are employed as polymer standards. However, it is well known that the shape and the density of nanogel particles are quite different than those of linear polymers. The internal crosslinking in the nanogel particles makes them rather compact. Hence, there is always a deviation between the values of GPC measurements and membrane osmometry, if they are used for the calculation of intramolecularly crosslinked nanogel particles. Moreover, this deviation would become larger when the size of the nanogels becomes bigger, because the size increases as the square, while the volume increases as the cube.

Such a phenomenon was also observed in the investigation in Ref. 79. With an increase in crosslinking degree from 50% to 70%, the factor M_{abs}/M_n decreased steadily from 24.0 to 13.0.

The results of kinetic experiments with **ING8** were quite satisfactory. They showed an enhancement of k_{impr} / k_{soln} of 90.4. This is about six times better than with **ING1** and three times better than with **ING6**, which showed a factor of 31.4 in relative enhancement factor.

Accordingly, it can be stated that, among all the attempts tried up to now, the change of the monomer concentration was the most influential factor, both for the morphological status of the nanogel structure, as well as for the enhancement of the reaction rate.

Table 20-5. Results of kinetic experiments of imprinted nanogels prepared with 1.5% monomer concentration.[a]

Nanogel	k_{impr} (min^{-1})	k_{impr} / k_{soln}	k_{impr} / k_{contr}	Enhancement factor compared to **ING1** [b]
ING8	2.20 X 10^{-6}	90.4	- [c]	6.1
ING1	*3.59 X 10^{-7}*	*14.8*	*1.42*	-

[a] Experimental condition: 0.05N HEPES (pH=7.3) + MeCN = 1 : 1 (v/v), at 10°C. 2eq. of cavities to 1eq. of substrate. Acetophenone as internal standard.
[b] Relative enhancement factor with comparing the rate constant measured by **ING1**.
[c] No corresponding control nanogel was prepared.

5) The influence of the post-dilution method

The next attempt to increase the rigidity of nanogel structure was the "post-dilution" method. According to Lee *et al.*, an important factor in the formation of nanogels takes place at the beginning of the free radical chain growth polymerization reaction.[94] They pointed out that the characteristics of the nanogels are determined during the initial stages of the reaction. In the homopolymerization of EDMA, it was observed that particles of two different sizes were formed from the very beginning of the reaction. The larger particles consisted of an aggregation of the smaller ones. In the early stage, the crosslinking density was found to be quite low. However, as the reaction proceeded, the pendant double bonds on the surface of the primary polymers were consumed rapidly and the crosslinking degree increased accordingly. Near to the gelation point, the degree of double bond conversion became lower and, at the end, macrogelation occurred.

This investigation suggests that the crosslinking degree of the system reaches the highest value at a point just before the macrogelation takes place. It is apparent that more rigid polymer structures could be obtained when the reaction goes further, but then only insoluble polymer would be available.

In other words, if the reaction is stopped at the point of time just prior to gelation and if then the whole system is diluted extensively at this point to keep the monomer concentration under the C_m, then no macrogelation would take place and it would be possible to obtain soluble nanogel particles with a crosslinking degree as high as possible.

With this novel method, which is called the "post-dilution" method, a series of imprinted nanogels was synthesized, expecting nanogel particles with more rigid structures.

Table 21-1. Preparation of molecularly imprinted nanogels with the post-dilution method.

Nanogel	EDMA (g)	MMA (g)	DEVPA (g)	Template (g)	Initiator (-wt.%)	Solvent (g)	t_{gel} [a] (min)	Monomer conc.	Crosslinking ratio
ING9 [b]	1.60	0.22	0.08	DPP 0.10	AIBN 3.0	CyP [c] 2+196.00	90	1.0%	80.0%
ING10	4.00	0.55	0.20	DPP 0.25	AIBN [d] 3.0 / 1.0 / 1.0	CyP 5+495.00	120	1.0%	80.0%
CNG4	1.60	0.22	0.08	formic acid 0.02	AIBN 3.0 / 1.0 / 1.0	CyP 2+196.00	120	1.0%	83.4%

[a] Critical gelation time. Determined in prior experiments.
[b] Prepared without the polymerization temperature modification. Polymerized at 80°C for 4 days as **ING1** was prepared.
[c] Before t_{gel} the same amount of solvent and monomer were mixed. After t_{gel} the rest of solvent was added for extensive dilution.
[d] Initiator was added three times for each polymerization phase.

Before starting the reaction, the critical gelation time, t_{gel}, should be determined. t_{gel} can be defined as the time period after which the macrogelation takes place and is dependent on a number of factors, such as temperature, type and amount of crosslinker, initiator, solvent, monomer concentration, etc. Therefore, it should be determined experimentally for each case

of polymerization, like the determination of C_m. After determining t_{gel}, a series of imprinted nanogels was prepared (*Table 21-1*).

t_{gel} for **ING9** was 90 minutes, while that of **ING10** was 120 minutes. The determination of t_{gel} of **ING9** was carried out at 80°C, whereas for **ING10** t_{gel} was measured at 60°C. Interestingly, when formic acid was added as a template instead of DPP, t_{gel} for the corresponding control nanogel **CNG4** (control to **ING10**) was determined as 120 minutes, like **ING10**. It can therefore be assumed that the change of the template molecule does not cause a great influence upon t_{gel}.

In *Table 21-2*, some experimental data for **ING10** and **CNG4** is given, including the intermediate conversion degrees.

Table 21-2. Properties of molecularly imprinted nanogels with post-dilution method.

Nanogel		Polymerization condition [a]			Properties of intermediates
		Temp. (°C)	Time (hours)	AIBN (-wt.%)	Conversion (%) [b]
ING10	phase 1	60	114 [c]	3.0	53.5
	phase 2	70	100	1.0	87.1
	phase 3	80	63	1.0	91.0
CNG4	phase 1	60	113 [c]	3.0	52.5
	phase 2	70	96	1.0	58.5
	phase 3	80	90	1.0	54.0

[a] Each probe was collected at the end of the corresponding polymerization phase.
[b] Determined by evaporation of the resultant polymerization solution.
[c] Not including t_{gel}.

Table 21-3. Properties of molecularly imprinted nanogels with post-dilution method.

Nanogel	Conversion (%)		The amount of DPP (%) [a]		Available cavities (mmol/g)	pKa range
	by evaporation	by precipitation	by HPLC	by titration		
ING9	43.5	38.0	79.3	42.6	0.0850	8.67~8.97
ING10	91.0	83.7	74.4	37.2	0.0733	8.66~8.91
CNG4	54.0	42.1	61.2	31.1	0.0946	8.55~8.81
ING1	*63.5*	*53.6*	*67.1*	*33.5*	*0.0670*	*8.68~8.96*
ING6	*85.3*	*77.0*	*87.9*	*62.0*	*0.1240*	*8.48~8.81*

[a] They are expressed in percentages as a proportion to the amount of DPP added in the beginning of the polymerization (*a*). See *Scheme 10* for detail.

In *Table 21-3*, the data for the analysis of **ING9**, **ING10** and **CNG4** are shown. The conversion for **ING10** determined by precipitation is 83.7%, which is more than double that shown by **ING9** (38.0%). Moreover, **ING10** shows a larger conversion compared even to **ING6**, both by evaporation and by precipitation. This value is the highest conversion percentage determined by precipitation up to now; even **ING8,** which is prepared with a monomer concentration of 1.5%, showed only 79.9%.

With respect to the amount of incorporated DPP, however, an unexpected tendency was observed. All the three imprinted nanogels prepared with the post-dilution method showed relatively large differences in the values determined by HPLC and titration. Around 30-40% of the added DPP was not included into the polymers. Accordingly, the amount of available cavities detected in all cases was less than 0.1 mmol/g.

The results of the characterization of **ING9**, **ING10** and **CNG4** by GPC and membrane osmometry are shown in *Table 21-4*.

Table 21-4. Characterization of the imprinted nanogels with post-dilution method by GPC and membrane osmometry.

Nanogel		M_w	M_n	polydispersity	M_{abs}	M_{abs}/M_n
ING9	non-extracted	2.14×10^5	2.61×10^4	8.20	6.39×10^5	24.5
	extracted	1.58×10^5	2.18×10^4	7.25	5.94×10^5	27.2
ING10	non-extracted	2.21×10^5	2.85×10^4	7.75	7.06×10^5	24.8
	extracted	1.47×10^5	2.45×10^4	6.00	6.24×10^5	25.5
CNG4	non-extracted	1.48×10^4	5.88×10^3	2.52	1.31×10^5	22.3
	extracted	1.22×10^4	5.75×10^3	2.12	1.28×10^5	22.3
ING1	*non-extracted*	*2.18×10^5*	*2.56×10^4*	*8.52*	*4.39×10^5*	*17.1*
	extracted	*1.97×10^5*	*2.31×10^4*	*8.53*	*3.81×10^5*	*16.5*
ING6	*non-extracted*	*1.63×10^5*	*2.71×10^4*	*6.01*	*4.66×10^5*	*17.2*
	extracted	*1.45×10^5*	*2.55×10^4*	*5.69*	*4.33×10^5*	*17.0*

At a glance, a striking increase in M_{abs}/M_n values can be noticed. **ING9** showed 24.5 and 27.2, with and without template, respectively. **ING10** displayed 24.8 and 25.5 and even the control nanogel **CNG4** exhibited more than twenty for the factor M_{abs}/M_n.

It can be seen that the apparent values for the molecular weight determined by GPC are not greatly changed between post-dilution and no post-dilution. **ING9** with post-dilution had a M_w of 2.14×10^5 before extraction, while **ING1** without post-dilution showed 2.18×10^5. M_n of **ING9** was found to be 2.61×10^4, while for **ING1** it was 2.56×10^4. **ING10** and **ING6**, representing a comparative pair of nanogels with the post-dilution method, also revealed a similar tendency. The value of 1.47×10^5 was determined for M_w of **ING10** after extraction, whereas **ING6** showed 1.45×10^5 for the same category. M_n values were also similar, 2.45×10^4 for **ING10** and 2.45×10^4 for **ING6**.

On the other hand, with respect to M_{abs}, a significant increase was observed. **ING9** had $M_{abs} = 6.39 \times 10^5$ and $M_{abs} = 7.06 \times 10^5$ was shown by **ING10**. Even after extraction they displayed 5.94×10^5 and 6.24×10^5, respectively. These numbers are significantly higher when

compared with M_{abs} of **ING1** and **ING6**. This is the reason why the M_{abs}/M_n factors in this series of nanogels are so high.

A high value of M_{abs}/M_n indicates a high degree of structural rigidity. Obviously, it can be expected that particles of **ING9** or **ING10** prepared via post-dilution are more densely packed than **ING1** or **ING6**. Since the number-averaged molecular weights are found to be quite similar for both groups of nanogels, the same hydrodynamic volumes of both are expected. On the other hand, the M_{abs} of **ING9** and **ING10** are larger than those of **ING1** and **ING6**. As a consequence, **ING9** and **ING10** have a higher density than **ING1** and **ING6**, because they are heavier with the same volume.

The results of kinetic experiments of the imprinted nanogels prepared with post-dilution are reported in *Table 21-5*.

Table 21-5. Results of kinetic experiments of imprinted nanogels with post-dilution method.[a]

Nanogel	k_{impr} (min^{-1})	k_{impr}/k_{soln}	k_{impr}/k_{contr}	Enhancement factor compared to **ING1** [b]
ING9	1.01×10^{-6}	41.5	-	2.8
ING10	1.28×10^{-6}	52.7	5.52	3.6 [1.7][c]
CNG4	4.71×10^{-7}	19.4	-	-
ING1	*3.59×10^{-7}*	*14.8*	*1.42*	*-*
ING6	*7.64×10^{-7}*	*31.4*	*2.46*	*2.1*

[a] Experimental condition: 0.05N HEPES (pH=7.3) + MeCN = 1 : 1 (v/v), at 10°C. 2eq. of cavities to 1eq. of substrate. Acetophenone as internal standard.
[b] Relative enhancement factor with comparing the rate constant measured by **ING1**.
[c] In bracket is shown the relative enhancement factor with comparing the rate constant measured by **ING6**.

The observed rate enhancement with **ING10** (52.7) is greater than that with **ING9** (41.5), indicating the effectiveness of the temperature variation method. These values almost

approach those of the TRIM-based nanogels, like **ING7** with 55.8, but they inevitably fall below the values of **ING8** (90.4), prepared with a monomer concentration of 1.5%. This is surprising, because the degree of compactness of the particles seems highest in **ING9** and **ING10**. Despite their extraordinary rigidity, the catalytic activity has not increased in relation to the M_{abs}/M_n value.

However, the selectivity k_{impr} / k_{contr} increased considerably. For the pair of nanogels **ING10** and **CNG4**, the value of k_{impr} / k_{contr} was calculated to give 5.52, which is almost double that which **ING6** and **ING7** presented (2.46 and 2.88, respectively). It indicates that the rigid structure of the nanogel particles improves the selectivity. This might be due to stabilization of the cavities.

- Variation of monomer concentration with the post-dilution method

Nanogels with monomer concentrations of 0.5% and 0.1% were synthesized (*Table 22-1*).

Table 22-1. Preparation of molecularly imprinted nanogels with 0.5% and 0.1% of monomer concentration under the post-dilution method.

Nanogel	EDMA (g)	MMA (g)	DEVPA (g)	Template (g)	Initiator (-wt.%)	Solvent (g)	t_{gel} [a] (min)	Monomer conc.	Crosslinking ratio
ING11	1.20	0.17	0.06	DPP 0.07	AIBN [b] 3.0 / 1.0 / 1.0	CyP [c] 1.5+297.0	120	0.5%	80.0%
CNG5	1.20	0.17	0.06	formic acid 0.02	AIBN 3.0 / 1.0 / 1.0	CyP 1.5+297.0	120	0.5%	83.4%
ING12	1.60	0.22	0.08	DPP 0.10	AIBN 3.0 / 1.0 / 1.0	CyP 2+1996.0	120	0.1%	80.0%
CNG6	1.60	0.22	0.08	formic acid 0.02	AIBN 3.0 / 1.0 / 1.0	CyP 2+1996.0	120	0.1%	83.4%

[a] Critical gelation time. Determined by the prior experiment to the main polymerization.
[b] Initiator was added three times for each polymerization phase.
[c] Before t_{gel} the same amount of solvent and monomer were mixed. After t_{gel} the rest of solvent was added for extensive dilution.

Since the monomer concentration is seen to be the most influential factor in the preparation of imprinted nanogels, some variations of this factor were applied together with the post-dilution method. t_{gel} was the same in all cases.

Table 22-2. Properties of molecularly imprinted nanogels with 0.5% and 0.1% of monomer concentration under the post-dilution method.

Nanogel		Polymerization condition [a]			Properties of intermediates
		Temp. (°C)	Time (hours)	AIBN (-wt.%)	Conversion (%) [b]
ING11	phase 1	60	100 [c]	3.0	50.9
	phase 2	70	60	1.0	69.0
	phase 3	80	50	1.0	78.6
CNG5	phase 1	60	100 [c]	3.0	42.3
	phase 2	70	60	1.0	59.9
	phase 3	80	50	1.0	52.2
ING12	phase 1	60	135 [c]	3.0	46.6
	phase 2	70	75	1.0	47.0
	phase 3	80	80	1.0	55.2
CNG6	phase 1	60	135 [c]	3.0	25.5
	phase 2	70	75	1.0	28.1
	phase 3	80	80	1.0	33.7

[a] Each probe was collected at the end of the corresponding polymerization phase.
[b] Determined by evaporation of the resultant polymerization solution.
[c] Not including t_{gel}.

The experimental data for the preparation of the nanogels is shown in *Table 22.2*. It can easily be noticed that the overall conversion of **ING11** and **ING12** was relatively low, with the conversion of **ING12** being barely over 50%. A relatively large increase in conversion was observed between 60°C and 70°C in the case of **ING11**, though not with **ING12**. This might be due to the exceedingly dilute monomer concentration.

After separation and extraction, the nanogels were analyzed by HPLC and titration. The results are shown in *Table 22-3*. All the values were found to be relatively low.

Table 22-3. Properties of molecularly imprinted nanogels with low monomer concentration under the post-dilution method.

Nanogel	Conversion (%)		The amount of DPP (%) [a]		Available cavities (mmol/g)	pK_a range
	by evaporation	by precipitation	by HPLC	by titration		
ING11	78.6	61.1	63.0	34.4	0.0699	8.20~8.50
CNG5	52.2	34.9	65.2	21.9	0.1120	8.04~8.39
ING12	55.2	27.6	55.6	26.4	0.0409	8.19~8.29
CNG6	33.7	29.7	51.2	21.4	0.0521	8.12~8.42

[a] They are expressed in percentages as a proportion to the amount of DPP added in the beginning of the polymerization (*a*). See *Scheme 10* for detail.

Except **ING11**, the other nanogels showed around only one third or even one quarter of the amount of monomer originally added in the nanogel. With respect to the amount of incorporated DPP, they all displayed relatively low values, with the differences being quite large. By titration, around 20~30% of the cavities were found to have survived. This tendency of diminution is believed to be caused by the excessive dilution. The characterization results of the nanogels by GPC and membrane osmometry are listed in *Table 22-4*.

Table 22-4. Characterization of the imprinted nanogels with low monomer concentration under the post-dilution method.

Nanogel		M_w	M_n	polydispersity	M_{abs}	M_{abs}/M_n
ING11	non-extracted	4.05×10^4	9.87×10^3	4.10	2.75×10^5	27.9
	extracted	3.22×10^4	8.91×10^3	3.61	2.61×10^5	29.3
CNG5	non-extracted	3.77×10^3	2.49×10^3	1.52	6.95×10^4	27.9
	extracted	3.64×10^3	2.51×10^3	1.45	6.76×10^4	26.9
ING12	non-extracted	2.33×10^3	1.43×10^3	1.63	4.88×10^4	34.1
	extracted	2.07×10^3	1.34×10^3	1.54	4.43×10^4	33.0
CNG6	non-extracted	1.16×10^3	8.37×10^2	1.38	2.67×10^4	31.9
	extracted	1.09×10^3	7.97×10^2	1.37	2.42×10^4	30.3
ING10	*non-extracted*	2.21×10^5	2.85×10^4	*7.75*	7.06×10^5	*24.8*
	extracted	1.47×10^5	2.45×10^4	*6.00*	6.24×10^5	*25.5*

Surprisingly, the factor M_{abs}/M_n went up markedly. Even though the M_w or M_n decreased by around a few tenths compared with **ING10**, around $M_{abs}/M_n = 27\sim29$ was seen for **ING11** and **CNG5**, while **ING12** and **CNG6** gave more than 30. Moreover, it was noticed that the polydispersity of **ING12**, **CNG5** and **CNG6** was exceptionally low.

Actually, the remarkably high value of M_{abs}/M_n is a characteristic feature of the post-dilution method. As seen in *Figure 12*, two groups can be distinguished in the imprinted nanogels series. In *Figure 12A*, a plot of relative number-averaged molecular weights *vs.* absolute number-averaged molecular weights for the non-extracted imprinted nanogels is shown. In this plot it can be seen that the imprinted nanogels prepared by the post-dilution method (**ING9 - ING16**, ▲) show higher M_{abs} values than the nanogels prepared without the post-dilution method (**ING1 - ING8**, ●) (Note: **ING13 - ING16** are not introduced yet). A plot of the polydispersity *vs.* M_{abs}/M_n was also made (*Figure 12B*); here one can see the tendency for higher M_{abs}/M_n values in the post-diluted nanogels.
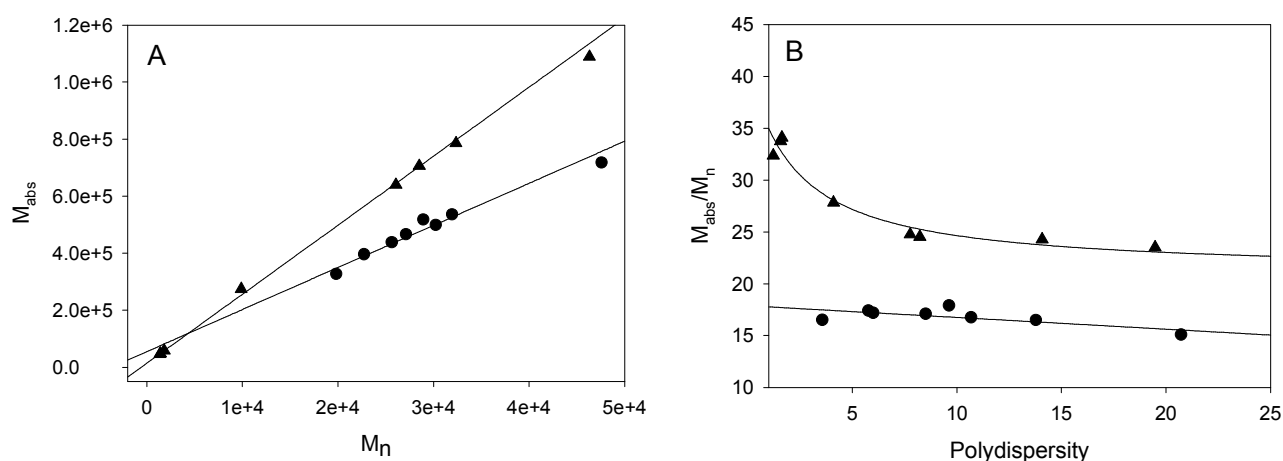
Figure 12.   Plots of (A) relative number-average molecular weights (M_n) *vs.* absolute number-average molecular weights (M_{abs}) and (B) polydispersity *vs.* M_{abs}/M_n values of the non-extracted imprinted nanogels. Results of the extracted nanogels and the control nanogels are omitted. The triangle dots (▲) represent the imprinted nanogels prepared by post-dilution method, and the circle dots (●) stand for the imprinted nanogels without post-dilution method.

In the characterization of the imprinted nanogels for the recognition of sugar derivatives by Biffis, it was shown that the molecular weights measured by membrane osmometry were about twenty times larger than the apparent values determined by GPC. This observation was explained via the assumption that the intramolecularly crosslinked nanogel particles dissolved in a good solvent should possess a much more densely packed structure than a statistical coils of linear polymer molecules of the same molecular weight. This means that they are significantly heavier than linear polymer standards used in GPC with the same hydrodynamic volume.

The M_{abs}/M_n values of the imprinted nanogels prepared *without* the post-dilution method (**ING1 - ING8**, ●) were around 15~18, whereas in the case of the imprinted nanogels prepared *with* the post-dilution method (**ING9 - ING16**, ▲) these values were found to be more than 25. In some specific cases, even values of around 30~35 are seen, especially with lower polydispersity. In other words, the post-diluted nanogels have denser polymeric structures; thus, they are more rigid than the others.

Table 22-5. Results of kinetic experiments of imprinted nanogels with low monomer concentration under the post-dilution method.[a]

Nanogel	k_{impr} (min^{-1})	k_{impr} / k_{soln}	k_{impr} / k_{contr}
ING11	3.77×10^{-7}	15.5	3.20
CNG5	1.18×10^{-7}	4.8	-
ING12	3.48×10^{-7}	14.3	2.58
CNG6	1.35×10^{-7}	5.5	-
ING10	*1.28×10^{-6}*	*52.7*	*5.52*

[a] Experimental condition: 0.05N HEPES (pH=7.3) + MeCN = 1 : 1 (v/v), at 10°C. 2eq. of cavities to 1eq. of substrate. Acetophenone as internal standard.

In *Table 22-5* are shown the results of the kinetic experiments using the imprinted nanogels prepared with low monomer concentration under the post-dilution method. **ING11** and **ING12**, containing lower contents of monomer concentration, exhibited rate enhancements of 15.5 and 14.3, respectively. Even though they were highly diluted in the preparation, they showed rate enhancements as good as **ING1** (14.8). This supports the positive effects of the post-dilution and the polymerization temperature modification.

6) The influence of different types of subsequent treatments of the nanogels

The establishment of sufficient rigidity in the structure has been regarded as a key for increased catalytic activity of the imprinted nanogels. The last possibility is an additional, subsequent polymerization of the imprinted nanogels, since they still contain unreacted double bonds. Additional monomer may or may not be added (see *Table 23-1*). As described in the experimental section, imprinted nanogels were dissolved in chloroform or CyP and then reacted further by thermal- or photo-initiation. Further UV-radiated reactions in CyP were not carried out because in this case there were always side reactions due to the complex photochemistry of CyP.

Table 23-1. Preparation of the subsequently polymerized nanogels.

Entry	Weighed microgel (g) [a]	Added monomer (g) [b]	Added solvent (g) [c]	Added initiator	Polymerization condition	Yield [e] (%)
FP1	ING1 / 0.26	0.26	CyP / 52.13	AIBN / 3-wt.%	thermal, 80°C, 4 days	66.3
FP2	ING1 / 0.30	0.30	$CHCl_3$ / 59.44	AIBN / 3-wt.%	thermal, 60°C, 4 days	54.8
FP3	ING1 / 0.20	0.20	$CHCl_3$ / 39.61	V70 [d] / 3-wt.%	UV radiation, 40 hours	47.0
FP4	ING1 / 0.50	none	$CHCl_3$ / 50.00	V70 / 3-wt.%	UV radiation, 40 hours	85.0
FP5	ING1 / 0.40	none	CyP / 39.66	AIBN / 3-wt.%	thermal, 80°C, 4 days	80.0
FP6	ING1 / 0.40	none	$CHCl_3$ / 39.87	AIBN / 3-wt.%	thermal, 60°C, 4 days	80.0
FP7	ING11 / 0.20	none	$CHCl_3$ / 39.91	AIBN / 5-wt.%	thermal, 60°C, 4 days	98.3
FP8	ING11 / 0.20	none	$CHCl_3$ / 39.84	V70 / 5-wt.%	UV radiation, 85 hours	78.6
FP9	ING10 / 0.10	none	$CHCl_3$ / 25.95	AIBN / 5-wt.%	thermal, 60°C, 4 days	87.1
FP10	ING10 / 0.10	none	$CHCl_3$ / 24.65	V70 / 5-wt.%	UV radiation, 65 hours	81.2

[a] ING1 was used for the investigation in FP1~FP6, ING11 for FP7, FP8 and ING10 for FP9, FP10.
[b] Monomer mixture ratio: EDMA : MMA = 8 : 2 (wt/wt).
[c] Solvent was degassed before polymerization by freeze-thaw cycle 3 times in the case of thermal initiated polymerization. However, in the case of UV-radiated polymerization only dried N_2 gas was bubbled to remove atmospheric oxygen.
[d] V70 is an initiator for photo-initiated free radical polymerization.
[e] Yield was calculated by the precipitating method.

In each case, the concentration of the nanogel or monomer was diluted to 1% to avoid undesirable aggregation. The overall yield in this series was found to be larger in the case of nanogels reacted without addition of monomer. For nanogels prepared with addition of the monomer mixture, the yield was around 50%, which indicates that most of the added monomer is not included in the nanogel particles. Without monomer addition, yields of around 80% were obtained, which is similar to a reprecipitation yield.

The characterization of this series of microgels with GPC yielded some important information (see *Table 23-2*).

Table 23-2. Characterization and results of kinetic experiment of further polymerized microgel.

Entry	M_w [a]	M_n [b]	D	M_{abs} [c]	M_{abs}/M_n	Relative enhancement [d]	Enhancement ratio
ING1	**2.18×10^5**	**2.56×10^4**	**8.5**	**4.39×10^5**	**17.1**	**14.8**	---
FP1	5.94×10^5	3.49×10^4	17.1	4.82×10^5	13.8	17.0	1.15
FP2	4.08×10^5	2.81×10^4	14.5	4.32×10^5	15.3	15.2	1.03
FP3	2.98×10^5	2.73×10^4	10.9	4.28×10^5	15.7	12.2	0.83
FP4	2.21×10^5	2.52×10^4	8.8	4.37×10^5	17.3	10.3	0.70
FP5	2.09×10^5	2.45×10^4	8.6	4.41×10^5	18.0	15.4	1.04
FP6	2.05×10^5	2.21×10^4	9.2	4.39×10^5	19.9	17.6	1.19
ING11	**4.05×10^4**	**9.87×10^3**	**4.1**	**2.75×10^5**	**27.8**	**15.5**	---
FP7	3.48×10^4	9.16×10^3	3.8	2.72×10^5	29.7	29.4	1.90
FP8	4.02×10^4	9.38×10^3	4.3	3.16×10^5	33.7	28.5	1.84
ING10	**2.21×10^5**	**2.85×10^4**	**7.8**	**7.06×10^5**	**24.8**	**52.7**	---
FP9	1.98×10^5	2.32×10^4	8.5	7.19×10^5	31.6	57.0	1.08
FP10	2.11×10^5	2.50×10^4	8.4	7.32×10^5	29.2	55.4	1.05

[a] Weight-averaged molecular weight by GPC.
[b] Number-averaged molecular weight by GPC.
[c] Absolute number-averaged molecular weight by membrane osmometry.
[d] Compared with the rate constant in buffer solution.

First, the number-averaged molecular weights of the microgels prepared by addition of monomer were slightly increased, whereas the weight-averaged molecular weights showed a significant increase. This tendency results in a broader polydispersity, about two times larger than that of the original nanogel (compare **ING1** with **FP1**, **FP2** and **FP3**). Even the M_{abs}/M_n

values, which can be interpreted as the degree of compactness in the crosslinked coil structure, showed a tendency to decrease in this series. Since this is the opposite direction with regard to the purpose of this investigation, it was decided not to continue with this method.

On the other hand, nanogels prepared without adding any monomer showed better M_{abs}/M_n values and a constant level of polydispersity (compare **ING1** with **FP4**, **FP5** and **FP6**). However, the most favorable result in this series is the drop in the M_n values. This phenomenon indicates a shrinking of the nanogel particles during the reaction. It can be explained as the result of intramolecular crosslinking in the nanogel particles. The results of the membrane osmometry measurements support this assumption, since most values of M_{abs} are not changed during the treatment. The same situation was observed in the **FP7**, **FP8**, **FP9**, and **FP10** series, which was also prepared without addition of monomers.

Notwithstanding, the kinetic experiments of these further polymerized nanogels showed only a mediocre enhancement in rate constant. Polymers **FP7** and **FP8** displayed some small improvement, while the others showed no enhancement or were even worse. This can be explained by the fact that the nanogel **ING11** has a more loose structure than **ING1** or **ING10**, so that a further polymerization can improve the structural rigidity with respect to **ING11**.

7) Synthesis of nanogels by combining the optimization methods

As described previously, several methods were developed to increase the rate of the catalysis by the imprinted nanogels. These were: A) Increase of the crosslinker contents (**ING1** *vs*. **ING5**), B) Modification of the polymerization temperature (**ING1** *vs*. **ING6**), C) Use of higher functionalized crosslinker (**ING1** *vs*. **ING7**), D) Increase of monomer concentration (**ING1** *vs*. **ING8**), and E) Application of the post-dilution method (**ING1** *vs*. **ING9** and **ING10**). Thus, it was assumed that there are several independent factors in optimizing the catalytic activity of the imprinted nanogels. *Table 24* shows the enhancement factors achieved by each individual optimization method to increase the rigidity of the imprinted nanogel particles. They present the respective enhancement in rate constant of the DPC hydrolysis.

Table 24. The enhancement factors achieved by each individual optimization method.

Optimization method	Corresponding nanogel	k_{impr} / k_{soln}	Enhancement factor [a]
A) Increase of crosslinker contents	**ING5**	25.3	1.7
B) Modification of the polymerization temperature	**ING6**	31.4	2.1
C) Use of more functional crosslinker	**ING7**	55.8	3.8
D) Increasing of the monomer concentration	**ING8**	90.4	6.1
E) Application of the post-dilution method	**ING9**	41.5	2.8

[a] Relative enhancement factor in comparing with the rate constant measured by **ING1**.

Interestingly, some remarkable enhancements in rate constant were observed when these factors were combined (**ING10** and **ING13**). **ING10** was prepared by combining methods B and E, and exhibited a rate enhancement of 52.7 in comparison to the rate constant of DPC hydrolysis in buffer solution. **ING13**, synthesized by the combination of methods B, C and E, showed an enhancement of 78.6.

This implies that, by combination of these methods, a synergistic effect can be expected in catalytic activity of the imprinted nanogels by causing more rigid polymeric structure. Inspired by this implication, an imprinted nanogel with all the factors (A+B+C+D+E) combined was prepared to maximize the optimization for catalytic activity (*Scheme 11*).
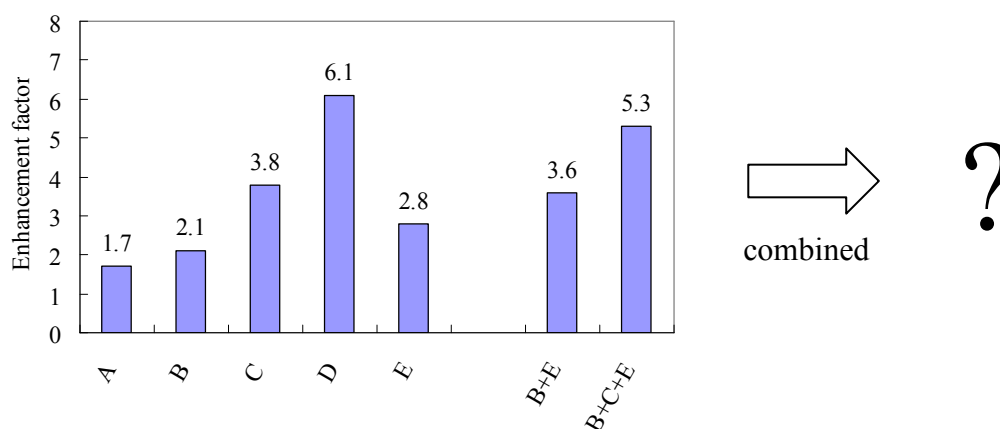
Scheme 11. The enhancement factors achieved by each individual optimization method. Some nanogels displayed better results when the individual methods were combined.

An imprinted nanogel, **ING14**, was prepared for this purpose with a content of 90% TRIM as the crosslinker, using post-dilution and polymerization temperature modification methods (*Table 25-1*). The monomer concentration, the most influential factor in catalytic activity, was determined to be 1.5% after determining the C_m value under the polymerization conditions. The aim here was to prepare an intramolecularly crosslinked particle which would have the highest possible rigidity, while remaining soluble. The corresponding control nanogel **CNG7** was prepared in parallel.

Table 25-1. Preparation of molecularly imprinted nanogels by combining the optimization methods.[a]

Nanogel	TRIM (g)	MMA (g)	DEVPA (g)	Template (g)	Initiator (-wt.%)	Solvent (g)	t_{gel} (min)	Monomer conc.	Crosslinking ratio
ING14	1.80	0.02	0.08	DPP 0.10	AIBN [b] 3.0 / 1.0 / 1.0	CyP 2+126	45	1.5%	90.0%
CNG7	1.80	0.04	0.08	formic acid 0.02	AIBN 3.0 / 1.0 / 1.0	CyP 2+117	45	1.5%	92.8%

[a] Polymerization was carried out at 60°C, 70°C, and 80°C for 133, 112, and 96 hours, respectively.
[b] Initiator was added three times for each polymerization phase.

It was observed that the critical gelation time, t_{gel}, decreased to 45 minutes. The use of TRIM and the increase of crosslinking ratio (90.0%) are thought to be the reason why t_{gel} is shorter under these conditions.

In *Table 25-2* the experimental data and the degree conversion determined by evaporation for **ING14** and **CNG7** are listed. Both **ING14** and **CNG7** showed complete conversions, similar to the results of the pair **ING7** and **CNG3**, prepared with TRIM as a crosslinker (see *Table 19-3*).

Table 25-2. Properties of molecularly imprinted nanogels with combining of the optimizing methods.

Nanogel		Polymerization condition [a]			Properties of intermediates
		Temp. (°C)	Time (hours)	AIBN (-wt.%)	Conversion (%) [b]
ING14	phase 1	60	120 [c]	3.0	> 100.0
	phase 2	70	72	1.0	> 100.0
	phase 3	80	70	1.0	> 100.0
CNG7	phase 1	60	120 [c]	3.0	> 100.0
	phase 2	70	72	1.0	> 100.0
	phase 3	80	70	1.0	> 100.0

[a] Each probe was collected at the end of the corresponding polymerization phase.
[b] Determined by evaporation of the resultant polymerization solution.
[c] Not including t_{gel}.

The data for the analysis of **ING14** and **CNG7** are shown in *Table 25-3*. Interestingly, the degree of conversion obtained from the calculation by precipitation also showed quite high values (99.5% and 89.8%, respectively). In the case of **ING7** and **CNG3**, the TRIM-based nanogels prepared under the condition of 1.0% monomer concentration and 80.0% crosslinking, however, without post-dilution method, showed relatively low conversion by precipitation, even though they had a nearly complete conversion by evaporation (67.9% and 34.8%, respectively. See *Table 19-2*). These results show that nearly all of the monomers have been included in the polymer network and, therefore, more rigidly structured nanogel particles are expected. The difference between the amounts of the incorporated DPP determined by HPLC and titration support this explanation. For ING14, the difference is only around 10%.

Table 25-3. Properties of molecularly imprinted nanogels with combining of the optimizing methods.

Nanogel	Conversion (%)		The amount of DPP (%) [a]		Available cavities (mmol/g)	pK_a range
	by evaporation	by precipitation	by HPLC	by titration		
ING14	> 100.0	99.5	88.9	79.5	0.1023	8.37~8.49
CNG7	> 100.0	89.8	83.5	61.8	0.1360	8.22~8.53
ING1	*63.5*	*53.6*	*67.1*	*33.5*	*0.0670*	*8.68~8.96*

[a] They are expressed in percentages as a proportion to the amount of DPP added in the beginning of the polymerization (*a*). See *Scheme 10* for detail.

After the characterization by GPC and membrane osmometry, the molecular weights of **ING14** and **CNG7** were revealed to be considerably high (*Table 25-4*). M_w of non-extracted **ING14** was 9.02×10^5 whereas M_n was 4.63×10^4. Polydispersity of **ING14** was found to be 19.5, which indicates quite high non-uniformity of the particles. The remarkably high polydispersity of **ING14** was still observable after extraction, giving a value of 18.6. As has

already been pointed out, the high degree of nanogel aggregation might be the reason. With a relatively high concentration of monomers, the probability of interaction between particles would increase. Furthermore, for the preparation of **ING14**, TRIM was employed as a crosslinker; this would provide stronger crosslinking than EDMA. The crosslinking percentage was as high as 90%, so that the overall agglomeration would be most prominent. Looking at the M_{abs}/M_n values, the degree of rigidity is expected to be rather high for good catalytic activity. Membrane osmometry analysis revealed the absolute number-averaged molecular weight of **ING14** to be extremely high, with one million. This is especially interesting since it was found that **ING14** is still soluble in appropriate solvents.

Table 25-4. Characterization of the imprinted nanogels with combining of the optimizing methods.

Nanogel		M_w	M_n	Polydispersity	M_{abs}	M_{abs}/M_n
ING14	non-extracted	9.02×10^5	4.63×10^4	19.5	1.09×10^6	23.5
	extracted	7.85×10^5	4.22×10^4	18.6	9.24×10^5	21.9
CNG7	non-extracted	7.36×10^4	9.08×10^3	8.1	2.07×10^5	22.8
	extracted	6.84×10^4	8.13×10^3	8.4	1.62×10^5	19.9
ING1	*non-extracted*	*2.18×10^5*	*2.56×10^4*	*8.5*	*4.39×10^5*	*17.1*
	extracted	*1.97×10^5*	*2.31×10^4*	*8.5*	*3.81×10^5*	*16.5*

In the kinetic experiments, **ING14** showed a rate enhancement k_{impr} / k_{soln} of 291.4-fold, this being the highest value among the imprinted nanogels (*Table 25-5*). By comparison with the results of **ING1**, it displayed around 20 times higher rate constant (291.4 to 14.8). Furthermore, a fascinating result was obtained by calculating the k_{impr} / k_{contr} value. With a series of parallel kinetic experiments with the corresponding control nanogel **CNG7**, it showed a selectivity of 18.5. In the results of molecularly imprinted macroporous polymer **DP1** for the catalysis of diphenylcarbonate hydrolysis, a selectivity value of 7.8 was

obtained.[32] The imprinted nanogel **ING14** prepared for the same purpose showed a much higher imprinting selectivity than the bulk-type imprinted polymer. The reason may be the better mass transfer properties of the nanogels.

Table 25-5. Results of kinetic experiments of imprinted nanogels with combining of the optimization methods.[a]

Nanogel	k_{impr} (min^{-1})	k_{impr} / k_{soln}	k_{impr} / k_{contr}	Enhancement factor from **ING1** [b]
ING14	7.09 X 10^{-6}	291.4	18.5	19.8
CNG7	4.71 X 10^{-7}	19.4	-	-
ING1	*3.59 X 10^{-7}*	*14.8*	*1.42*	-
DP1 [c]	*7.9 X 10^{-4}*	*588*	*7.8*	-

[a] Experimental condition: 0.05N HEPES (pH=7.3) + MeCN = 1 : 1 (v/v), at 10°C. 2eq. of cavities to 1eq. of substrate. Acetophenone as internal standard.
[b] Relative enhancement factor with comparing the rate constant measured by **ING1**.
[c] Corresponding imprinted macroporous polymer. The composition of the monomer mixture for the preparation of the imprinted polymers consisted of 79.6 wt % of EDMA, 10.4 wt % MMA, and 9.0 wt % of DEVPA-DPP-complex, and 1 wt % of AIBN, diluted by the same weight of the porogen, acetonitrile.[32]

8) Imprinted nanogels bearing one catalytic site per one particle (enzyme analogy)

The ability to determine the number of active sites per individual nanogel particle became available due to the possibility of measuring the molecular weight of the corresponding imprinted nanogels. This is especially interesting for soluble imprinted nanogels, with respect to mimicking enzyme.

Most natural enzymes have only one active site per individual unit. This is considered to be a unique property of this type of catalyst. If we can control the number of active sites in imprinted nanogels, down to one active site per one polymer particle, this is a challenging approach in the mimicry of natural enzymes.

The absolute number-averaged molecular weight M_{abs} (unit: g/mol) is simply multiplied by the number of available active sites of the nanogel (unit: mol/g) to give the number of cavities

per individual particle. In *Table 26* the results of this calculation for the imprinted nanogels are shown. A series of the virtual number of active sites per 40,000 of M_{abs} is inserted for comfortable comparison.

Table 26. Results of calculation of estimated number of cavities per individual imprinted nanogel particle.

Entry	M_{abs} (g/mol) [a]	available cavities after extraction (mmol/g) [b]	number of cavities per individual particle	number of cavities per 40K M_{abs}
ING1	3.81×10^5	0.0670	25.5	2.68
ING2	2.82×10^5	0.0737	20.8	2.95
ING3	3.48×10^5	0.0822	28.6	3.32
ING4	4.32×10^5	0.0897	38.7	3.59
ING5	4.92×10^5	0.0970	47.7	3.88
ING6	4.33×10^5	0.1240	53.7	4.96
ING7	4.72×10^5	0.1097	51.8	4.39
ING8	6.23×10^5	0.0984	61.3	3.94
ING9	5.94×10^5	0.0850	50.5	3.40
ING10	6.24×10^5	0.0733	45.7	2.93
ING11	2.61×10^5	0.0699	18.2	2.80
ING12	4.43×10^4	0.0409	1.8	1.64
ING13	6.92×10^5	0.0852	59.0	3.41
ING14	9.24×10^5	0.1023	94.5	4.09

[a] Absolute number-averaged molecular weight determined by membrane osmometry.
[b] Determined by acid-base titration.

The general tendency was observed that more active sites were available when the corresponding nanogel had a more rigid structure or a higher molecular weight. A series of imprinted nanogels with increasing crosslinking ratio (from **ING2** to **ING5**) showed a simple dependence in this respect. Moreover, with application of the various optimization methods, the nanogels from **ING6** to **ING9** displayed a relatively high number of active sites per individual particle, yielding over 50 in all cases. In case of **ING14**, which was prepared to obtain a highly rigid structure, this polymer showed 94.5 catalytic sites per particle, the highest value.

Of general interest is also the number of active sites per 40K M_{abs}. This value shows the relative density of active sites in the nanogel. In this case there is a correction for the different M_{abs}. It is clear that a nanogel of high molecular weight will contain more active sites. From the value per 40K M_{abs}, however, a relative high incorporation of active sites can be seen, *e.g.* in **ING6**, **ING7**, and **ING14**.

An interesting result was obtained with **ING12**. This nanogel showed an extremely low number (1.8) of active sites per particle. One reason is the small size of these particles. Inspired by this result, the synthesis of another imprinted nanogel was planned to have, on average, just one active site on one individual particle. **ING16** and the corresponding control nanogel **CNG8** were prepared analogously as **ING12**, except that only half of the complex of the functional amidine monomer DEVPA **3** and the template DPP **2** was added (*Table 27-1*).

Table 27-1. Preparation of molecularly imprinted nanogels possessing one active site per one individual nanogel particle.

Nanogel	EDMA (g)	MMA (g)	DEVPA (g)	Template (g)	Initiator (-wt.%)	Solvent (g)	t_{gel} (min)	Monomer conc.	Crosslinking ratio
ING16	1.60	0.31	0.04	DPP 0.05	AIBN 3.0 / 1.0 / 1.0	CyP 2+1996.0	90	0.1%	80.0%
CNG8	1.60	0.31	0.04	formic acid 0.01	AIBN 3.0 / 1.0 / 1.0	CyP 2+1996.0	90	0.1%	83.4%

The critical gelation times, t_{gel}, of **ING16** and **CNG8** were 90 minutes, while those of **ING12** and the corresponding control nanogel **CNG6** were 120 minutes. Experimental data and the results of the analysis are presented in *Tables 27-2* and *27-3*.

Table 27-2. Properties of molecularly imprinted nanogels possessing one active site per one individual nanogel particle.

Nanogel		Polymerization condition [a]			Properties of intermediates
		Temp. (°C)	Time (hours)	AIBN (-wt.%)	Conversion (%) [b]
ING16	phase 1	60	135 [c]	3.0	43.0
	phase 2	70	75	1.0	47.8
	phase 3	80	80	1.0	51.9
CNG8	phase 1	60	135 [c]	3.0	15.8
	phase 2	70	75	1.0	18.1
	phase 3	80	80	1.0	21.9

[a] Each probe was collected at the end of corresponding polymerization phase.
[b] Determined by evaporation of the resultant polymerization solution.
[c] Not including t_{gel}.

Table 27-3. Properties of molecularly imprinted nanogels possessing one active site per one individual nanogel particle.

Nanogel	Conversion (%)		The amount of DPP (%) [a]		Available cavities (mmol/g)	pK$_a$ range
	by evaporation	by precipitation	by HPLC	by titration		
ING16	51.9	31.4	56.3	25.6	0.0265	8.26~8.68
CNG8	21.9	20.2	59.0	19.3	0.0242	8.25~8.54
ING12	*55.2*	*27.6*	*55.6*	*26.4*	*0.0528*	*8.19~8.29*

[a] They are expressed in percentages as a proportion to the amount of DPP added in the beginning of the polymerization (*a*). See *Scheme 10* for detail.

The degree of conversion of **ING16** was quite similar to that of **ING12**. By evaporation it showed more than 50% of conversion; however, by precipitation it was only around 30%. **CNG8** was found to have the poorest conversion among the nanogels prepared. It exhibited around 20% conversion by both of evaporation and precipitation. At very low monomer concentration the conversion is generally low.

The most interesting value in the table might be the number of available cavities of **ING16** determined by potentiometric titration. After removing the template, it was found to possess

0.0265 mmol/g of active sites. This value is just half that of **ING12**, which is not surprising because only half the amount of amidine-template complex was added in the preparation.

To calculate the number of free cavities per one nanogel particle, **ING16** and **CNG8** were characterized by GPC and membrane osmometry (*Table 27-4*).

Table 27-4. Characterization of the imprinted nanogels possessing one active site per one individual nanogel particle.

Nanogel		M_w	M_n	polydispersity	M_{abs}	M_{abs}/M_n
ING16	non-extracted	2.15×10^3	1.37×10^3	1.57	4.63×10^4	33.8
	extracted	1.99×10^3	1.30×10^3	1.54	3.90×10^4	30.1
CNG8	non-extracted	1.08×10^3	7.92×10^2	1.37	2.63×10^4	33.2
	extracted	9.89×10^2	7.35×10^2	1.35	2.31×10^4	31.5
ING12	*non-extracted*	*2.33×10^3*	*1.43×10^3*	*1.63*	*4.88×10^4*	*34.1*
	extracted	*2.07×10^3*	*1.34×10^3*	*1.54*	*4.43×10^4*	*33.0*

Similar to **ING12**, relatively low molecular weights were observed for both **ING16** and CNG8. M_{abs}/M_n values were also high, with values around 30.

Table 27-5. Results of calculation of estimated number of cavities per individual imprinted nanogel particle **ING16** and **CNG8**.

Entry	M_{abs} (g/mol) [a]	available cavities after extraction (mmol/g) [b]	number of cavities per individual particle	number of cavities per 40K M_{abs} ($\times 10^{24}$)
ING16	3.90×10^4	0.0265	1.03	1.06
CNG8	2.31×10^4	0.0242	0.56	0.97

[a] Absolute number-averaged molecular weight determined by membrane osmometry.
[b] Determined by acid-base titration.

The result of the calculation of the number of active sites per particle in **ING16** was 1.03 (*Table 27-5*). The value of the corresponding control nanogel **CNG8** was, with 0.56, about half that of **ING16**. This is a very encouraging outcome, since a nanogel with approximately only one active site in a single particle was synthesized, like a natural enzyme.

Of special interest is the catalytic activity of these enzyme models. The results of the kinetic experiments with **ING16** and **CNG8** are shown in *Table 27-6*.

Table 27-6. Results of kinetic experiments of imprinted nanogels for approximately possessing of one active site per one individual nanogel particle.[a]

Nanogel	k_{impr} (min^{-1})	k_{impr}/k_{soln}	k_{impr}/k_{contr}
ING16	3.91 X 10^{-7}	16.1	2.43
CNG8	1.61 X 10^{-7}	6.6	-
ING12	*3.48 X 10^{-7}*	*14.3*	*2.58*

[a] Experimental condition: 0.05N HEPES (pH=7.3) + MeCN = 1 : 1 (v/v), at 10°C. 2eq. of cavities to 1eq. of substrate. Acetophenone as internal standard.

As presented in *Table 27-6*, the kinetic experiment with **ING16** gave very similar results to **ING12** (14.3 for **ING12**, 16.1 for **ING16**). This shows that the amount of active sites per individual nanogel particle itself does not affect the catalytic activities. Even the values for the imprinting selectivity k_{impr}/k_{contr} were found to be similar for both nanogels (2.58 for **ING12**, and 2.43 for **ING16**).

Michaelis-Menten kinetics

Up to this point, it has been consistently proven that the nanogels imprinted with DPP **2** are catalytically active in DPC **1** hydrolysis. Through several optimizations they showed up to a 290-times enhancement in rate constant compared with the reaction in buffer. In addition, typical enzymatic behavior was observed with these imprinted nanogels. Similarly to enzymes, typical data like V_{max}, K_m, and k_{cat} could be derived (see *Figure 2*).
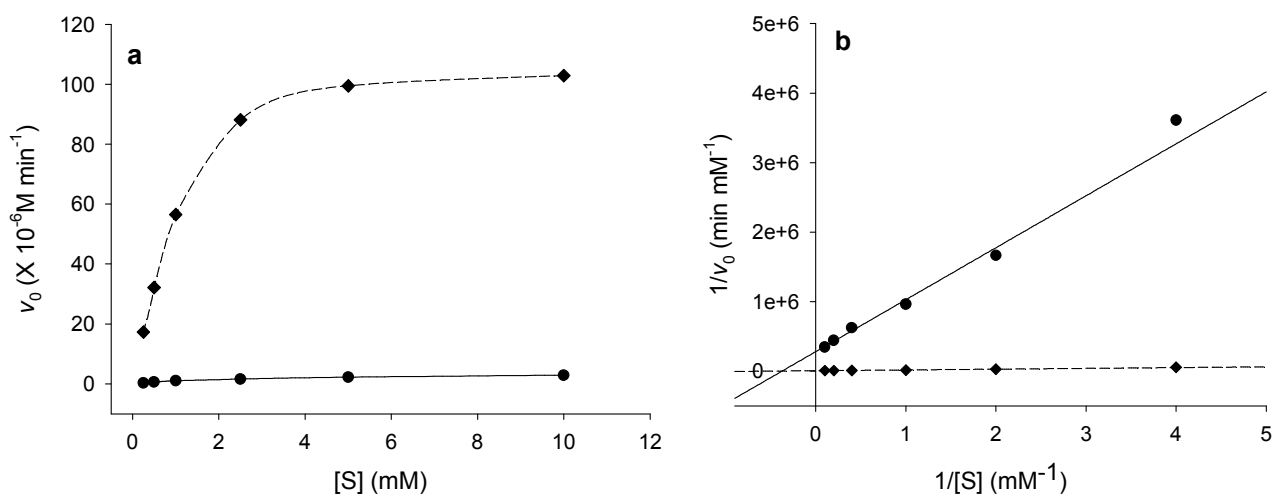
Figure 13. (a) Michaelis-Menten curve and (b) Lineweaver-Burk plot of imprinted nanogel (**ING14**, dashed line, ♦) and control nanogel (**CNG7**, solid line, •).

Imprinted nanogel **ING14**, which was proven to be the most effective catalyst among the imprinted nanogels, was investigated in detail. A plot of initial rates of the reaction versus the substrate concentration was measured to clarify the mechanism of the reaction. The hydrolysis of DPC was carried out in the presence of either the imprinted nanogel **ING14** or the control nanogel **CNG7**, respectively, with variation of substrate DPC concentration. In *Figure 13a* the obtained graph is shown; it displays a typical Michealis-Menten curve. The Lineweaver-Burk plot is also drawn for calculation of the kinetic parameters (*Figure 13b*). The results of the plot interpretation are shown in *Table 28-1*.

Table 28-1. Results of Michaelis-Menten kinetics using the imprinted nanogel **ING14** and the corresponding control nanogel **CNG7**.

catalyst	ING14	CNG7
K_m [mM]	1.82	3.66
V_{max} [mM min^{-1}]	1.45×10^{-4}	4.47×10^{-6}
k_{cat} [min^{-1}]	7.27×10^{-5}	2.23×10^{-6}
k_{cat}/K_m [min^{-1} M^{-1}]	3.99×10^{-2}	6.10×10^{-4}
Ratio of k_{cat}/K_m of **ING14** and **CNG7**	65.6	

In the case of **ING14** the values were found to be $K_m = 1.82$ mM, $k_{cat} = 7.27 \times 10^{-5}$, $V_{max} = 1.45 \times 10^{-4}$ mM min^{-1} and $k_{cat}/K_m = 0.0399$ min^{-1}M^{-1}, respectively. The corresponding control nanogel **CNG7** was also investigated for comparison purposes, yielding $K_m = 3.66$ mM, $k_{cat} = 2.23 \times 10^{-6}$, $V_{max} = 4.47 \times 10^{-6}$ mM min^{-1} and $k_{cat}/K_m = 6.10 \times 10^{-4}$ min^{-1}M^{-1}. These values are lower compared with those for insoluble imprinted bulk-type polymers (*Table 28-2*).

The soluble imprinted nanogel **ING14** showed a better value for K_m than the corresponding imprinted macroporous polymer **DP1**. However, the other parameters, such as V_{max} and k_{cat}, are poorer for **ING14** than for **DP1**. Especially, the factor k_{cat}/K_m showed that the efficiency of **DP1** is around 60 times better than that of **ING14**, with k_{cat}/K_m of **ING14** being around 0.04, whereas that of **DP1** is 2.30.

Table 28-2. Results of Michaelis-Menten kinetics using the imprinted insoluble polymers **DP1** and the corresponding control polymer **DPF**.

catalyst	DP1 (bulk)	DPF (bulk) [a]
K_m [mM]	5.01	2.57
V_{max} [mM min^{-1}]	2.27×10^{-2}	5.89×10^{-3}
k_{cat} [min^{-1}]	0.0115	0.0030
k_{cat}/K_m [min^{-1} M^{-1}]	2.30	1.16
Ratio of k_{cat}/K_m of **DP1** and **DPF**	1.98	

[a] Imprinted with formic acid as a template.

These results indicate that the substrate affinity for the free cavities in **ING14** is quite appreciable, but that the catalytic step from substrate to product is slower. This phenomenon might be explained by the poorer rigidity of the imprinted nanogels. If they are too flexible, the transition state stabilization is lower.

On the other hand, it was shown that the selectivity of the imprinted nanogels was better than that of the imprinted bulk polymers (see *Table 25-5*). The imprinted nanogel **ING14** and the corresponding control nanogel **CNG7** showed a k_{impr} / k_{contr} value of 18.5, whereas **DP1** and the control polymer **DPF** exhibited a value of 7.8.

Comparing the k_{cat}/K_m values of **ING14** and the control **CNG6**, the soluble imprinted nanogel **ING14** show a 65.6-fold higher value than the control. This shows a very good imprinting selectivity that is much higher compared to macroporous imprinted polymers **DP1** and **DPF** with a ratio of 1.98.

Investigations by electron microscopy

In recent years a number of analytical techniques involving transmission electron microscopy have been employed in the field of materials science in order to study the structure and chemistry of both perfect crystals and their interfaces at the atomic level. There are only two widely accepted atomic-resolution methods that can actually help us visualize the atomic structures: high-resolution transmission electron microscopy (HRTEM) and high-resolution scanning transmission electron microscopy (STEM).

HRTEM images are mainly sensitive to the changes in a phase of the incoming parallel electron wave as it passes through the specimen. Such images provide very reliable information about the crystallography of the specimen in a chosen crystallographic orientation. Moreover, even the chemical composition of single dots can be addressed with additional TEM tools such as electron energy loss spectroscopy (EELS). The local structure can be obtained from HRTEM images only by image simulation including all the parameters that influence the final HRTEM images, such as lens aberrations, defocus value and the thickness of the specimen.[95]

Although the reciprocity theorem of scattering theory for electron microscopy states that a HRTEM and a bright-field (BF) high-resolution STEM should provide the same information, the basic difference between HRTEM and STEM is that in STEM the image is formed with no refocus of the scattered electrons. The STEM image is produced by detecting the intensity of the electron flux in a convergent-beam electron diffraction pattern that is integrated over the detector geometry as a function of the scanning electron probe position. The advantage of STEM for the investigation of organic materials is the lower energy of the electron beam. With HRTEM, decomposition of organic material is frequently encountered, while in STEM this is less pronounced.

As an initial attempt, **ING1** was investigated by ordinary scanning electron microscopy (SEM). **ING1** was first dissolved in chloroform (1mg/ml) and the solution was dropped on an iron plate. The measurement was carried out after evaporation of the solvent under vacuum. The results are shown in *Figure 14*. The size of the **ING1** particles is 200~500nm, as shown in *Figure 14A*.
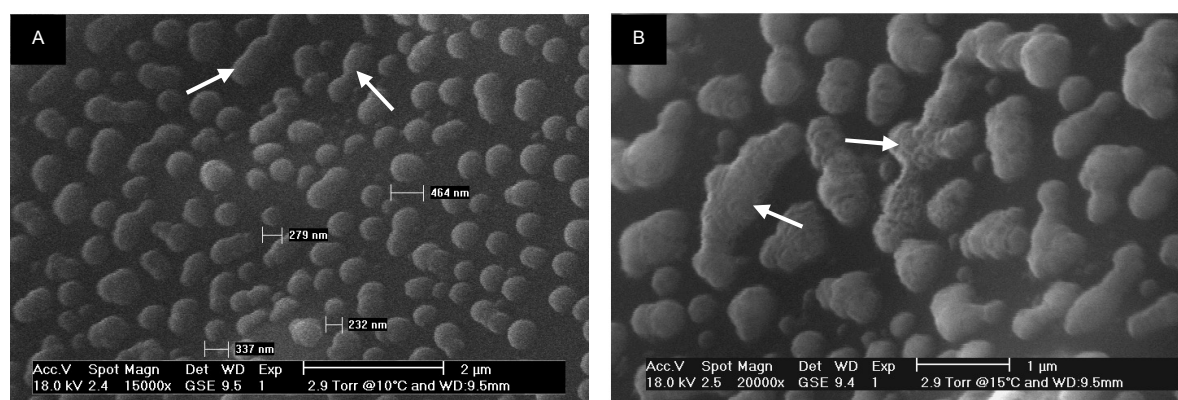

Figure 14. Scanning electron micrographs of **ING1**.

It was also shown that some of the particles participated in inter-particle interactions to form aggregates (see arrows in *Figure 14A*). At higher magnification, irregular shapes of the particles were clearly observed, as shown in *Figure 14B*. The aggregation here was more pronounced, since particles of more than 1 μm were observed (see arrows in *Figure 14B*).

This type of aggregation is already well known from several investigations on nanogel formation. Especially, it has been reported that the nanogels became insoluble once they were dried.[96,97] This might be due to unreacted double bonds in the nanogel particles. The existence of these unreacted double bonds was confirmed by the doublet at 5 - 6 ppm in the ^{1}H NMR spectrum of the imprinted nanogels. During the drying process, these unreacted double bonds can interact with each other as they become less separated as the solvent is removed. The observed insolubility after drying might be due to the aggregation of the particles caused by these interactions.

In order to avoid interactions between particles another nanogel was synthesized (**ING15**) that was never subjected to a drying step. It was prepared with only 0.1% of monomer concentration *cf.* **ING14** (*Table 29*). **ING15** was only prepared for the microscopic measurement and, thus. it was not investigated further.

Table 29. Preparation of molecularly imprinted nanogels by combination of the optimization methods.[a]

Nanogel	EDMA (g)	MMA (g)	DEVPA (g)	Template (g)	Initiator (-wt.%)	Solvent (g)	t_{gel} (min)	Monomer conc.	Crosslinking ratio
ING15	1.60	0.22	0.08	DPP 0.10	AIBN [b] 3.0 / 1.0 / 1.0	CyP 2+1996	120	0.1%	80.0%

[a] Polymerization was carried out at 60°C, 70°C, and 80°C for 92, 70, and 72 hours, respectively.
[b] Initiator was added three times for each polymerization phase.

Ordinary scanning electron microscopy (SEM) has a relatively low resolution. The resolution in transmission electron microscopy is much better. For the transmission electron microscopy (TEM) measurements, the samples had to be stained. There were two staining methods used, (i) using uranyl acetate $(UO_2)(CH_3COO)_2 \cdot 2H_2O$ (UAc$_2$) in solution and (ii) using ruthenium tetraoxide RuO_4 in the gas phase. Of these two different staining methods, RuO_4 was preferred due to the easier preparation and more homogeneous staining. The measurements were performed in the imaging mode (HRTEM) as well as in the scanning mode (STEM). In addition, elemental analysis (EDX) was performed using an EDAX system with Si/Li detector. For the measurements, bigger particle size portions of **ING15** were removed by centrifugation under mild condition (300 rpm over 5 min). The measurement of **ING15** was performed with two samples, i.e. one which had been centrifuged and one which had not. A dilute solution of the nanogel in chloroform was dropped onto a carbon coated Cu-grid. After evaporation of the solvent, the sample was investigated by STEM and HRTEM under liquid N_2 cryo-condition (FEI Tecnai F30 ST at 300 KV equipped with a field emission gun).

In *Figure 15* a STEM image of **ING15** particles is shown with uranium contrast. Around 20 - 40 nm sized particles were observed. This size range was confirmed again by HRTEM (*Figure 16*).
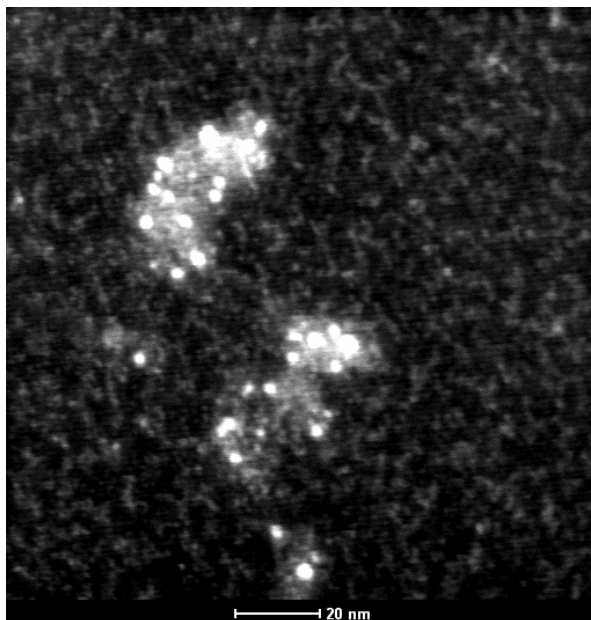

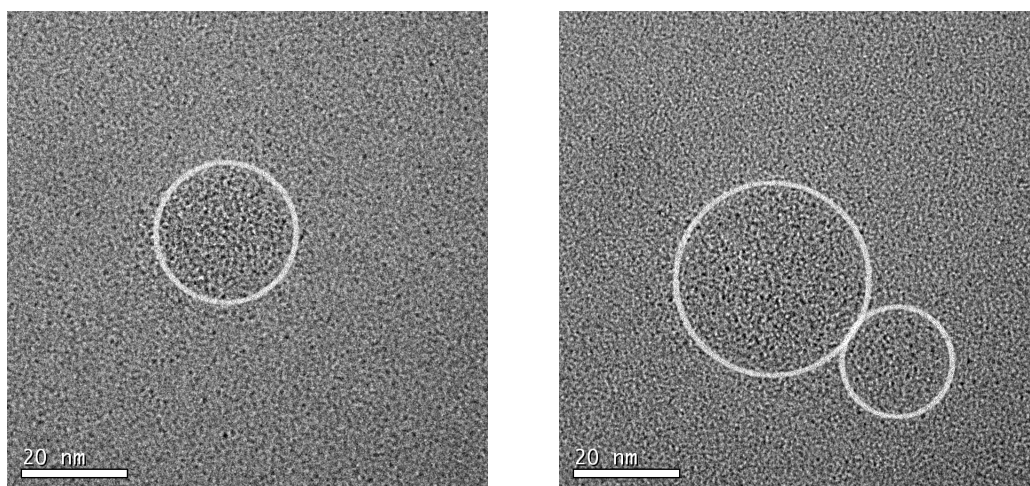Figure 15. Transmission electronic microscopy in scanning mode (STEM) of centrifuged **ING15**. Stained with UAc_2.

Figure 16. Transmission electronic microscopy in imaging mode (HRTEM) of centrifuged **ING15**. Stained with RuO_4.

These HRTEM images in *Figure 16* were obtained from particles stained using ruthenium tetraoxide. The staining with ruthenium was confirmed by EDX analysis. Although the overall contrast of the images seems relatively poor, such that the shape of the particles cannot be distinguished, the size range is approximately 20~40 nm (in marked circles).
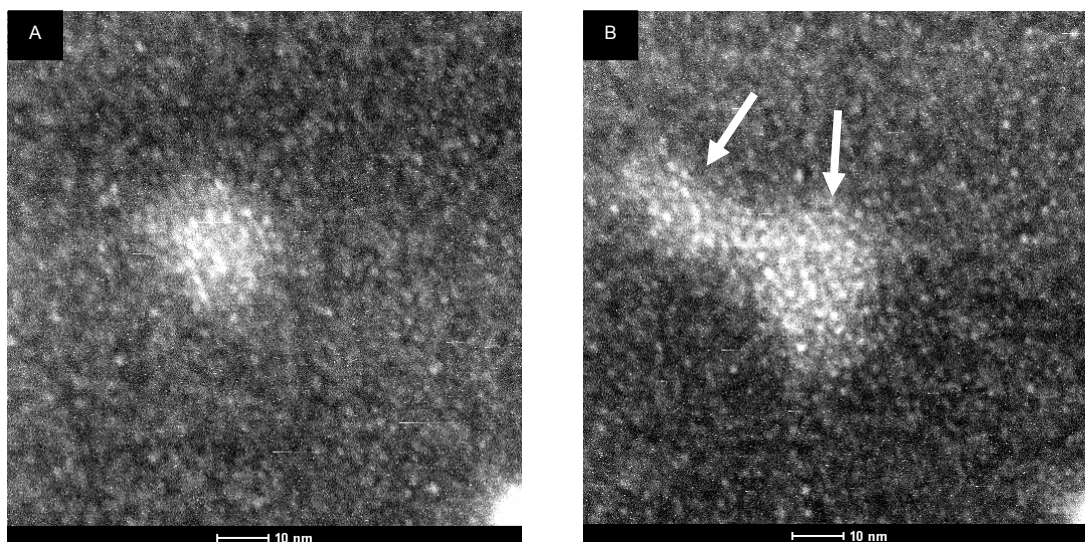

Figure 17. Transmission electron microscopy in scanning mode (STEM) of centrifuged **ING15**. Stained with RuO$_4$.

The investigation with STEM of the ruthenium stained particles brought better images. As seen in *Figure 17*, centrifuged **ING15** nanogel particles stained with RuO$_4$ were investigated by STEM. The micrograph indicates that particles of 15~20 nm are present (*Figure 17A*) and that there are still aggregated particles, even though the sample was centrifuged (see arrows in *Figure 17B*).

It was noticed that the concentration of the centrifuged sample was too low to produce overviews with many particles. Actually, it was found that the concentration of the nanogel particles was 0.25mg/mL, which was determined after drying of solvent. This means that most of the particles, including the bigger particle portions, were removed during the centrifugation.

However, in the case of non-centrifuged **ING15** nanogel particles, overview images were obtained more clearly (*Figure 18A*).
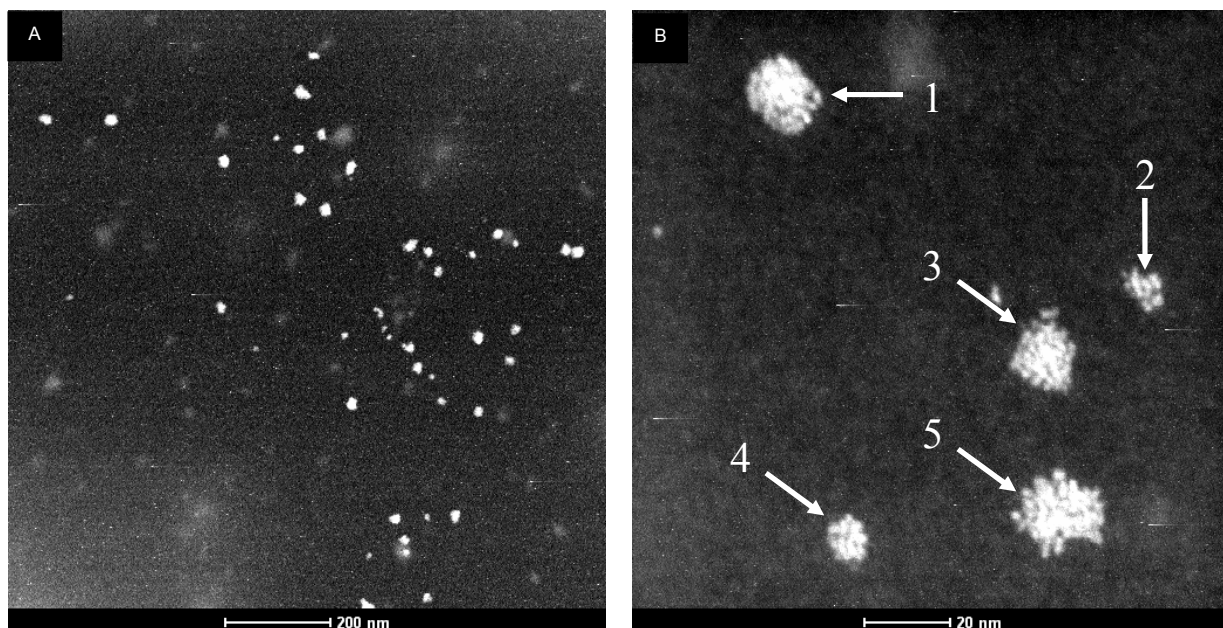
Figure 18. Transmission electron microscopy in scanning mode (STEM) of non-centrifuged **ING15**. Stained with RuO$_4$.

In more magnified image on the right hand side (*Figure 18B*), the size of the particles was determined to be around 8~20 nm. The approximate diameters measured for each particle in *Figure 18B* are 1: 16 nm, 2: 10 nm, 3: 17 nm, 4: 11 nm, and 5: 20 nm, respectively. An EDX analysis confirmed the staining with ruthenium in **ING15** (*Figure 19*).

In *Figure 20* a HRTEM image of non-centrifuged **ING15** particles stained with RuO$_4$ is shown. The size of each particle
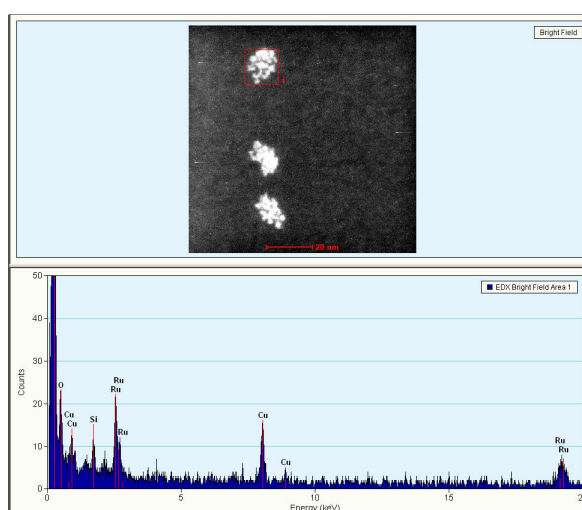
Figure 19. Proof of ruthenium contrast in ING15 by EDX analysis.

was also determined approximately to give 1: 18nm, 2: 21nm, 3: 18nm, 4: 21nm, and 5: 17nm, respectively. The size range of this sample was 17~21nm, i.e. a more narrow size distribution.

Figure 20. Transmission electronic microscopy in imaging mode (HRTEM)
of non-centrifuged **ING15**. Stained with RuO_4.

In the non-centrifuged **ING15** sample the aggregated particles were also detected. As seen in
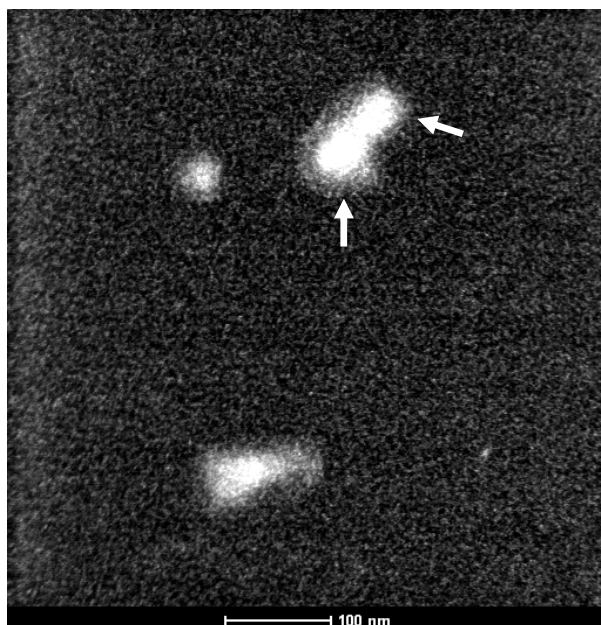
Figure 21. Transmission electronic microscopy in imaging mode
(HRTEM) of non-centrifuged **ING15**. Stained with UAc_2.

Figure 21, the STEM image of the particles stained with UAc_2, the upper right particle seems to consist of two individual particles (see arrows in *Figure 21*).

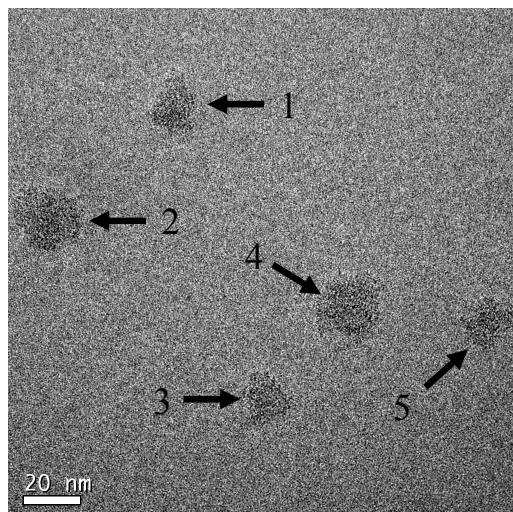However, it was generally observed that only a few particles were agglomerated in pairs. The particles are essentially separated and show a spherical shape. The size distribution is quite small. Through a tilt series of approx. ±40°, the shape and size of the particles did not change. Therefore, it can be assumed that they are rigid and do not collapse onto the support film.

These investigations clearly show that it was indeed possible to prepare soluble nanogels with narrow size distributions in the order of 8 - 20 nm. This is a similar diameter to that possessed by natural enzymes. The same is true with respect to the molecular weight of the nanogels, at around 40,000 Dalton. Since these particles contain, on average, one active catalytic site, a high analogy to natural enzymes was obtained for the first time.

Experimental Section

An overview of the instrumentation

1H-NMR Spectrometer	Varian VXR 200 (200MHz)
	Bruker AC 200 (200MHz)
	Varian VXR 300 (300MHz)
	Bruker DRX 500 (500MHz)
	(TMS as an internal standard)
$^{13}C\{^1H\}$-NMR Spectrometer	Bruker DRX 500 (125MHz)
	Bruker AC 200 (50MHz)
^{31}P-NMR Spectrometer	Bruker DRX 500 (202MHz)
	Varian VXR 200 (81MHz)
Infrared Spectrophotometer	Bruker Vector 22 FT-IR Spectrophotometer
Ultraviolet Spectrophotometer	Perkin-Elmer UV-Spectrophotometer 554
Membrane Osmometer	Knauer A0330 Membrane Osmometer
Semi-permeable Membrane	Knauer Regenerated Cellulose Membrane fein f. 101/102 (cutoff 10K and 20K Dalton)
Elemental Analysis	Institut für Pharmazeutische Chemie der

Universität Düsseldorf

Perkin-Elmer 2400

Milling Machine   Janke & Kunkel, IKA-Werke, A10

Sieves   Siebetechnik GmbH, Mühlheim, Retsch

Sieving Machine   Retsch RV

GPC-system   Pump: Waters 510 pump

Injector: S5200 autosampler

Degasser: Gastorr 150 from SFD

Detector: Waters 486 tunable absorbance detector

Waters 410 differential refractometer

Column: Waters HEMA Columns

Integrator: NTeq GPC-Software V6.1.13

HPLC   Isocratic Pump: Waters 410

Injector: Rheodyne

Column: RP-18 (Merck)

RP-18 ACE-EPS

(Bischoff)

UV-detector: Waters 486

Syringe Filter   SPARTAN RC/0.2, Schleicher & Schuell

Thermostat   F25-MV, Julabo

pH Meter   691 pH Meter, Metrohm

Ultrafitration   Stirring cylinder: Schleicher & Schuell SC 300

                                    Membrane: Celfa CMF-DY-040

Ultracentrifugation   Beckman L8-55

                                    Institut für Biophysik, Universität Düsseldorf

                                    Rotor: Beckman Ti 55.2

Electron Microscopy   Scanning Electron Microscopy (SEM):

                                    Institut für Physikalische Chemie II

                                    Philips XL 30 ESEM

                                    Transmission Electron Microscopy (TEM):

                                    Institut für Physikalische Chemie

                                    Johannes Gutenberg-Universität Mainz

                                    Philips Tecnai F30 analytical TEM instrument

Use of the Instruments

^{1}H (500MHz) and ^{13}C{^{1}H} NMR (125.8MHz) spectra were recorded on a Bruker DRX 500, while ^{31}P-NMR (81MHz) spectra were recorded on a Bruker AC 200, with TMS as internal standard. NMR spectra were measured in CDCl$_3$ at 25°C if not otherwise stated.

Membrane osmometry was performed in chloroform at 28°C with a Knauer A0330 membrane osmometer. Regenerated cellulose membrane fein f. 101/102 (cutoff 10K and 20K Dalton) from Knauer was employed as semi-permeable membrane.

GPC was performed on a GPC-System consisting of a Waters 486 tunable absorbance detector, set at 275 nm, and a Waters 410 differential refractometer with a Waters 510 pump and a degasser gastorr 150 from SFD with an S5200 autosampler unit from SFD with NTeq GPC-Software V6.1.13, using THF as eluent. The system was calibrated with polystyrene standards with a molecular weight range from 580 to 1,186,000 D. The flow rate was 1mL/min. 100µL of a 0.125% (w/w) polymer solution was injected onto a HEMA-column-combination consisting of a pre-column of 40Å and main columns of 40, 100 and 300Å porosities.

pH values were measured with a 691 pH Meter from Metrohm. Before the measurements, a two point calibration was performed using buffer pH 2.0 and 7.0 from Bernd Kraft GmbH.

All HPLC measurements were performed with a set-up consisting of a Waters 410 pump, a Waters 486 UV-detector and a spectral recording and integration software CSW Chromatography Station for Windows, Version 1.7, 2000, Apex Data Ltd. As column, an RP-18 ACE-EPS (Bischoff) or an RP-18 (Merck) was used. Acetophenone or benzylalcohol, distilled before use, was used as internal standard.

STEM and HRTEM measurements were performed using a Philips Tecnai F30 analytical TEM instrument, operated at an accelerating voltage of 300 kv.

Materials

- Solvents

HPLC solvents (acetonitrile: isocratic grade) and all solvents for the kinetic reactions and polymerizations, methylene chloride (peptide grade), chloroform (dry), methanol (extra dry), toluene (dry), acetonitrile (dry) tetrahydrofuran (dry) and ethanol (dry), were supplied by Biosolve. Cyclopentanone (CyP) and cyclohexanone (CyH) were purchased from Acros, extracted with 1 mM aqueous $KMnO_4$ and then distilled before use. Dimethylformamide (DMF), dimethylsulfoxide (DMSO) and 1,4-dioxane were purchased from Merck.

- Initiators

2,2'-Azobisisobutyronitrile (AIBN) from Aldrich was further purified by recrystallization from dry methanol. 2,2'-Azobis(4-methoxy-2,4-dimethylvaleronitrile) (V70) was supplied from Wako and purified by recrystallization in dry ethanol.

- Monomers

Ethylene glycol dimethacrylate (EDMA) and methyl methacrylate (MMA) were purchased from Aldrich and purified by drying over calcium hydride (24 hours), followed by distillation under reduced pressure. Trimethylolpropane trimethacrylate (TRIM) was also purchased from Aldrich and distilled before use. All monomers were stored in a freezer (-26°C).

The functional monomer *N,N'*-diethyl(4-vinylphenyl)amidine (DEVPA) was synthesized in seven steps according to a literature procedure.[98] DEVPA was purified by sublimation twice prior to use.

- Templates and other chemicals

Diphenyl phosphate (DPC, Aldrich), formic acid (Riedel de Haën) and trifluoroacetic acid (Riedel de Haën) were used as received. Diphenylcarbonate (DPC, substrate) was purchased from Merck, recrystallized from dry ethanol and purified by sublimation prior to use. Phenol was supplied from Riedel de Haën and purified by sublimation.

Acetophenone and benzylalcohol, used as internal standards for HPLC investigations, were distilled prior to use. Polyvinylpyrollidone 90 K and polyvinylalcohol 72000 were purchased from Fluka and used as received.

Preparation of the Imprinted Polymers with Varying Crosslinker Ratio

- Highly crosslinked macroporous polymers

For the preparation of the macroreticular imprinted polymers for the catalysis of DPC hydrolysis (**IP**), a functional monomer *N,N'*-diethyl(4-vinylphenyl)amidine (DEVPA) was used for providing of a binding site as well as a catalytic site. A mixture of 0.404 g of DEVPA (2.0 mmol) and an equimolar amount of corresponding template (see *Table 30*) was dissolved in 10.0 ml of acetonitrile to form a complex. 8.00 g of EDMA (40.36 mmol, 7.61 ml) and 1.10 g of MMA (10.95 mmol, 1.17 ml) were added to the solution. The mixtures were homogenized in an ultrasonic bath at 40°C. Finally, 1% (w/w total monomers) of azobisisobutyronitrile (AIBN) was added as an initiator. The monomer mixture was degassed via a "freeze- thaw" procedure. The polymerization was carried out in bulk at 60°C for 72 h in an evacuated ampoule. The polymers were crushed and sieved and only the fraction from 45 to 125 μm was used for the measurements. The corresponding control polymer **CPF**, prepared using formic acid as a template, was also synthesized for comparison.

Table 30. Preparation of a series of imprinted polymers for catalysis.

Entry	EDMA (g) (-wt.%)	MMA (g)	DEVPA (g)	Template (g)	Porogen (ml)	Polymerization method	Yield (%)
IP	8.0 (80.0 %)	1.096	0.404	DPP 0.500	ACN 10.00	bulk	90.1
CPF	8.0 (80.0 %)	1.096	0.404	formic acid 0.092	ACN 10.00	bulk	92.3
2%-IP	0.2 (2.0 %)	8.896	0.404	DPP 0.500	toluene 10.00	suspension	85.1
5%-IP	0.5 (5.0 %)	8.596	0.404	DPP 0.500	toluene 10.00	suspension	83.0
10%-IP	1.0 (10.0 %)	8.096	0.404	DPP 0.500	toluene 10.00	suspension	76.5
S-IP	None	9.096	0.404	DPP 0.500	ACN 10.00	bulk	88.8

- Slightly crosslinked imprinted polymers

A series of slightly crosslinked, imprinted polymers (with 2%, 5%, and 10% of crosslinker (**2%-IP**, **5%-IP**, and **10%-IP**, respectively) was prepared. For the preparation of such polymers with a low amount of crosslinker, the suspension polymerization method was employed. 2.0 mmol of the complex of DEVPA and DPP and corresponding amounts of EDMA and MMA (see *Table 30*) were placed in a 50 ml flask with 0.100 g of AIBN (1.0% w/w total monomers) and 10.00 ml of toluene. After homogenizing in an ultrasonic bath, the mixture was placed in a reactor and bubbled with dried N_2 gas for ten minutes to remove atmospheric oxygen. Afterwards, 150ml of 0.1% of polyvinylpyrrolidone + 0.2% of polyvinylalcohol solution in H_2O were added as surfactant and N_2 bubbling was continued over another 20 minutes. The reactor was then sealed tightly and the contents stirred at 400 rpm for 15 minutes as a pre-stirring. Finally, the polymerization was started by heating the reactor to 70°C overnight. The resulting polymers were washed with freshly distilled H_2O and methanol, filtered and dried in a vacuum oven.

- Non-crosslinked imprinted polymers

A molecularly imprinted polymer prepared without any crosslinker was synthesized (**S-IP**). A mixture of 0.404g of DEVPA (2.00mmol) and 0.500g of DPP (2.00mmol) was mixed with 9.096g of MMA (90.85mmol, 9.718ml) and 10.00ml of acetonitrile in an ampoule. After adding 0.100g of AIBN (1.0% w/w total monomers) the mixed solution was homogenized in an ultrasonic bath and degassed via a "freeze- thaw"-procedure. Subsequently, the ampoule was sealed under vacuum and placed in a 60°C oil bath for 16 hours. The polymerized solution was diluted with 15ml of 1,4-dioxane and added dropwise to isopropanol for precipitation. 8.88 g of white solid were obtained after isolation by filtration, washing and drying under vacuum (yield = 88.8%).

To remove the template, the polymer was first swollen in acetonitrile and, after one hour, the template was washed out by shaking 3-5 times in a 1:1 mixture of 0.1 M sodium hydroxide and acetonitrile in an ice bath until no more template could be removed. The amount of released template was determined by HPLC (eluent: 0.2% (v/v) trifluoroacetic acid in H_2O : acetonitrile 90:20 (v/v), internal standard 5mM benzylalcohol, flow rate 1 ml/min, detected at 218nm). A calibration curve for the determination of the template in presence of the internal standard benzylalcohol was established. At the time when no more template was detectable the polymer solution was washed until neutral using water and acetonitrile. All polymers were dried over phosphorous pentoxide before use in an evacuated drying oven set at 40°C.

Determination of the critical monomer concentration (C_m)

The critical monomer concentration (C_m) is the highest monomer concentration at which the nanogels can remain as a stable solution. To determine C_m, a stock monomer mixture containing ethylene glycol dimethacrylate (EDMA) and methyl methacrylate (MMA) was prepared. Azobisisobutyronitrile (AIBN) (3.0% w/w total monomers) was added as an initiator to this solution. Exact amounts of the resulting solution were poured into pre-weighed borosilicate flasks and diluted with a precise amount of the solvent of choice, to yield from 0.5 - 5 % w/v monomer concentrations with increments of 0.5%. The flasks were sealed and subjected to "freeze -thaw" cycles. Finally, they were placed in an oven at 80°C for 4 days.

The highest monomer concentration that could be employed without sample gelation was taken as the C_m in the solvent of choice. Whenever the polymerization condition was changed, C_m was determined anew experimentally.

Preparation of the Imprinted nanogels

In order to prepare the imprinted nanogels **ING1** and **CNG1**, a monomer mixture of EDMA/MMA (80/20 w/w), binding site functional monomer *N,N'*-diethyl(4-vinylphenyl)amidine (DEVPA, **3**) and template molecule diphenylphosphate (DPP, **2**) were placed in a glass vial with a cap. The mixtures were put into an ultrasonic bath to be homogenized. The well-mixed solutions were transferred to a pre-weighed round-bottomed flask and diluted with the desired amount of solvent, maintaining the monomer concentration below the C_m.

Finally, AIBN (3% w/w total monomers) was added to the solution, the flask sealed tightly and degassed three times through "freeze -thaw" procedure. The polymerization was usually

carried out at 80°C for 4 days. **ING2**, **ING3**, **ING4** and **ING5** were prepared with the same method but with variation of the crosslinking ratio.

*- Modification of the polymerization temperature (**ING6, ING7**)*

A monomer mixture of EDMA/MMA with the complex between DEVPA and template molecule DPP was homogenized using an ultrasonic bath. The well-mixed solutions were placed in a pre-weighed round-bottomed flask and diluted with the desired amount of solvent, maintaining the monomer concentration below the C_m. AIBN (3% w/w total monomers) was added to the solution, the flask sealed tightly and degassed three times using a "freeze"-thaw procedure. The polymerization was carried out at 60°C for six days as the first phase. The polymerization solution was then cooled to ambient temperature and a small portion was collected to determine the halfway degree of conversion using the evaporation method. Additional initiator was put in and the solution degassed again. The second phase started when the polymerization solution was placed in an oven set at 70°C and continued for four days. The final phase was the same as the second, except that the temperature was increased to 80°C for 4 days. For **ING7**, TRIM was used as the crosslinker instead of EDMA (**ING6**).

*- The post-dilution method (**ING9**)*

The monomer mixture containing crosslinker, comonomer, functional monomer-template complex and initiator was mixed with the same weight of the solvent of choice. After "freeze-thaw" cycling, the mixed solution was placed in an oven set at 60°C for the critical polymerization period. The critical gelation time t_{gel} is the longest time in which the resultant mixture does not get turbid after polymerization.

Just after this period the solution was immediately diluted with the selected solvent to the dilution required. After degassing with N_2, the solution was polymerized.

A quick overview of all imprinted nanogels formulations is shown in *Table 31*.

Table 31. Imprinted nanogels by radical polymerization in solution.

Entry [a]	Template	Monomer conc. wt.-%	Crosslinker Class	Crosslinker wt.-%	Temperature increased [b]	Post dilution [c]
ING1	DPP	1.0	EDMA	80	No	No
CNG1	formic acid	1.0	EDMA	80	No	No
ING2	DPP	1.0	EDMA	60	No	No
ING3	DPP	1.0	EDMA	70	No	No
ING4	DPP	1.0	EDMA	85	No	No
ING5	DPP	1.0	EDMA	90	No	No
ING6	DPP	1.0	EDMA	80	Yes	No
CNG2	formic acid	1.0	EDMA	83	Yes	No
ING7	DPP	1.0	TRIM	80	Yes	No
CNG3	formic acid	1.0	TRIM	83	Yes	No
ING8	DPP	1.5	EDMA	80	Yes	No
ING9	DPP	1.0	EDMA	80	No	Yes
ING10	DPP	1.0	EDMA	80	Yes	Yes
CNG4	formic acid	1.0	EDMA	83	Yes	Yes
ING11	DPP	0.5	EDMA	80	Yes	Yes
CNG5	formic acid	0.5	EDMA	83	Yes	Yes
ING12	DPP	0.1	EDMA	80	Yes	Yes
CNG6	formic acid	0.1	EDMA	83	Yes	Yes
ING13	DPP	1.0	TRIM	80	Yes	Yes
ING14	DPP	1.5	TRIM	90	Yes	Yes
CNG7	formic acid	1.5	TRIM	93	Yes	Yes
ING15 [d]	DPP	0.1	EDMA	80	Yes	Yes
ING16	DPP(half) [e]	0.1	EDMA	80	Yes	Yes
CNG8	formic acid(Half)	0.1	EDMA	80	Yes	Yes

[a] ING: Imprinted nanogel, CNG: Control nanogel in pairing with imprinted nanogel just above presented in row.
[b] Polymerization was carried out at 60, 70 and 80°C.
[c] Solvent was added after beginning of polymerization.
[d] Prepared only for the purpose of transmission electronic microscopic measurement. Thus, it was never extracted.
[e] Only half of amidine **3** and DPP complex was added.

Stepwise Polymerization

To increase the rigidity of the nanogel structure, stepwise polymerization was carried out. This was done in two ways, either with or without addition of extra monomers. A specific amount of non-extracted nanogel was dissolved in chloroform or cyclopentanone, followed by

polymerization via thermal initiation or UV irradiation. The general preparation is described in *Table 23-1*. In all cases, the concentration of the nanogel or the monomer was kept below the value of C_m.

Determination of the degree of conversion

A pre-weighed glass vial was filled with a defined amount of the polymerization solution. The solution was evaporated under vacuum at room temperature and finally dried to constant weight in a vacuum oven set at 80°C. The degree of conversion can be calculated from the weight of the residue, which is the amount of nanogel formed in the polymerization and the total amount of the solution. The other way to calculate the degree of conversion is to determine it directly from the weight of the isolated nanogel. It was found to be comparable with the values calculated by sample evaporation.

Isolation of the nanogels

Petroleum ether (60 - 80°C boiling point fraction) was chosen as the precipitating solvent for the nanogels that were synthesized in cyclopentanone (CyP) or cyclohexanone (CyH). A mixed solvent comprising toluene and petroleum ether (2/5, v/v) was used for precipitation of the nanogels prepared in dimethylformamide (DMF).

In all cases, the polymerization solution was cooled down to ambient temperature and evaporated to around one third its original volume. The chosen precipitating solvent was added cautiously until the polymerization solution became turbid. The turbid solution then was added dropwise into about five times its volume of vigorously stirred precipitating solvent.

The precipitated nanogel was separated by filtration, ultrafiltration or ultracentrifugation. When the nanogel was ultracentrifuged, the condition was 9000 rpm for 20 minutes.

Determination of the molecular weight of the nanogels

The relative molecular weight of nanogels was determined by gel permeation chromatography (GPC). Samples were prepared by dissolving *ca.* 10 mg of nanogel in 4 ml of tetrahydrofuran (THF). Polystyrene standards were used for the calibration, with THF as the mobile phase.

Membrane osmometry was employed to determine the absolute molecular weight of nanogels. The measurements were carried out in chloroform at 28°C using a Knauer A0330 membrane osmometer. A regenerated cellulose membrane fein f. 101/102 from Knauer was used for the measurements. Before the measurements, lower molecular weight portions were removed by ultracentrifugation, ultrafiltration or reprecipitation. The osmotic pressure was measured for at least 4 samples in a concentration range between 0.001 and 0.01 g/ml. The molecular weights were obtained from the π/c *vs* c plots (π is the osmotic pressure and c is the concentration). In all cases, the correlation coefficient was greater than 0.95.

Extraction of the imprinted nanogels

To remove the template molecule DPP from the imprinted nanogel, liquid-liquid extraction was employed. This is possible due to the solubility of the nanogels in appropriate solvents.

The imprinted nanogel was dissolved in chloroform and extracted with ice-cooled aqueous 0.05N NaOH solution (three times) as quickly as possible. Neutralization was followed by distilled water 3 times. The organic layer was dried with magnesium sulphate, filtered and then evaporated until a small volume remained. The remainder was added dropwise in petroleum ether to be precipitated and finally isolated by ultracentrifugation.

The amount of template molecule extracted was quantified by HPLC (mobile phase: 0.2% (v/v) trifluoroacetic acid in water / acetonitrile 90:20 (v/v), internal standard 5mM benzyl alcohol, flow rate 1.0 mL/min, at 218 nm detected by UV detector, C18 reverse column). A

calibration curve for the determination of the template in the presence of the internal standard benzyl alcohol was established prior to the measurements.

Table 32 shows the amount of DPP incorporated, as determined by HPLC, along with the titration of the amidine moieties in the polymers for all imprinted nanogels.

Table 32. The amount of the incorporated DPP/amidine determined by HPLC and titration.

Nanogel	The amount (%)		Nanogel	The amount (%)		Nanogel	The amount (%)	
	of DPP by HPLC	of amidine by titration		of DPP by HPLC	of amidine by titration		of DPP by HPLC	of amidine by titration
ING1	67.1	33.5	ING7	77.2	55.4	ING12	55.6	26.4
CNG1	74.3	44.7	CNG3	59.3	33.2	CNG6	51.2	21.4
ING2	63.1	36.9	ING8	92.5	91.9	ING13	82.1	42.2
ING3	66.8	41.5	ING9	79.3	42.6	ING14	88.9	79.5
ING4	65.2	45.9	ING10	74.4	37.2	CNG7	83.5	61.8
ING5	71.4	49.1	CNG4	61.2	31.1	ING15	N/A [a]	N/A
ING6	87.9	62.0	ING11	63.0	34.4	ING16	56.3	25.6
CNG2	61.3	42.0	CNG5	65.2	21.9	CNG8	59.0	19.3

[a] Prepared only for the purpose of transmission electronic microscopic measurement. Thus, not extracted ever.

Titration of the imprinted nanogels

For the calculation of the amount of the remaining available active sites, acid-base titrations were performed. A mixed solvent containing aqueous 0.1N NaCl : acetonitrile (1:1 v/v) was prepared and 60.0 mL of the mixed solvent was placed in 100 mL 2-necked round-bottomed flask. The solvent was degassed using a "boiling-and-cooling" method. The solvent is refluxed, using a condenser, and then dry nitrogen gas was bubbled while it was cooling. The extracted nanogel (30.0mg) was dispersed and then stirred for 3 hours to be swollen. The pH value was checked, using a pH-microelectrode, with addition of aqueous 0.02N HCl. The

resulting curve from the measured pH-value plotted versus the HCl concentration had an inflection point from which the amount of accessible amidine groups could be calculated.

General Procedure for the kinetic measurements

The hydrolysis of the carbonates was carried out under optimal conditions for the amidine based nanogels in an 1:1 mixture of aqueous 2-[4-(2-hydroxyethyl)-1-piperazino]-ethanesulfonic acid (HEPES) buffer with a pH of 7.3 and acetonitrile at a temperature of 10°C. For this purpose, dried polymer with 4×10^{-6} mol of free cavities was dissolved in 1.97 mL of the buffer mixture at room temperature in a 3 mL screw-capped vial . After liquefying, 10 µL of an internal standard solution (acetophenone in acetonitrile) were added and stirred overnight to assure equilibration of the amidine groups in the nanogel.

To start the measurement, 20 µL from a 0.10 M (2×10^{-6} mol) of a freshly prepared substrate solution in acetonitrile were added. During the reactions, 6-9 aliquots of 150 µL were taken, the polymer was filtered off through a syringe membrane filter (0.2 µm-pore size, Schleicher & Schuell), the sample collected in an Eppendorf vessel and deep-frozen in liquid nitrogen to stop the reaction. Afterwards each sample was defrosted to room temperature and measured by injecting 20 µL into the HPLC-system. As mobile phase, acetonitrile and 0.2% (v/v) trifluoroacetic acid in water (30:70 v/v) was employed, with a flow rate of 1 mL/min and, as stationary phase, an RP-18 column (Merck). The chosen wavelength was the λ_{max} of phenol at 218 nm, which is optimal to detect the product of the reaction. The system was optimized to control the product peak and the internal standard. A detection software package was used to record and integrate the chromatograms.

A calibration curve for the determination of the product phenol in presence of the internal standard acetophenone was established prior to the measurements.

Michaelis-Menten kinetics

For the imprinted and the control nanogels, substrate saturation curves could be obtained. For these investigations, the initial reaction rates were determined at a constant concentration of active sites and increasing substrate concentration. We chose six different substrate concentrations and the procedure to measure the velocities were the same as in case of the pseudo-first order kinetics. The calculation of the Michaelis-Menten scheme was performed via fitting with Hyperbola using Origin 7.0.

Literature

[1] A. J. Kirby, *Angew. Chem., Int. Ed. Engl.,* **1996**, *35*, 707-724.

[2] J. K. M. Sanders, *Chem. Eur. J.,* **1998**, *4*, 1378-1383.

[3] R. Breslow, and S. D. Dong, *Chem. Rev.,* **1998**, *98*, 1997-2011.

[4] J. M. Lehn, *Angew. Chem., Int. Ed. Engl.,* **1988**, *27*, 89-104.

[5] D. J. Cram, *Angew. Chem., Int. Ed. Engl.,* **1988**, *27*, 1009-1020.

[6] W. K. Fife, *Trends Polym. Sci.,* **1995**, *3*, 214-221.

[7] Y. Murakami, J. Kikuchi, Y. Hisaeda, and O. Hayashida, *Chem.Rev.,* **1996**, *96*, 721-758.

[8] W. B. Motherwell, M. J. Bingham, and Y. Six, *Tetrahedron*, **2001**, *57*, 4663-4686.

[9] K. Johnsson, R. K. Allemann, H. Widmer, and S. A. Benner, *Nature*, **1993**, *365*, 530.

[10] S. J. Pollack, and P. G. Schultz, *J. Am. Chem. Soc.,* **1989**, *111*, 1929-1931.

[11] P. Wirsching, J. A. Ashley, S. J. Benkovic, K. D. Janda, and R. A. Lerner, *Science*, **1991**, *252*, 680-685.

[12] G. Wulff, *Chem. Rev.,* **2002**, *102*, 1-28.

[13] A. S. Lindsay, *Rev. Macromol. Chem.*, **1970**, *4*, 1-41.

[14] C. G. Overberger, and J. C. Salamone, *Acc. Chem. Res.,* **1969**, *2*, 217-224.

[15] T. Kunitake, and Y. Okahata, *J. Am. Chem. Soc.*, **1976**, *98*, 7793-7799.

[16] C. G. Overberger, J. C. Salamone, and B. Yaroslovski, *J. Am. Chem. Soc.*, **1967**, *89*, 6231-6236.

[17] D. M. Blow, and T. A. Steitz, *Annu. Rev. Biochem.*, **1970**, *39*, 63-100.

[18] D. E. Koshland, Angew. *Chem. Int. Ed. Engl.*, **1994**, *33*, 2408-2412.

[19] G. Wulff, A. Sarhan, and K. Zabrocki, *Tetrahedr. Lett.*, **1973**, *44*, 4329-4332.

[20] Y. Okahata, and T. Kunitake, *J. Polym. Sci. Polym. Chem. Ed.*, **1977**, *15*, 2571-2585.

[21] M. Fridkin, and H. J. Goren, *Eur. J. Biochem.*, **1974**, *41*, 273-283.

[22] H. C. Kiefer, W. I. Congdon, I. S. Scarpa, and I. M. Klotz, *Proc. Natl. Acad. Sci. U.S.A.*, **1972**, *69*, 2155-2159.

[23] I. M. Klotz, *Ann. N. Y. Acad. Sci.*, **1984**, *434*, 302-320.

[24] R. Schwyzer, *Proc. 4th Int. Congr. Pharmacol.*, **1970**, *5*, 196-209.

[25] G. Wulff, *Angew. Chem.*, **1995**, *107*, 1958-1979; *Angew. Chem. Int. Ed. Engl.*, **1995**, *34*, 1812-1832.

[26] G. Wulff, T. Gross, R. Schönfeld, T. Schrader, and C. Kirsten, In *Molecular and Ionic Recognition with Imprinted Polymers, Vol. 703* (Eds.: R. A. Bartsch, M. Maeda), Washington D.C., **1998**, pp 10-28.

[27] G. Wulff and A. Sarhan, *Angew. Chem.*, **1972**, *84*, 364.; *Angew. Chem. Int. Ed. Engl.*, **1972**, *11*, 341.

[28] G. Wulff and A. Sarhan, German Patent, Offenlegungsschrift DE-A 2242796, **1974**. *Chem. Abstr.*, **1975**, *83*, P 60300*w*; US Patent, continuation in part US-A 4127730, **1978**.

[29] R. A. Lerner, S. J. Benkovic and P. G. Schultz, *Science*, **1991**, *252*, 659-667.

[30] J. D. Stewart, L. J. Liotta and S. J. Benkovic, *Acc. Chem. Res.,* **1993**, *26*, 396-404.

[31] G. Wulff, T. Gross and R. Schönfeld, *Angew. Chem.*, **1997**, *109*, 2049-2052; *Angew. Chem. Int. Ed. Engl.*, **1997**, *36*, 1961-1964.

[32] A. G. Strikovsky, D. Kasper, M. Grün, B. S. Green, J. Hradil and G. Wulff, *J. Am. Chem. Soc.*, **2000**, *122*, 6295-6296.

[33] V. Henri, *Lois Générales de l'Action des Diastases.* Paris, Hermann, **1903**.

[34] L. Michaelis and M. L. Menten, *Biochemische Zeitschrift*, **1913**, *49,* 333.

[35] A. L. Lehninger, D. L. Nelson, and M. M. Cox, *Principles of Biochemistry*, 2nd ed, Worth Publishers: Seoul, **1993**, pp 214.

[36] A. Fersht, *Enzyme Structure and Mechanism*, W. H. Freeman and Company, New York, **1985**, pp 152.

[37] G. Wulff, W. Vesper, R. Grobe-Einsler and A. Sarhan, *Makromol. Chem.*, **1977**, *178*, 2799-2816.

[38] G. Wulff, R. Grobe-Einsler, W. Vesper and A. Sarhan, *Makromol. Chem.*, **1977**, *178*, 2817-2825.

[39] G. Wulff, J. Vietmeier and H. G. Poll, *Makromol. Chem.*, **1987**, *188*, 731-740.

[40] K. Hosoya, K. Yoshizako, N. Tanaka, K. Kimata, T. Araki and J. Haginaka, *Chem. Lett.*, **1994**, 1437-1438.

[41] L. Ye, P. A. G. Cormack and K. Mosbach, *Anal. Commun.* **1999**, *36*, 35-38.

[42] A. G. Strikovski, J. Hradil and G. Wulff, *React. Func. Polym.*, **2003**, *54*, 49-61.

[43] D. L. Van Vranken, D. Panomitros and P. G. Schultz, *Tetrahedron Lett.* **1994**, *35*, 3873-3876.

[44] K. Landfester, N. Bechthold, F. Tiarks and M. Antonietti, *Macromolecules*, **1999**, *32*, 2679-2683.

[45] H. Staudinger and E. Husemann, *Chem. Ber.*, **1935**, *68*, 1618.

[46] D. Saatweber, B. Vogt-Birnbrich, *Prog. Org. Coat.*, **1996**, *28*, 33.

[47] N. Sasa and T. Yamaoks, *Adv. Mater.,* **1994**, *6*, 417.

[48] J. Zhang, S. Xu and E. Kumacheva, *J. Am. Chem. Soc.*, **2004**, *126*, 7908-7914.

[49] P. F. Kiser, G. Wilson and D. Needham, *Nature,* **1998**, *394*, 459.

[50] C. Schunicht, A. Biffis, and G. Wulff, *Tetrahedron*, **2000**, *56*, 1693-1699.

[51] S. L. Goh, N. Murthy, M. Xu and J. M. J. Fréchet, *Bioconjugate Chem.*, **2004**, *15*, 467-474.

[52] C. Spanka, B. Clapham and K. D. Janda, *J. Org. Chem.*, **2002**, *67,* 3045-3050.

[53] C. D. Jones and L. A. Lyon, *Macromolecules,* **2000,** *33,* 8301-8306.

[54] W. O. Baker, *Ind. Eng. Chem.*, **1949**, *41*, 511-520.

[55] IUPAC Macromolecular Division (**1998**) Commission on Macromolecular Nomenclature.

[56] Glossary of Basic Terms in Polymer Science by IUPAC**,** *Pure & Appl. Chem.,* **1996**, *68*, 2298.

[57] N. B. Graham, and A. Cameron, *Pure Appl. Chem.*, **1998**, *70*, 1271-1275.

[58] S. Kadlubowski, J. Grobelny, W. Olejniczak, M. Cichomski and P. Ulanski, *Macromolecules,* **2003**, *36*, 2484-2492.

[59] K. Ogawa, A. Nakayama and E. Kokufuta, *Langmuir,* **2003**, *19,* 3178-3184.

[60] W. H. Carothers, *Chem. Rev.*, **1931**, *8*, 353-426.

[61] P. J. Flory, *J. Am. Chem. Soc.*, **1941**, *63*, 3083-3090.

[62] P. L. Kuo, N. J. Turro, C. M. Tseng, M. S. El-Aasser, and J. W. Vanderhoff, *Macromolecules*, **1987**, *20*, 1216-1221.

[63] S. S. Atik, and J. K. Thomas, *J. Am. Chem. Soc.*, **1981**, *103*, 4279-4280.

[64] Y. T. Choi, M. S. El-Aasser, E. D. Sudol, and J. W. Vanderhoff, *J. Polym. Sci., Part A: Polym. Chem.*, **1985**, *23*, 2973-2987.

[65] D. Zou, S. Ma, R. Guan, M. Park, L. Sun, J. J. Aklonis, and R. Salovey, *J. Polym. Sci., Part A: Polym. Chem.*, **1992**, *30*, 137-144.

[66] K. Tauer, R. Deckwer, I. Kuhn, and C. Schellenberg, *Colloid. Polym. Sci.*, **1999**, *277*, 607-626.

[67] W. Funke, O. Okay, B. Joos-Müller, *Adv. Polym. Sci.*, **1998**, 136, 139-234.

[68] K. Dušek, H. Galina, and J. Mikes, *Polym. Bull.*, **1980**, *3*, 19-25.

[69] M. C .A. Donkersloot, J. H. Gouda, J. J. van Aartsen, and W. Prins, *Recl. Trav. Chim. Pays-Bas.*, **1967**, *86*, 321.

[70] L. M. Croll, and H. D. H. Stöver, *Langmuir*, **2003**, *19*, 10077-10080.

[71] A. Matsumoto, *Adv. Polym. Sci.*, **1995**, *123*, 41-80.

[72] N. B. Graham, and C. M. G. Hayes, *Macromol. Symp.*, **1995**, *93*. 293-300.

[73] N. B. Graham, J. Mao, and A. Urquhart, *Angew. Makromol. Chem.*, **1996**, *240*, 113-121.

[74] K. E. J. Barrett, H. R. Thomas, *Dispersion polymerization in organic media*, Wiley, London, **1975**.

[75] J. S. Downey, R. S. Frank, W. Li, and H. D. H. Stöver, *Macromolecules*, **1999**, *32*, 2838-2844.

[76] F. W. Billmeyer Jr., *Textbook of polymer Science*, 3rd ed., Wiley: New York, **1984**, pp 152-154.

[77] H. F. Mark, N. M. Bikales, C. G. Overberger, and G. Menges, *Encyclopedia of Polymer Science and Engineering*, 2nd ed., Wiley: New York, **1986**, pp.394.

[78] S. C. Maddock, P. Pasetto and M. Resmini, *Chem. Comm.*, **2004**, 536-537.

[79] A. Biffis, N. B. Graham, G. Siedlaczek, S. Stalberg, and G. Wulff, *Macromol. Chem. Phys.*, **2001**, *202*, 163-171.

[80] G. Wulff, R. Schönfeldt, M. Grün, R. Baumstark, G. Wildburg, and L. Häussling, (BASF AG). German Patent, Offenlegungsschrift DE A 19720345, **1998**.

[81] G. Wulff and K. Knorr, *Bioseparation*, **2002**, *10*, 257-276.

[82] G. Wulff, R. Schönfeld, *Adv. Mater.* **1998**, *10*, 957-959.

[83] G. Wulff, and A. Biffis, In *Molecularly Imprinted Polymers-Man-Made Mimics of Antibodies and their Application in Analytical Chemistry*, B. Sellergren, Ed., Elsevier, Amsterdam, **2001**, pp 71-111.

[84] X. Yan, *Diploma Thesis*, Heinrich-Heine-University Düsseldorf, **1999**.

[85] D. Kasper, *PhD Thesis*, Heinrich-Heine-University Düsseldorf, **1999**.

[86] V. S. Soldatov, *Ind. Eng. Chem. Res.*, **1995**, *34*, 2605-2611.

[87] H. R. Allcock, and F. W. Lampe, *Contemporary Polymer Chemistry*, 2nd ed., Prentice Hall, **1992**, pp 339.

[88] P. G. Higgs, and J. F. Joanny, *J. Chem. Phys.*, **1991**, *94*, 1543-1554.

[89] M. Antonietti, A. Rriel, and S. Förster, *J. Chem. Phys.*, **1996**, *105*, 7795-7807.

[90] G. Odian, *Principles of Polymerization*, 2nd ed., Wiley: New York, **1981**, pp 196.

[91] J. Brandrup, E. H. Immergut, and E. A. Grulke, Eds., *Polymer Handbook*, 4th ed., Wiley: New York, **1999**, *II*, 3.

[92] M. Glad, P. Reinholdsson, and K. Mosbach, *React. Polym.*, **1995**, *25*, 47-54.

[93] M. Yoshida, Y. Hatate, K. Uezu, M. Goto, and S. Furusaki, *J. Polym. Sci. Pol. Chem.*, **2000**, *38*, 689-696.

[94] Y.Y.Chiu, L.J.Lee (1995) *J. Polym. Sci. :Part A: Polym. Chem.*, 33, 257-267

[95] L. Reimer, *Transmission Electron Microscopy*, Springer-Verlag, Berlin, **1997**.

[96] W. Funke, *Brit. Polym. J.*, **1989**, *21*, 107-115.

[97] A. Biffis, *PhD Thesis*, Heinrich-Heine-University Düsseldorf, **1998**.

[98] R. Schönfeld, Dissertation, Heinrich-Heine-University Düsseldorf, **1998**.